AN ABSTRACT OF THE DISSERTATION OF

Daniel J. Coleman for the degree of Doctor of Philosophy in Molecular and Cellular Biology presented on April 17, 2014

Title: Roles for Retinoid-X-Receptors in Solar UV-Induced Melanocyte Homeostasis and Melanomagenesis

Abstract approved: _____

Arup K. Indra

Melanoma is the deadliest form of skin cancer, arising from malignant transformation of pigment-producing melanocytes. The primary risk factor for melanoma and other skin cancers is DNA damage resulting from unprotected solar ultraviolet radiation (UVR). If incorrectly repaired, this damage can result in incorporation of mutations that cause aberrant cell cycling and/or other functional defects that promote tumorigenesis. Rates of melanoma incidence are on the rise in Oregon and throughout the U.S.; thus better understanding of the molecular mechanisms underlying its formation and progression are needed for the purposes of diagnosis and therapeutic targeting. In this work we have used mouse models to establish multiple roles for Retinoid-X-Receptors (RXRs) in UVR-induced melanocyte homeostasis and melanomagenesis. Ablation of RXRα expression in epidermal keratinocytes (*Rxrα*$^{ep-/-}$) enhances melanocyte proliferation following an acute UVR dose; stemming from increased expression of mitogenic paracrine factors. Combining *Rxrα*$^{ep-/-}$ mice with activated CDK4

(R24C) or oncogenic NRAS (Q61K) mutations in a bigenic model results in enhanced UVR-induced melanomagenesis compared to control mice with the CDK4 or NRAS mutations alone. These melanomas show increased expression of malignant melanoma and tumor angiogenesis markers; and increased metastases of pigment-producing cells to draining lymph nodes. Interestingly, the tumor adjacent normal skin of these mice have reduced expression of p53 and PTEN, tumor suppressors commonly downregulated in melanoma; suggesting that in addition to enhancing melanomagenesis, keratinocytic RXRα loss results in a microenvironment favorable to primary tumor formation. By ablating RXRs α and β specifically in the melanocytes (*Rxrα/β*$^{mel-/-}$), we observed differential alterations in the post-UVR survival of the melanocytes and the dermal fibroblasts. Loss of melanocytic RXR expression results in defective homeostasis of chemoattractive/chemorepulsive chemokines secreted by melanocytes to attract macrophages and other immune cells post-UVR. An overall reduction of immune cell infiltration in *Rxrα/β*$^{mel-/-}$ mice results in less available interferon-γ available in the microenvironment which has a negative effect on post-UVR survival of fibroblasts and melanocytes. However, as the genetic defect in these mice is specifically in the melanocytes, there are dysregulations in cell-intrinsic apoptosis signaling that allow these cells to overcome reduced available IFN-γ and have enhanced survival post-UVR. Therefore RXRs in melanocytes modulate post-UVR survival of dermal fibroblasts in a “non-cell autonomous” manner, underscoring their role in immune surveillance; while independently mediating post-UVR melanocyte survival in a

“cell autonomous” manner. Altogether these results establish a multitude of roles for RXRs in melanocyte homeostasis and melanomagenesis, and identifies them as potential targets for melanoma diagnosis and therapeutics.

Roles for Retinoid-X-Receptors in Solar UV-Induced Melanocyte Homeostasis and Melanomagenesis

by

Daniel J. Coleman

A DISSERTATION

Submitted to

Oregon State University

In partial fulfillment of
the requirements for the
degree of

Doctor of Philosophy

Presented April 17, 2014
Commencement June 2014

Doctor of Philosophy dissertation of Daniel J. Coleman presented on April 17, 2014

APPROVED:

Major Professor, representing Molecular and Cellular Biology

Director of the Molecular and Cellular Biology Program

Dean of the Graduate School

I understand that my dissertation will become part of the permanent collection of the Oregon State University libraries. My signature below authorizes release of my dissertation to any reader upon request.

Daniel J. Coleman, Author

ACKNOWLEDGMENTS

All Indra Lab members past and present!!!

Molecular and Cellular Biology Program (OSU)

College of Pharmacy (OSU)

EHSC (OSU) for NIEHS predoctoral trainee funding (2010-2012)

Dermatology Research Division (OHSU) for NCI predoctoral trainee funding (2012-2013)

Walter Vogel (OSU College of Pharmacy) and Chris Sullivan (OSU CGRB) for bioinformatics advice and support

C. Samuel Bradford (OSU EHSC) for flow cytometry and LCM support

Pierre Chambon's Group (IGBMC, France) for floxed RXR mice

Mariano Barbacid (Spain) for CDK4 mice

Gary Miller, Debra Peters, and Patty Beaumont (OSU College of Pharmacy) for all of their help over the years!!!

CONTRIBUTION OF AUTHORS

Chapter 1: Daniel J. Coleman wrote the chapter with editing by Dr. Arup K. Indra. Data was excerpted from Wang et al 2010 (J Invest Dermatol 131(1): 177-187) and Hyter et al 2012 (Pigment Cell Melanoma Res 26(2): 247-258). In these studies, Daniel J. Coleman helped to perform these experiments in close collaboration with Dr. Arup K. Indra and either Zhixing Wang (Figures 1.1-1.3) or Stephen Hyter (Figure 1.4).

Chapter 2: Dr. Arup K. Indra and Daniel J. Coleman worked together to design research experiments, analyze data, and write the manuscript; with input from Sharmeen Chagani and Stephen Hyter. Daniel J. Coleman primarily performed the experimental research in addition to contributions from other Indra Lab members, namely Sharmeen Chagani (sample collection, western blotting, histology and imaging) Stephen Hyter (mouse breeding, UVR treatment, sample collection, western blotting, histology and imaging), Anna M. Sherman (histology and imaging), Xiaobo Liang (western blotting), Dr. Christiane V. Löhr (pathological assessments of histological tumor samples), and Dr. Gitali Ganguli-Indra (critical analyses of manuscripts).

Chapter 3: Dr. Arup K. Indra and Daniel J. Coleman worked together to design research experiments, analyze data, and write the manuscript. Daniel J. Coleman primarily performed the experimental research in addition to contributions from other Indra Lab members, namely Gloria Garcia (western

blotting and image analyses) Stephen Hyter (western blotting, histology, and imaging/analyses), Hyo Sang Jang (histology and imaging/analyses), Sharmeen Chagani (image analyses), Xiaobo Liang (western blotting), Dr. Lionel Larue (critical analyses of manuscripts) and Dr. Gitali Ganguli-Indra (critical analyses of manuscripts).

Chapter 4: Daniel J. Coleman wrote the chapter with editing by Dr. Arup K. Indra. All analyses and plotting of ChIP-seq data was performed by Daniel J. Coleman. Dr. Ling-juan Zhang and Shreya Bhattacharya isolated keratinocytes and performed ChIP to isolate DNA for use in high-throughput sequencing analyses.

TABLE OF CONTENTS

TABLE OF CONTENTS (Continued)

TABLE OF CONTENTS (Continued)

Page

LIST OF FIGURES

LIST OF FIGURES (Continued)

Figure Page

LIST OF FIGURES (Continued)

LIST OF FIGURES (Continued)

Figure Page

LIST OF TABLES

DEDICATION

To my family for their unconditional love and support; and to the State of Oregon for being an awesome place to grow up, live, and receive an education.

General Introduction: Melanocytes, Ultraviolet Radiation-Induced DNA Damage and Mutation; and the Involvement of Retinoid-X-Receptors in Melanomagenesis

Chapter 1

Daniel J. Coleman and Arup K. Indra

1.1 Abstract

Melanoma is the deadliest form of skin cancer, arising from malignant transformation of melanocytes, the pigment cells of the skin. The primary risk factor for development of melanoma and other skin cancers is unprotected ultraviolet radiation (UVR), which results in DNA damage. If incorrectly repaired, this damage can result in incorporation of mutations that render cells tumorigenic owing to aberrant cell cycling and/or other functional defects. In addition, these UVR-induced mutations may cooperate with heritable mutations that already predispose individuals to melanoma. Oregon has one of the highest melanoma incidence rates in the U.S. and with cases on the rise, the need to better understand the molecular mechanisms behind melanoma formation becomes more crucial. Retinoid-X-Receptors (RXRs) α, β, and γ are members of the Type II Nuclear Receptor (NR) superfamily of DNA-binding transcription factors. RXRs ubiquitously regulate gene expression via ligand binding and heterodimerization with various other NRs; depending on ligand and heterodimeric partner they are able to function as transcriptional co-repressors or co-activators. Progressive loss of RXRα expression has been reported during progression from benign nevi to invasive malignant melanoma in humans, both in melanoma cells themselves and in the adjacent keratinocytes that comprise the epidermis of the skin. We have found that keratinocyte-specific ablation of RXRα in a mouse model (*Rxrα*$^{ep-/-}$) results in increased melanoma formation as a result of DMBA/TPA induced chemical carcinogenesis. Melanocytes in those mice exhibit enhanced proliferation in response to an acute dose of UVR, suggesting altered

keratinocyte-melanocyte crosstalk. We aim to better elucidate the molecular mechanisms of RXR function in UVR-induced melanocyte homeostasis and in melanomagenesis.

1.2 The Biology of the Skin

Skin is the largest organ in the body and provides the main barrier between our internal organs and the external environment. It is comprised of three layers, the epidermis, dermis, and hypodermis [1]. The epidermis is the uppermost layer, of which the outermost surface is exposed to the environment. The epidermis is a multilayered stratified epithelium comprised primarily of keratinocytes and is a constantly self-renewing tissue [1]. A proliferating basal layer gives rise to the terminally differentiated spinous and granular layers [1]. The outermost layer, the stratum corneum, is comprised of flattened, dead cells that are continually shed and replaced by cells underneath [1]. These dead cells retain some metabolic functions [1]; and form a tight barrier to prevent water loss from the skin and also to keep insults, such as harmful pathogens, out. Beneath the epidermis is the dermis, which connects to the epidermis via a basement membrane [1]. This layer is comprised primarily of fibroblasts, which secrete a collagenous extracellular matrix [1]. At the base of the dermis are sub-cutaneous (cutaneous = within the skin) fat cells, known as adipocytes. This sub-cutaneous layer is known as the hypodermis [1]. The purpose of this layer is to cushion the skin against underlying structures such as bone and to provide an energy reserve [1]. Also present throughout the skin are various immune cells, such as Langerhans cells [1], monocytes, macrophages, mast cells [1], and T-cells [2]. Additionally, melanin-producing melanocytes reside within the epidermis, dermis, and hair follicles.

1.3 Melanocyte Biology

Melanocytes give skin and hair their pigment via synthesis and transfer of melanin to other cells. Due to their dendritic nature, one melanocyte is capable of contacting and transferring melanin to 36 keratinocytes simultaneously [1]. Melanin pigment also functions to shield cells from ultraviolet radiation (UVR) that can damage DNA and result in mutations that cause cancers of the skin. This UVR-induced pigmentation of the skin, or melanogenesis, is commonly known as tanning. Rates of UVR-induced DNA damage have been inversely correlated with cellular melanin content [3]. In response to UVR, keratinocytes upregulate secretion of mitogenic paracrine factors to enhance melanogenesis, for example a >30 fold increase in melanocyte stimulating hormone (αMSH) is observed in UVR-treated keratinocytes from both mice and humans [4]. Addition of thymine dinucleotides (pTpTs) to simulate presence of DNA photoproducts directly activates tumor suppressor p53 [5] and enhances DNA repair efficiency when topically applied to skin [5,6]. When added to cultured pigment cells, pTpT increases melanogenesis [7] and upregulates expression of Tyrosinase, the rate-limiting enzyme involved in melanin synthesis [8]. This suggests that melanocytes can also directly sense DNA damage and enhance their melanogenesis without signaling from other cell types.

Throughout the animal kingdom, colors of feathers, fur, skin, eyes, etc. are determined primarily by pigment-producing melanocytes [4]. Melanin pigment is classified into two main types, pheomelanin and eumelanin, which are red/yellow

and brown/black in color, respectively [4]. The melanin is packaged into unique organelles known as melanosomes and transferred to other cells, largely keratinocytes [4,9], resulting in pigmentation of the skin and hair. While melanocyte numbers are consistent, alterations in the composition of melanosomes can produce varying pigmentation patterns within a species [4].

Unlike other cell types in the skin, melanocytes arise from pluripotent neural crest cells. During development, the immature cells, known as melanoblasts, migrate from the neural crest to populate the skin, as well as the inner ear and eyes [10-12]. Melanocyte development, survival and migration is heavily influenced by signaling via the c-KIT receptor and its mitogenic ligand Stem Cell Factor (SCF, aka Kit Ligand (KITL)) [13-17]; including its function as a chemotactic factor for migration from the dermal mesenchyme into the hair follicles of the skin [17]. Within the hair follicles, a population of undifferentiated melanocyte stem cells resides in the bulge region, giving rise to differentiated melanocytes that populate the hair follicle bulb to incorporate melanin during hair synthesis; and also to populate the epidermis for skin pigmentation [4]. Other receptor-mediated signaling pathways, such as Endothelin signaling via the ENDRB receptor [18], Hepatocyte Growth Factor (HGF) signaling via the c-MET receptor [19], and αMSH signaling via the MC1R receptor have also been found to have significant roles in melanocyte development, migration, and homeostasis. MC1R receptor signaling has been found to be crucial for skin pigmentation. Paracrine αMSH secretion from keratinocytes is largely upregulated following UVR exposure [4]; agonist-bound MC1R results in production of cyclic AMP [4],

leading to downstream activation of the transcription factor MITF [4], which regulates expression of several factors of melanocyte differentiation and pigment-production [4]. Numerous (>30) allelic variations of human MC1R exist [4], specific variants have been associated with red hair phenotype [4,20] and/or increased melanoma risk [20,21].

Recent findings have suggested that different signaling pathways are required to maintain cutaneous melanocyte populations in the dermal layer as opposed to those cells residing in the epidermis [10,22]. In a mouse model, melanocytes residing in the epidermis are highly sensitive to SCF-cKIT signaling [10,13]. Meanwhile similar to non-cutaneous melanocytes, those residing in the dermal layer are relatively insensitive to SCF owing to reduced expression of the c-KIT receptor on their cell surface, and instead respond strongly to mitogens Hepatocyte Growth Factor (HGF), via the c-MET receptor; and Endothelin-3 (EDN3, aka ET-3) via the ENDRB receptor [10]. Keratinocyte-specific overexpression of SCF results in localization of melanocytes to the mouse epidermis [10,13], while HGF or EDN3 overexpression results in melanocytes populating the dermal layer [10]. Furthermore, a hair reconstitution assay revealed that dermal melanocytes are unable to repopulate hair follicles [22]. These data suggest that two distinct populations of melanocytes exist in the skin.

Specific localizations of melanocytes can vary amongst species. For example, the skin of mice is strikingly similar to human skin in morphology, but being a furry nocturnal animal, most murine melanocytes in the skin are contained within the hair follicle for coat pigmentation; and the number of innate

extrafollicular epidermal melanocytes is low compared to human skin [4]. However, as mentioned previously, keratinocyte-specific overexpression of SCF [10,13] results in enhanced melanocyte localization to the extrafollicular epidermis in a similar manner to human skin [4,13]. Additionally, studies from our own group [23,24] and others [25] have shown that exposure of murine skin to ultraviolet-B radiation (UVB) results in robust activation and outmigration of melanocytes from the hair follicles into the epidermis and dermis; demonstrating that their photoprotective function in response to UVR is conserved in mice despite their nocturnal nature in the wild. Thus, murine skin is being utilized as a very suitable model to study UVR-induced pathogenenesis, including the roles of melanocytes.

1.4 Ultraviolet Radiation and Mutagenic DNA Damage

1.4.1 Solar UV-induced DNA Damage

Solar ultraviolet radiation (UVR) is an environmental carcinogen owing to its ability to directly and indirectly cause DNA damage, which can result in harmful mutations if not properly repaired. UV light is comprised of three bands: UVA (315-400 nm), UVB (280-315 nm), and UVC (< 280 nm) [26]. The atmospheric ozone layer filters out UVC radiation and the bulk of UVB [26]. Therefore, the solar UVR that reaches the earth's surface and has implications in biology is comprised largely of UVA and some UVB [26]. UVA is able to penetrate deeper into the skin, with 30-50% of its energy able to reach the dermis, while only 10-20% of UVB penetrates beyond the epidermis and into this layer [26]. Both bands are able to inflict DNA damage. The DNA damage caused by UVA is largely indirect, it is absorbed by chromophores within the cell which results in formation of reactive oxygen species (ROS); which then react with DNA to cause oxidative-induced DNA damage, such as 8-Oxo-2'-deoxyguanosine (8-oxo-dG) [26-28]. Red/yellow pheomelanin may itself be a photosensitizer, producing ROS as a result of UVR [4]. Meanwhile, UVB has a largely direct effect. UVB radiation can result in formation of covalent bonds between adjacent pyrimidines, such as cyclobutane pyrimidine dimers (CPDs) and 6-4 photoproducts (6-4 PPs) [4,9,26-28]; though UVB can also result in oxidative DNA damage [28]. Oxidative DNA lesions can be repaired by either base excision repair (BER) or nucleotide excision repair (NER) [26]. CPDs and

6-4 PPs are generally repaired using NER [26,28]. Individuals with compromised NER, such as xeroderma pigmentosum (XP) sufferers, are highly sensitive to sunlight and are extremely susceptible to UVR-induced skin cancers as many mutations are improperly repaired [9,26-28]. Even in otherwise healthy individuals, UVR-induced mutations can occur when the NER repair capacity is exceeded [26]. A mere 15% reduction in NER capacity can separate healthy individuals from those developing skin cancers such as basal cell carcinoma (BCC) at an early age [27]. It has also been suggested that defects in mismatch repair (MMR) can reduce NER capacity and may also have a role in UVR-induced tumorigenesis [26].

UVR-induced DNA lesions are not completely random. DNA structure can favor mutagenicity at particular sites in what are known as UVR fingerprint mutations [9]. “Hotspots” of UVR-induced mutation correspond with regions of the genome where DNA repair is slow [28,29]. Point mutations induced by UVB generally occur at di-pyrimidine sites containing cytosine [30], with C to T transitions most common [31,32]; while mutations resulting from oxidative stress most often result in G to T transversions [32,33]. Thus, certain genetic regions are at higher risk for incorporating tumorigenic mutations as a result of UVR.

1.4.2 Melanoma Etiology

Malignant melanoma arises from malignant transformation of melanocytes. While melanomas make up less than 10% of total skin cancer

incidences [28], they account for the majority of deaths [27,28]. Unprotected exposure to UVR is the primary risk factor for melanoma and other skin cancers [Centers for Disease Control and Prevention (CDC), 2010; American Cancer Society, 2013]. Despite our often cloudy and wet weather, Oregon has one of the highest melanoma incidence rates in the U.S.; with a diagnosis rate 36% higher than the national average from 2002-2006, ranking 4th nationally [34,35]. Approximately 120 melanoma-related deaths occur in Oregon each year [36] and the death rate from 2002-2006 ranked 8th nationally [37]. As of 2009, Josephine County has the 5th highest melanoma death rate among all counties in the U.S. [36]. Melanoma is the second most common cancer to arise in young adults [38], and the diagnosis rate for people born in 2006 is estimated to be 30 times higher than for people born in 1930 [37,39]. Thus, better understanding of the molecular mechanisms underlying formation of malignant melanoma and progression to metastasis is crucial for developing new diagnostic and therapeutic strategies as the number of incidences continues to rise.

1.4.3 Hallmark Mutations in Melanoma

Mutational disruption of the INK4a/ARF locus and related genes are signature events in formation of familial melanoma. Partial or complete loss of INK4a/ARF has been reported to exist in ~60% of melanoma cell lines surveyed [32,40]. Via alternative splicing, the INK4a/ARF locus encodes two non-homologous proteins: p16^{INK4a} and p14^{ARF} (homolog is p19^{ARF} in mice) [41,42]. p16^{INK4a} has a role in the Rb-INK4a-CDK4 pathway; via inhibiting Cyclin

Dependent Kinases (CDK4/6) from phosphorylating the tumor suppressor protein retinoblastoma (pRb) [41,43]. When hypo-phosphorylated, pRb represses E2F1 transcription factor function and prevents exit from the G1 cell cycle phase [41]. Thus $p16^{INK4a}$ expression results in a G1 cell cycle arrest and limits excessive cellular proliferation. $p14^{ARF}$/$p19^{ARF}$ stabilizes tumor suppressor p53 via inhibition of MDM2 protein, which otherwise mediates p53 degradation [41]. Both genes encoded by the INK4a/ARF locus are crucial for preventing aberrant cell cycling and tumorigenesis. Heterozygous *Ink4a/arf* $^{+/-}$ mice combined with an overexpressing *HGF/SF* (Hepatocyte Growth Factor and Scatter Factor) transgene develop melanomas as a result of UVR, this melanomagenesis is accelerated in null *Ink4a/arf* $^{-/-}$ | *HGF/SF* mice [44].

Other mutations in the Rb-INK4a-CDK4 pathway can result in cell cycle defects analogous to INK4a/ARF inactivation, such as oncogenic point mutations in CDK4 that alter the protein encoded by open reading frame. The mutant CDK4 R24C protein (Arginine at amino acid position 24 mutated to Cysteine) is unable to bind $p16^{INK4a}$ [45] and thus the Rb-INK4a-CDK4 pathway is dysregulated similarly to if the INK4a/ARF locus had been inactivated. This mutation has been found to be a risk factor for hereditary melanoma in humans [45-47]. Homozygous *Cdk4*$^{R24C/R24C}$ mice have been found to have enhanced pRb phosphorylation, as well as increased cell proliferation rate and shorter cycling times [45]. Fibroblasts cultured from these mutant mice evade senescence and undergo neoplastic transformation when combined with a single oncogenic *Ha-ras*^{v12}, *v-myc*, or *E1A* mutation; wild–type *Cdk4*$^{+/+}$ cells required

expression of at least two of these oncogenes [45]. Additionally these mice develop more spontaneous tumors as a function of age compared to control mice, and addition of the *Cdk4*$^{R24C/R24C}$ mutation enhances tumorigenesis resulting from expression of oncogenic *Ras* [45]. Two-step DMBA/TPA induced chemical carcinogenesis treatment on the skin of *Cdk4*$^{R24C/R24C}$ mice results in formation of invasive melanomas [48].

The canonical mitogen-activated protein kinase (MAPK) pathway, consisting upstream to downstream of RAS-RAF-MEK-ERK, has been found to be important in melanoma formation. A point mutation consisting of a T-A transversion at position 1,799 accounts for 90% of all mutations in the human *BRAF* gene [49], resulting in a mutant protein known as BRAF^{V600E}. *BRAF* mutations are found in ~50% of melanomas; with 90+% of those mutations being *BRAF*^{V600E} [49]. This mutation results in constitutive downstream ERK activation and upregulation of Cyclin D1, the regulatory subunit of CDK4/6 required for G1-S transition; demonstrating synergism with the Rb-p16/INK4a-CDK4 pathway. Some clinical success has been obtained using the RAF inhibitor Vemurafenib to treat *BRAF*^{V600E} melanomas. However, acquired drug resistance often occurs, possibly due to aberrant mRNA splicing prior to protein translation [50]; underscoring a need for additional simultaneous therapeutic targets for melanoma treatment. Oncogenic RAS expression is prevalent in a broad range of human cancers; and an estimated 15-20% of melanomas express mutant oncogenic *NRAS* [51,52]. Direct targeting of RAS mutations has been unsuccessful thus far [51], but pharmacological inhibition of MEK resulted in

regression of melanomas in mice expressing $NRAS^{Q61K}$ [51], but interestingly only when CDK4/6 was also inhibited. MEK inhibition alone wasn't enough to produce this effect [51], again suggesting a synergism of the Rb-p16/INK4a-CDK4 and MAPK pathways in melanoma progression.

1.5 Retinoid-X-Receptors and Melanoma

1.5.1 Biology of Type II Nuclear Receptors

Retinoid-X-Receptors (RXRs) α, β, and γ are members of the Type II Nuclear Receptor (NR) superfamily of DNA-binding transcription factors. Type II NRs have a highly conserved DNA binding domain (DBD) consisting of two zinc finger motifs [53]. The NRs form either homo- or hetero-dimers with each other and bind response elements on the DNA as part of a transcriptional regulatory complex [53]. These elements generally consist of short direct-repeat sequences with a variable length of nucleotides in-between, for example a 5'-AGGTCAxxxxAGGTCA-3' consensus sequence is bound in the case of a RXR-LXR (Liver-X-Receptor) heterodimer [54]. Dimerization and DNA binding capabilities are aided by two activation domains (AF-1, AF-2) [53]. More variation exists between the NRs with regard to their carboxyl terminal ligand binding domain (LBD), which allows for binding of signaling molecules; specificity of which varies between individual NRs [53,55]. Receptors for which ligand specificity has yet to be determined are labeled as orphan receptors [53]. Examples of endogenous NR ligands expressed in skin include all-trans retinoic acid (RA) for retinoic acid receptors (RARs) [53,56,57], 9-cis RA for RXRs [53,58,59], 1,25-(OH)2-VD3 for Vitamin D receptor (VDR) [53,60], fatty acids/lipids for Peroxisome Proliferator-Activated Receptors (PPARs) [53,61,62] and oxysterols for LXR [53,63].

A distinguishing feature of Type II NRs function is the promiscuity of heterodimerization by the RXRs [53]. All of the NRs are capable of forming heterodimers with one of the three RXR isoforms; RXRα alone is able to heterodimerize with at least 15 NR family members [53]. These heterodimers occupy aforementioned direct repeat response elements within the promoter regions of target genes [53,64,65]; where they are able to regulate gene expression in a ligand-dependent manner [53]. Mediated via ligand binding, the NR heterodimers can regulate organization of complexes in a manner that either initiates or represses transcription [53,66,67]. Examples of coactivators include ATP-dependent chromatin remodelers, histone acetyltrasferases and the Mediator complex [53,68,69]. Corepressors comprise the N-CoR/Smart assembly and histone deacetylases [53,70,71]. Post-translational modifications of co-factors such as phosphorylation, methylation, sumoylation and ubiquitination add an additional layer of complexity and specificity to NR regulation [53,72]. Cell- and tissue-specific factors can also come into play, for example the PPARγ cofactor PGC-1 is present in adipose tissue but not fibroblasts, allowing a cell type-specific activation of genes related to adaptive thermogenesis [53,73]. Thus, NRs are able to influence gene expression in a diverse and dynamic manner via diversity in heterodimerization, ligand binding, and cell-intrinsic properties.

1.5.2 Role for RXRs in Melanoma

Although many of RXRs heterodimeric partners have been implicated in diseases of the skin, perhaps in many cases these could instead be associated with disrupted RXR function itself. Loss of RXRα expression is observed in human melanomas as tumors progress from benign nevi to malignant and metastatic lesions, both in the melanoma cells themselves [74], and interestingly also in adjacent keratinocytes [75]. These data indicate an importance for RXR-mediated gene expression in melanomagenesis. Work from our own group has previously established that in a mouse model, loss RXRα expression in keratinocytes has a role in melanomagenesis. Interestingly, tissue-specific ablation of RXRα expression in keratinocytes (*Rxrα*$^{ep-/-}$ mice) results in enhanced formation and malignant conversion of melanomas as a result of chronic chemical DMBA-TPA carcinogenesis treatment on the skin [76]. This effect was exacerbated when combined with mutant CDK4 in a bigenic mouse model. *Rxrα*$^{ep-/-}$| *Cdk4*$^{R24C/R24C}$ mice formed a higher number of large (>2mm) melanomas than either regular *Rxrα*$^{ep-/-}$ or *Cdk4*$^{R24C/R24C}$ mice; and the melanomas exhibited higher expression of markers of malignant progression and had increased metastasis to lymph nodes relative to mice expressing only the mutant CDK4^{R24C} [75]. These results suggested that loss of RXRα expression in keratinocytes can promote malignant transformation of melanocytes, possibly via dysregulated cross-talk between keratinocytes and melanocytes; and that cooperativity with oncogenic mutations in key signaling pathways such as the Rb-INK4a-CDK4 pathway may enhance this effect.

Being a more biologically-relevant model of melanoma susceptibility than chemical carcinogens, we wanted to assess the role of keratinocytic RXRα loss on melanocyte homeostasis following UVR. While no change in formation/clearance of CPDs was observed as a result of keratinocytic RXRα ablation (Figure 1.1 a), we did observe increased levels of 8-oxo-dG+ melanocytes in *Rxrα*$^{ep-/-}$ skin 48 hours post-UVR (Figure 1.1 b) [23]. We observed that the number of epidermal and total extrafollicular melanocytes was increased in UVR-irradiated floxed *Rxrα*$^{L2/L2}$ control (CT) skin over untreated mice, this increase was significantly higher yet in the mutant *Rxrα*$^{ep-/-}$ (MT) group (Figure 1.2 a-d) [23]. Additionally, an increase in TRP2-positive melanocytes was consistently detected in the dermis of mutant skin 48 hours after UVR (Figure 1.1 b) [23]. These results suggest that loss of keratinocytic RXRα expression makes melanocytes more sensitive to UVR-induced activation/proliferation in both the epidermis and dermis, possibly via altered paracrine signals from the keratinocytes. Primary murine melanocytes showed enhanced proliferation when cultured in conditioned keratinocyte medium (KM) derived from cultured primary keratinocytes isolated from either CT or MT skin (Figure 1.2 e) [23]. This effect was enhanced when using KM from MT *Rxrα*$^{ep-/-}$ keratinocytes, and more so when KM was collected from MT keratinocytes exposed to UVR (Figure 1.2 e) [23]. In *Rxrα*$^{ep-/-}$ keratinocytes we observed increases in relative mRNA expression levels of mitogenic paracrine factors secreted by keratinocytes to stimulate melanocyte proliferation, in particular EDN1 (aka ET-1) FGF2, and SCF were more than two-fold higher in mutant skin

prior to and 24 hours post-UVR (Figure 1.3) [23]. Overall, the results of our study provide compelling evidence that keratinocytic RXRα, in cooperation with UVR, regulates melanocyte homeostasis by repressing secretion of paracrine mitogenic growth factors Additionally, the finding of increased melanocytes with incorporated oxidative DNA damage following UVR suggests an enhanced susceptibility to malignant transformation of these cells in *RXRα*$^{ep-/-}$ mice.

We then decided to thoroughly investigate the role of keratinocytic EDN1 expression in UVR-induced melanocyte homeostasis, as endothelin signaling via the EDNRB receptor is known to be crucial in melanocyte biology, and EDN1 expression is significantly upregulated in the skin of our *RXRα*$^{ep-/-}$ mice. Keratinocyte-specific ablation of EDN1 (*EDN1*$^{ep-/-}$ mice) results in reduced numbers of both cutaneous epidermal and dermal melanocytes post-UVR compared to wild-type mice [24]. We observed that addition of exogenous EDN1 to cultured primary melanocytes activates both the downstream MAPK and Protein Kinase C (PKC) pathways in primary murine melanocytes (Figure 1.4) [24]. PKCs can also activate the MAPK pathway and aberrant PKC expression/function is thought to contribute to melanoma malignancy [77]. Parallel co-treatment of cells with EDN1 and the potent EDNRB receptor antagonist BQ788 completely abrogated both MAPK and PKC activation, indicating that both of these processes are specifically mediated by the EDNRB receptor (Figure 1.4) [24].

As EDN1 is upregulated in keratinocytes from *RXRα*$^{ep-/-}$ mice, it's possible that the MAPK and PKC pathways are indirectly activated as a consequence of

epidermal RXRα loss. EDN1 represents only one of several mitogenic paracrine factors that are dysregulated as a result of keratinocytic RXRα ablation, thus EDNRB-mediated activation of the MAPK and PKC pathways may be only one mechanism in which RXRα loss promotes melanomagenesis. As nuclear receptors function in a very diverse and dynamic manner to regulate gene expression, continuing work needs to be done to better understand the mechanistic roles of RXRs in melanocyte and melanoma biology. To that end, in the following chapters we have aimed to further elucidate the molecular biology of RXRs in UVR-induced melanocyte homeostasis and melanomagenesis. In Chapter 2, have we investigated the mechanistic role of keratinocytic RXRα loss in chronic UVB-induced melanomagenesis in combination with either activated $CDK4^{R24C}$ or oncogenic $NRAS^{Q61K}$ mutations. As RXRα has also been shown to be progressively lost in pigmented melanoma cells themselves [74], in Chapter 3, we have generated a unique mouse model containing a melanocyte-specific knockout of both RXRs α and β to elucidate the role of melanocytic RXRs in melanocyte and skin homeostasis post-ultraviolet radiation.

1.6 References

1. Haake A, Scott GA, Holbrook KA (2001) Structure and function of the skin: overview of the epidermis and dermis. The Biology of the skin 2001: 19-45.

2. Ariotti S, Beltman JB, Chodaczek G, Hoekstra ME, van Beek AE, et al. (2012) Tissue-resident memory CD8+ T cells continuously patrol skin epithelia to quickly recognize local antigen. Proc Natl Acad Sci U S A 109: 19739-19744.

3. Kobayashi N, Muramatsu T, Yamashina Y, Shirai T, Ohnishi T, et al. (1993) Melanin reduces ultraviolet-induced DNA damage formation and killing rate in cultured human melanoma cells. Journal of investigative dermatology 101.

4. Lin JY, Fisher DE (2007) Melanocyte biology and skin pigmentation. Nature 445: 843-850.

5. Eller MS, Maeda T, Magnoni C, Atwal D, Gilchrest BA (1997) Enhancement of DNA repair in human skin cells by thymidine dinucleotides: evidence for a p53-mediated mammalian SOS response. Proceedings of the National Academy of Sciences 94: 12627-12632.

6. Maeda T, Eller M, Gleason M, Hedayati M, Grossman L, et al. (1998) Thymidine dinucleotide enhances DNA repair in human skin cells. J Dermatol Sci 16: S17.

7. Eller MS, Yaar M, Gilchrest BA (1994) DNA damage and melanogenesis. Nature 372: 413.

8. Eller MS, Ostrom K, Gilchrest BA (1996) DNA damage enhances melanogenesis. Proceedings of the National Academy of Sciences 93: 1087-1092.

9. Agar N, Young AR (2005) Melanogenesis: a photoprotective response to DNA damage? Mutation Research/Fundamental and Molecular Mechanisms of Mutagenesis 571: 121-132.

10. Aoki H, Yamada Y, Hara A, Kunisada T (2009) Two distinct types of mouse melanocyte: differential signaling requirement for the maintenance of non-cutaneous and dermal versus epidermal melanocytes. Development 136: 2511-2521.

11. Hall BK (2009) The neural crest and neural crest cells in vertebrate development and evolution: Springer.

12. Le Douarin N, Kalcheim C (1999) The neural crest: Cambridge University Press.

13. Kunisada T, Lu SZ, Yoshida H, Nishikawa S, Mizoguchi M, et al. (1998) Murine cutaneous mastocytosis and epidermal melanocytosis induced by keratinocyte expression of transgenic stem cell factor. J Exp Med 187: 1565-1573.

14. Mackenzie MA, Jordan SA, Budd PS, Jackson IJ (1997) Activation of the receptor tyrosine kinase Kit is required for the proliferation of melanoblasts in the mouse embryo. Dev Biol 192: 99-107.

15. Yoshida H, Kunisada T, Grimm T, Nishimura EK, Nishioka E, et al. (2001) Review: melanocyte migration and survival controlled by SCF/c-kit expression. J Investig Dermatol Symp Proc 6: 1-5.

16. Steel KP, Davidson DR, Jackson IJ (1992) TRP-2/DT, a new early melanoblast marker, shows that steel growth factor (c-kit ligand) is a survival factor. Development 115: 1111-1119.

17. Jordan SA, Jackson IJ (2000) MGF (KIT ligand) is a chemokinetic factor for melanoblast migration into hair follicles. Dev Biol 225: 424-436.

18. Baynash AG, Hosoda K, Giaid A, Richardson JA, Emoto N, et al. (1994) Interaction of endothelin-3 with endothelin-B receptor is essential for development of epidermal melanocytes and enteric neurons. Cell 79: 1277-1285.

19. Kos L, Aronzon A, Takayama H, Maina F, Ponzetto C, et al. (1999) Hepatocyte growth factor/scatter factor-MET signaling in neural crest-derived melanocyte development. Pigment Cell Res 12: 13-21.

20. Abdel-Malek ZA, Knittel J, Kadekaro AL, Swope VB, Starner R (2008) The Melanocortin 1 Receptor and the UV Response of Human Melanocytes—A Shift in Paradigm†. Photochemistry and photobiology 84: 501-508.

21. Landi MT, Bauer J, Pfeiffer RM, Elder DE, Hulley B, et al. (2006) MC1R germline variants confer risk for BRAF-mutant melanoma. Science 313: 521-522.

22. Aoki H, Hara A, Motohashi T, Osawa M, Kunisada T (2011) Functionally distinct melanocyte populations revealed by reconstitution of hair follicles in mice. Pigment Cell Melanoma Res 24: 125-135.

23. Wang Z, Coleman DJ, Bajaj G, Liang X, Ganguli-Indra G, et al. (2011) RXRalpha ablation in epidermal keratinocytes enhances UVR-induced DNA damage, apoptosis, and proliferation of keratinocytes and melanocytes. J Invest Dermatol 131: 177-187.

24. Hyter S, Coleman DJ, Ganguli-Indra G, Merrill GF, Ma S, et al. (2013) Endothelin-1 is a transcriptional target of p53 in epidermal keratinocytes and regulates ultraviolet-induced melanocyte homeostasis. Pigment Cell Melanoma Res 26: 247-258.

25. Zaidi MR, Davis S, Noonan FP, Graff-Cherry C, Hawley TS, et al. (2011) Interferon-gamma links ultraviolet radiation to melanomagenesis in mice. Nature 469: 548-553.

26. Rass K, Reichrath J (2008) UV damage and DNA repair in malignant melanoma and nonmelanoma skin cancer. Sunlight, Vitamin D and Skin Cancer: Springer. pp. 162-178.

27. Epstein FH, Gilchrest BA, Eller MS, Geller AC, Yaar M (1999) The pathogenesis of melanoma induced by ultraviolet radiation. New England Journal of Medicine 340: 1341-1348.

28. Pfeifer GP, Besaratinia A (2012) UV wavelength-dependent DNA damage and human non-melanoma and melanoma skin cancer. Photochemical & Photobiological Sciences 11: 90-97.

29. Tornaletti S, Pfeifer GP (1994) Slow repair of pyrimidine dimers at p53 mutation hotspots in skin cancer. Science 263: 1436-1438.

30. Bastien N, Therrien J-P, Drouin R (2013) Cytosine containing dipyrimidine sites can be hotspots of cyclobutane pyrimidine dimer formation after UVB exposure. Photochemical & Photobiological Sciences 12: 1544-1554.

31. Brash DE, Haseltine WA (1982) UV-induced mutation hotspots occur at DNA damage hotspots.

32. de Gruijl FR, van Kranen HJ, Mullenders LH (2001) UV-induced DNA damage, repair, mutations and oncogenic pathways in skin cancer. Journal of Photochemistry and Photobiology B: Biology 63: 19-27.

33. Shibutani S, Takeshita M, Grollman AP (1991) Insertion of specific bases during DNA synthesis past the oxidation-damaged base 8-oxodG.

34. National Cancer Institute and Centers for Disease Control and Prevention. (2009) State Cancer Profiles. U.S. state-level and Oregon county-level incidence data query. Incidence data based on data from the State's Cancer Registry, the SEER November 2008 data submission, and the CDC's National Program of Cancer Registries Cancer Surveillance System (NPCR-CSS) November 2008 and January 2009 data submissions. Retrieved March 29, 2010, from http://statecancerprofiles.cancer.gov/.

35. Centers for Disease Control and Prevention. Melanoma diagnosis rates are the result of a number of different factors, including: race (melanoma affects Caucasians at a much greater rate than other racial groups), type of UV exposure (intermittent versus cumulative exposure), sun protection behaviors in childhood and adulthood, geographic mobility of the population, risk awareness of the population and geography (e.g., latitude and elevation).

36. National Cancer Institute and Centers for Disease Control and Prevention. (2009). State Cancer Profiles. U.S. state-level and Oregon county-level mortality data query. Mortality data based on the National Vital Statistics System public use data file. Retrieved March 29, 2010, from http://statecancerprofiles.cancer.gov/.

37. Horner MJ, Ries, L.A.G., Krapcho, M., Neyman, N., Aminou, R., Howlader, N., Altekruse, S.F., Feuer, E.J., Huang, L., Mariotto, A., Miller, B.A., Lewis, D.R., Eisner, M.P., Stinchcomb, D.G., & Edwards, B.K. (Eds.). (2009) SEER Cancer Statistics Review, 1975-2006, Section 16: Melanoma of the Skin. Based on November 2008 SEER data submission, posted to the SEER web site, 2009. National Cancer Institute. Bethesda, MD. Retrieved March 29, 2010, from http://seer.cancer.gov/csr/1975_2006/.

38. Bleyer A, O'Leary, M., Barr, R., & Ries, L.A.G. (Eds.). (2006) Cancer Epidemiology in Older Adolescents and Young Adults 15 to 29 Years of Age, Including SEER Incidence and Survival: 1975-2000. National Cancer Institute, NIH Pub. No. 06-5767. Bethesda, MD. Retrieved March 13, 2009, from http://seer.cancer.gov/publications/aya/.

39. Rigel DS, Friedman, R.J., & Kopf, A.W. (1996) The Incidence of Malignant Melanoma in the United States: Issues as We Approach the 21st Century. Journal of the American Academy of Dermatology, 34(5), 839-847.

40. Pollock PM, Yu F, Qiu L, Parsons PG, Hayward NK (1995) Evidence for uv induction of CDKN2 mutations in melanoma cell lines. Oncogene 11: 663-668.

41. Sharpless N, Chin L (2003) The INK4a/ARF locus and melanoma. Oncogene 22: 3092-3098.

42. Ouelle DE, Zindy F, Ashmun RA, Sherr CJ (1995) Alternative reading frames of the< i> INK4a</i> tumor suppressor gene encode two unrelated proteins capable of inducing cell cycle arrest. Cell 83: 993-1000.

43. Serrano M, Hannon GJ, Beach D (1993) A new regulatory motif in cell-cycle control causing specific inhibition of cyclin D/CDK4. Nature 366: 704-707.

44. Recio JA, Noonan FP, Takayama H, Anver MR, Duray P, et al. (2002) Ink4a/arf deficiency promotes ultraviolet radiation-induced melanomagenesis. Cancer Res 62: 6724-6730.

45. Rane SG, Cosenza SC, Mettus RV, Reddy EP (2002) Germ line transmission of the Cdk4R24C mutation facilitates tumorigenesis and escape from cellular senescence. Mol Cell Biol 22: 644-656.

46. Wolfel T, Hauer M, Schneider J, Serrano M, Wolfel C, et al. (1995) A p16INK4a-insensitive CDK4 mutant targeted by cytolytic T lymphocytes in a human melanoma. Science 269: 1281-1284.

47. Zuo L, Weger J, Yang Q, Goldstein AM, Tucker MA, et al. (1996) Germline mutations in the p16INK4a binding domain of CDK4 in familial melanoma. Nat Genet 12: 97-99.

48. Sotillo R, García JF, Ortega S, Martín J, Dubus P, et al. (2001) Invasive melanoma in Cdk4-targeted mice. Proceedings of the National Academy of Sciences 98: 13312-13317.

49. Cantwell-Dorris ER, O'Leary JJ, Sheils OM (2011) BRAFV600E: implications for carcinogenesis and molecular therapy. Molecular cancer therapeutics 10: 385-394.

50. Poulikakos PI, Persaud Y, Janakiraman M, Kong X, Ng C, et al. (2011) RAF inhibitor resistance is mediated by dimerization of aberrantly spliced BRAF (V600E). Nature 480: 387-390.

51. Kwong LN, Costello JC, Liu H, Jiang S, Helms TL, et al. (2012) Oncogenic NRAS signaling differentially regulates survival and proliferation in melanoma. Nat Med 18: 1503-1510.

52. Jakob JA, Bassett RL, Ng CS, Curry JL, Joseph RW, et al. (2012) NRAS mutation status is an independent prognostic factor in metastatic melanoma. Cancer 118: 4014-4023.

53. Hyter S, Indra AK (2013) Nuclear hormone receptor functions in keratinocyte and melanocyte homeostasis, epidermal carcinogenesis and melanomagenesis. FEBS Lett 587: 529-541.

54. Dave VP, Kaul D (2010) Coronary heart disease: Significance of liver X receptor α genomics. World journal of cardiology 2: 140.

55. Bourguet W, Germain P, Gronemeyer H (2000) Nuclear receptor ligand-binding domains: three-dimensional structures, molecular interactions and pharmacological implications. Trends Pharmacol Sci 21: 381-388.

56. Giguere V, Ong ES, Segui P, Evans RM (1987) Identification of a receptor for the morphogen retinoic acid. Nature 330: 624-629.

57. Petkovich M, Brand NJ, Krust A, Chambon P (1987) A human retinoic acid receptor which belongs to the family of nuclear receptors. Nature 330: 444-450.

58. Mangelsdorf DJ, Ong ES, Dyck JA, Evans RM (1990) Nuclear receptor that identifies a novel retinoic acid response pathway. Nature 345: 224-229.

59. Heyman RA, Mangelsdorf DJ, Dyck JA, Stein RB, Eichele G, et al. (1992) 9-cis retinoic acid is a high affinity ligand for the retinoid X receptor. Cell 68: 397-406.

60. Simpson RU, DeLuca HF (1980) Characterization of a receptor-like protein for 1,25-dihydroxyvitamin D3 in rat skin. Proc Natl Acad Sci U S A 77: 5822-5826.

61. Forman BM, Tontonoz P, Chen J, Brun RP, Spiegelman BM, et al. (1995) 15-Deoxy-delta 12, 14-prostaglandin J2 is a ligand for the adipocyte determination factor PPAR gamma. Cell 83: 803-812.

62. Kliewer SA, Sundseth SS, Jones SA, Brown PJ, Wisely GB, et al. (1997) Fatty acids and eicosanoids regulate gene expression through direct interactions with peroxisome proliferator-activated receptors alpha and gamma. Proc Natl Acad Sci U S A 94: 4318-4323.

63. Janowski BA, Willy PJ, Devi TR, Falck JR, Mangelsdorf DJ (1996) An oxysterol signalling pathway mediated by the nuclear receptor LXR alpha. Nature 383: 728-731.

64. Leid M, Kastner P, Lyons R, Nakshatri H, Saunders M, et al. (1992) Purification, cloning, and RXR identity of the HeLa cell factor with which RAR or TR heterodimerizes to bind target sequences efficiently. Cell 68: 377-395.

65. Orlov I, Rochel N, Moras D, Klaholz BP (2012) Structure of the full human RXR/VDR nuclear receptor heterodimer complex with its DR3 target DNA. EMBO J 31: 291-300.

66. Glass CK, Rosenfeld MG (2000) The coregulator exchange in transcriptional functions of nuclear receptors. Genes Dev 14: 121-141.

67. Perissi V, Rosenfeld MG (2005) Controlling nuclear receptors: the circular logic of cofactor cycles. Nat Rev Mol Cell Biol 6: 542-554.

68. Dilworth FJ, Fromental-Ramain C, Yamamoto K, Chambon P (2000) ATP-driven chromatin remodeling activity and histone acetyltransferases act sequentially during transactivation by RAR/RXR In vitro. Mol Cell 6: 1049-1058.

69. Rachez C, Lemon BD, Suldan Z, Bromleigh V, Gamble M, et al. (1999) Ligand-dependent transcription activation by nuclear receptors requires the DRIP complex. Nature 398: 824-828.

70. Underhill C, Qutob MS, Yee SP, Torchia J (2000) A novel nuclear receptor corepressor complex, N-CoR, contains components of the mammalian SWI/SNF complex and the corepressor KAP-1. J Biol Chem 275: 40463-40470.

71. Lee CH, Wei LN (1999) Characterization of receptor-interacting protein 140 in retinoid receptor activities. J Biol Chem 274: 31320-31326.

72. Hermanson O, Glass CK, Rosenfeld MG (2002) Nuclear receptor coregulators: multiple modes of modification. Trends Endocrinol Metab 13: 55-60.

73. Puigserver P, Wu Z, Park CW, Graves R, Wright M, et al. (1998) A cold-inducible coactivator of nuclear receptors linked to adaptive thermogenesis. Cell 92: 829-839.

74. Chakravarti N, Lotan R, Diwan AH, Warneke CL, Johnson MM, et al. (2007) Decreased expression of retinoid receptors in melanoma: entailment in tumorigenesis and prognosis. Clin Cancer Res 13: 4817-4824.

75. Hyter S, Bajaj G, Liang X, Barbacid M, Ganguli-Indra G, et al. (2010) Loss of nuclear receptor RXRalpha in epidermal keratinocytes promotes the formation of Cdk4-activated invasive melanomas. Pigment Cell Melanoma Res 23: 635-648.

76. Indra AK, Castaneda E, Antal MC, Jiang M, Messaddeq N, et al. (2007) Malignant transformation of DMBA/TPA-induced papillomas and nevi in the skin of mice selectively lacking retinoid-X-receptor alpha in epidermal keratinocytes. J Invest Dermatol 127: 1250-1260.

77. Denning MF (2012) Specifying protein kinase C functions in melanoma. Pigment Cell Melanoma Res 25: 466-476.

Figure 1.1: UVR-induced DNA damage responses in control (CT) and *Rxrα*$^{ep-/-}$ neonatal mouse skin.

(a) Ex vivo immunohistochemical (IHC) analysis of DNA damage in dorsal skin by detecting formation of cyclopyrimidine thymine dimers (CPDs) (red). (b) Co-IHC labeling of oxidative DNA damage (8-oxo-dG, red) and green labeled TRP2+ (aka DCT, TYRP2) melanocytes in skin. Yellow (merged panel) shows TRP2+/8-oxo-dG+ cells, indicating melanocytes with incorporated oxidative DNA damage. D, dermis; E, epidermis; RXRα, retinoid X receptor-α. Bar = 15.6 μm.

Data excerpted from:

"RXRα Ablation in Epidermal Keratinocytes Enhances UVR-Induced DNA Damage, Apoptosis, and Proliferation of Keratinocytes and Melanocytes"

Zhixing Wang, Daniel J. Coleman, Gaurav Bajaj, Xiaobo Liang,
Gitali Ganguli-Indra and Arup K. Indra

Journal of Investigative Dermatology
Published October 14, 2010
JID 131(1):177-187
doi: 10.1038/jid.2010.290

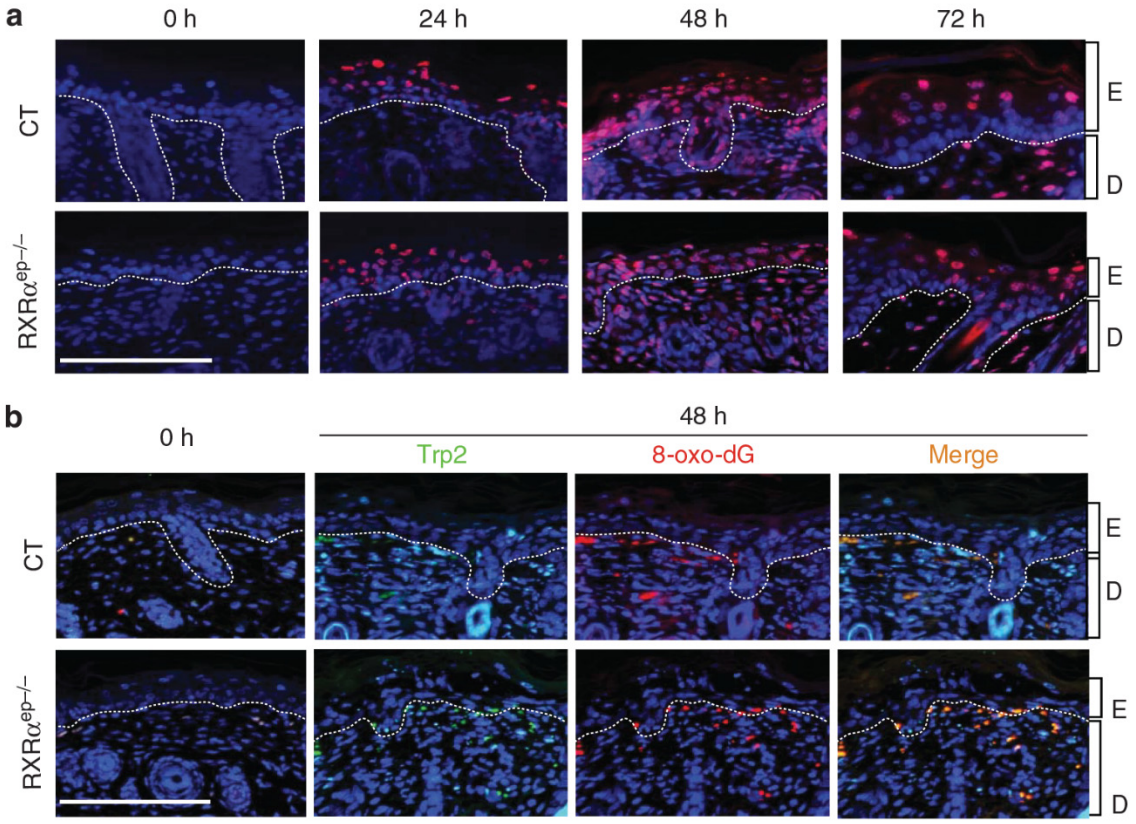

Figure 1.1

Figure 1.2: Effects of keratinocytic RXRα on melanocyte proliferation after UV exposure.

(a) Co-IHC staining for proliferating melanocytes using proliferation marker PCNA (green) and melanocyte-specific marker TRP1 (aka TYRP1) (red). Nuclei were labeled with DAPI (blue). Arrows indicate epidermal melanocytes. An overall increase in proliferating melanocytes over controls (CT) was observed in *Rxrα*$^{ep-/-}$ mice 48 h post-UVR. (b) Fontana–Masson staining for melanin pigment in CT and *Rxrα*$^{ep-/-}$ skin. Nuclei (pink-red), cytoplasm (pink), and melanin-producing melanocytes (black) are indicated. Arrows indicate melanin-producing melanocytes in dermis. Bar = 15.6 μm. Counts of melanocytes in CT and *Rxrα*$^{ep-/-}$ (c) epidermis and (d) dermis at different time points. More epidermal and total extrafollicular melanocytes were observed in *Rxrα*$^{ep-/-}$ skin over CT, particularly at 48 h post-UVR. (e) Proliferation assay of primary melanocytes 24 hours after culture in keratinocyte-derived conditioned medium (KM). KM enhanced proliferation of melanocytes, this effect was greater when using *Rxrα*$^{ep-/-}$ KM, and more so when using KM from *Rxrα*$^{ep-/-}$ keratinocytes exposed to UVR. Statistical analyses were performed by two-tailed unpaired t-test and corrected with Bonferroni step-down analysis using GraphPad Prism software; *P<0.1; **P<0.05; # = no statistical difference.

Data excerpted from:

"RXRα Ablation in Epidermal Keratinocytes Enhances UVR-Induced DNA Damage, Apoptosis, and Proliferation of Keratinocytes and Melanocytes"

Zhixing Wang, Daniel J. Coleman, Gaurav Bajaj, Xiaobo Liang,
Gitali Ganguli-Indra and Arup K. Indra

Journal of Investigative Dermatology
Published October 14, 2010
JID 131(1):177-187
doi: 10.1038/jid.2010.290

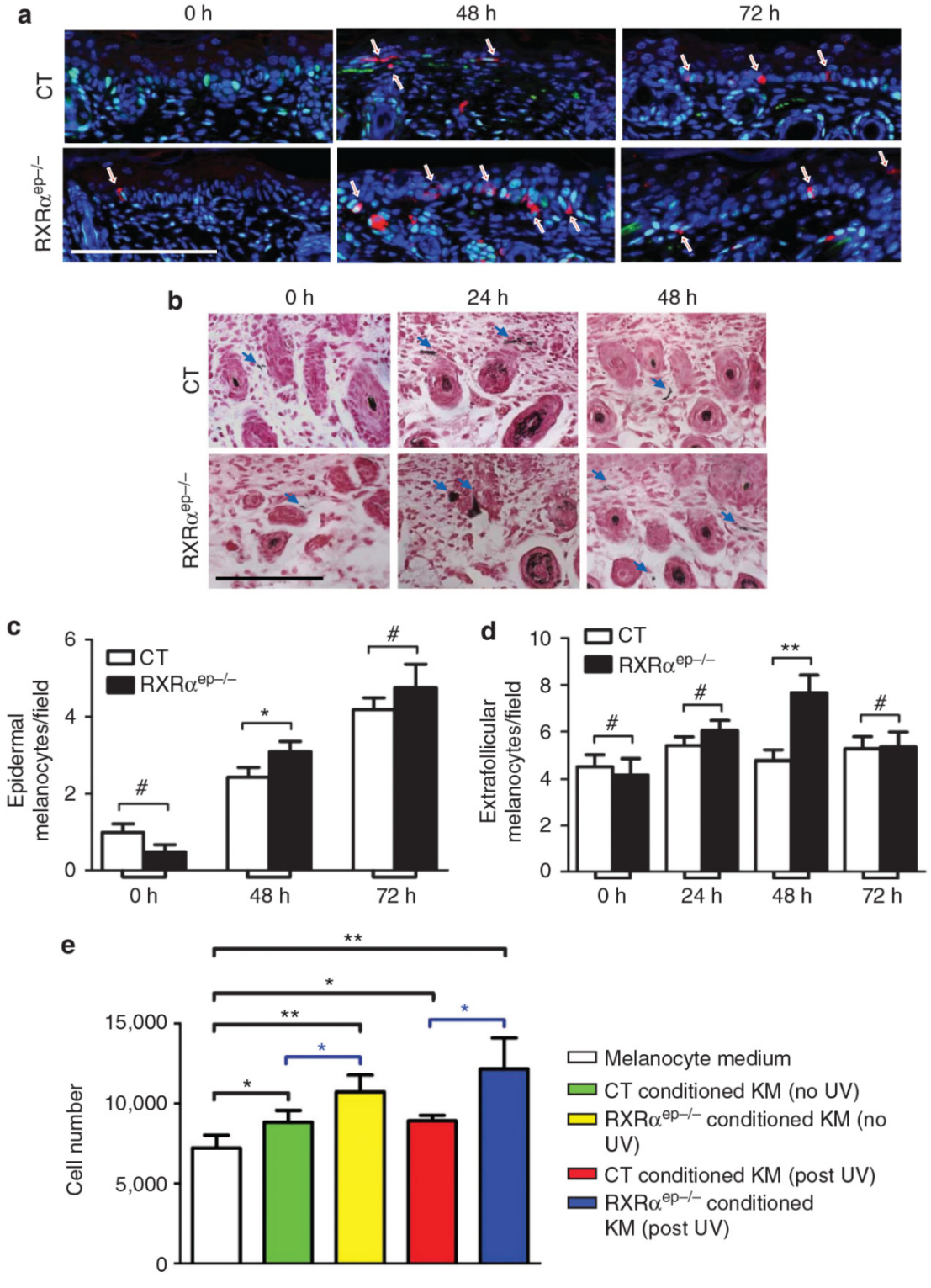
a
0 h
48 h
72 h
CT
RXRα^ep−/−
b
0 h
24 h
48 h
CT
RXRα^ep−/−
c
Epidermal melanocytes/field
CT
RXRα^ep−/−
0 h
48 h
72 h
d
Extrafollicular melanocytes/field
CT
RXRα^ep−/−
0 h
24 h
48 h
72 h
e
Cell number
Melanocyte medium
CT conditioned KM (no UV)
RXRα^ep−/− conditioned KM (no UV)
CT conditioned KM (post UV)
RXRα^ep−/− conditioned KM (post UV)

Figure 1.2

Figure 1.3: Quantitative RT-PCR analysis of expression of paracrine factors in skin of CT and *Rxrα*$^{ep-/-}$ (MT) mice.

Relative expression levels of (a) ET-1 (aka EDN1), FGF2; and (b) POMC, SCF at different time points after UVR are indicated. Known melanocyte mitogens ET-1, FGF2, and SCF were all significantly upregulated in *Rxrα*$^{ep-/-}$ skin both pre- and post-UVR. Values represent relative transcript level after normalization with HPRT transcripts. *P<0.2; **P<0.05; # = no statistical difference between CT and *Rxrα*$^{ep-/-}$ mice.

Data excerpted from:

"RXRα Ablation in Epidermal Keratinocytes Enhances UVR-Induced DNA Damage, Apoptosis, and Proliferation of Keratinocytes and Melanocytes"

Zhixing Wang, Daniel J. Coleman, Gaurav Bajaj, Xiaobo Liang,
Gitali Ganguli-Indra and Arup K. Indra

Journal of Investigative Dermatology
Published October 14, 2010
JID 131(1):177-187
doi: 10.1038/jid.2010.290

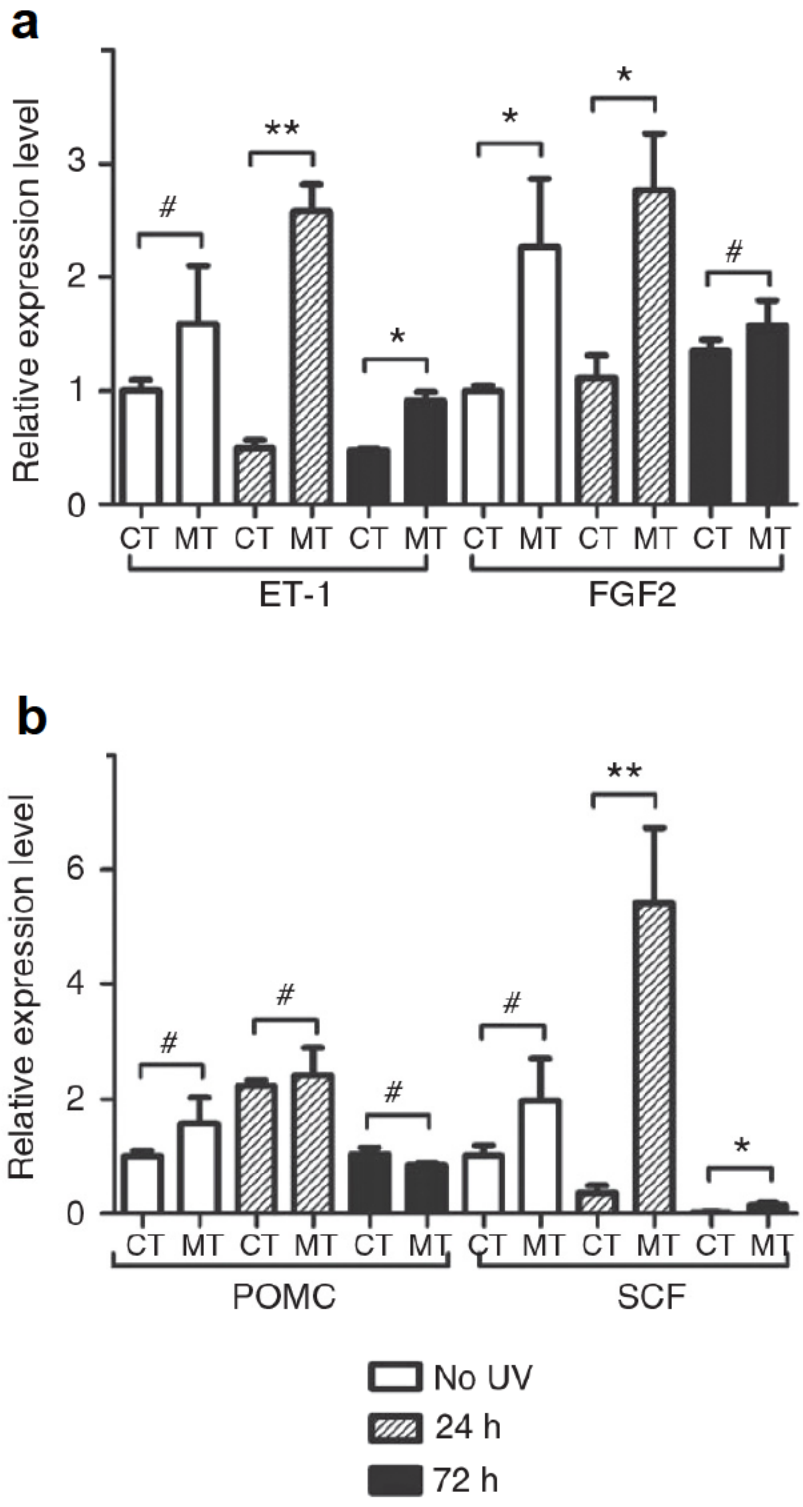
a
Relative expression level
0
1
2
3
#
**
*
*
*
#
CT MT CT MT CT MT CT MT CT MT CT MT
ET-1
FGF2
b
Relative expression level
0
2
4
6
#
#
#
#
**
*
CT MT CT MT CT MT CT MT CT MT CT MT
POMC
SCF
No UV
24 h
72 h

Figure 1.3

Figure 1.4: Activation of MAPK and PKC signaling by EDN1 is specific to EDNRB receptor.

(A) Immunoblot analysis of EDNRB receptor expression in lysates from primary murine keratinocytes [KC] and melanocytes [MC]. Both cell types express EDNRB. β-actin was used as a loading control. (B) Immunoblot analysis for ERK phosphorylation in melanocytes, a marker of MAPK pathway activation. Addition of exogenous EDN1 to minimal melanocyte growth medium results in ERK phosphorylation, which is abrogated by co-treatment with the EDNRB antagonist BQ788, demonstrating that the observed ERK activation is specifically via the EDNRB receptor. Total ERK and β-actin levels were used as loading controls. (C) Exogenous EDN1 also activates PKC, this is abrogated by co-treatment with BQ788, demonstrating that PKC activation by EDN1 is specific to the EDNRB receptor. All experiments were performed in triplicate and PKC activation results are expressed as mean ±SEM. (D) Real-time transwell migration assay comparing slopes for exponential phase of wild-type melanocytes. Exogenous EDN1 addition stimulates melanocyte migration. Results are expressed as mean ±SEM. All statistical analyses were performed using GraphPad Prism, ** = $P < 0.01$, *** = $P < 0.001$. For B-D, minimal growth medium with no additives was used as a negative control; a complete medium rich in melanocyte growth factors was used as positive control.

Data excerpted from:

"Endothelin-1 is a Transcriptional Target of p53 in Epidermal Keratinocytes and Regulates UV Induced Melanocyte Homeostasis"

Stephen Hyter, Daniel J. Coleman, Steven Ma, Masashi Yanagisawa, Gary F. Merrill, Gitali Ganguli-Indra and Arup K. Indra

Pigment Cell and Melanoma Research
Published October 13, 2012
PCMR 26(2):247-258
doi: 10.1111/pcmr.12063

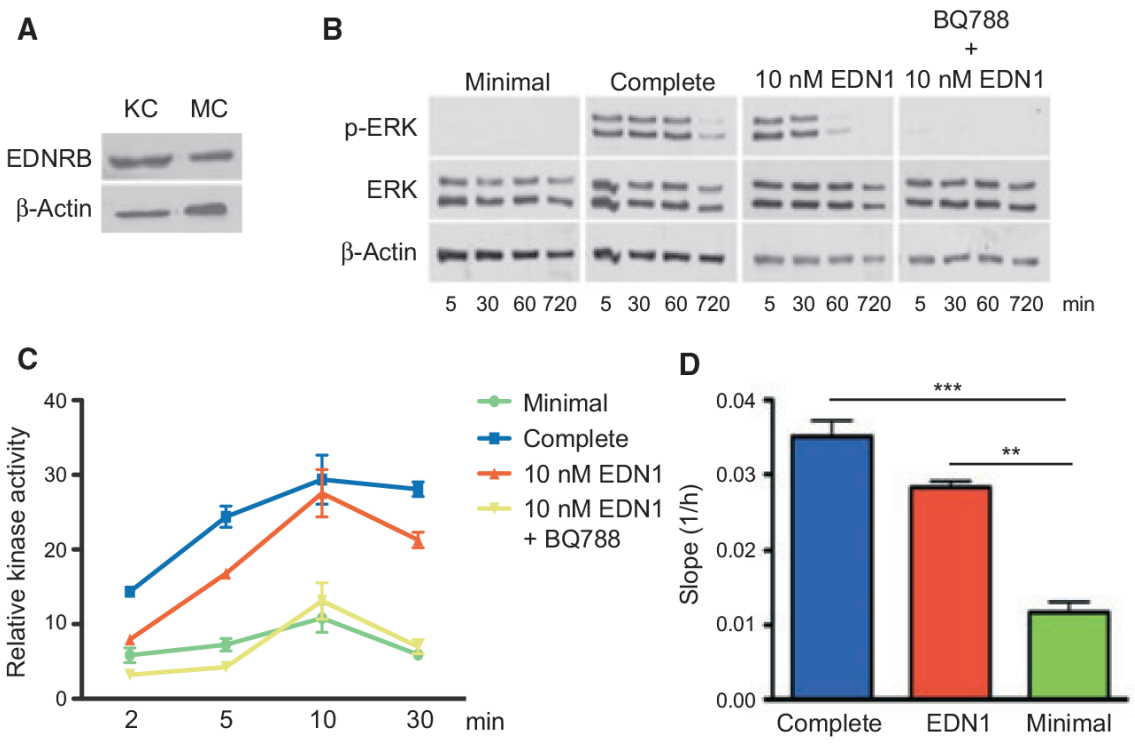
A
KC
MC
EDNRB
β-Actin
B
Minimal
Complete
10 nM EDN1
BQ788 + 10 nM EDN1
p-ERK
ERK
β-Actin
5 30 60 720 5 30 60 720 5 30 60 720 5 30 60 720 min
C
Relative kinase activity
40
30
20
10
0
2
5
10
30
min
Minimal
Complete
10 nM EDN1
10 nM EDN1 + BQ788
D
Slope (1/h)
0.04
0.03
0.02
0.01
0.00
***
**
Complete
EDN1
Minimal

Figure 1.4

Loss of keratinocytic *Rxrα* combined with activated *Cdk4* or oncogenic *NRAS* generates UVB-induced melanomas via loss of p53 and PTEN in the tumor microenvironment

Chapter 2

Daniel J. Coleman, Sharmeen Chagani, Stephen Hyter, Anna M. Sherman, Christiane V. Löhr, Xiaobo Liang, Gitali Ganguli-Indra and Arup K. Indra

Under Revision, Molecular Cancer Research

Submitted March 24, 2014

2.1 Abstract

Understanding the molecular mechanisms behind formation of melanoma, the deadliest form of skin cancer, is crucial for improved diagnosis and treatment. One key is better understanding of the cross-talk between epidermal keratinocytes and pigment-producing melanocytes. Here we report that in a bigenic mouse model, combining either activating *Cdk4* (*R24C*) or oncogenic NRAS (*Q61K*) mutations with an epidermis-specific knockout of *Rxrα* expression ($Rxr\alpha^{ep-/-}$) results in formation of larger, more proliferative and aggressive melanomas after chronic ultraviolet-B irradiation compared to control mice with functional *Rxrα*. Melanomas from bigenic $Rxr\alpha^{ep-/-}$ mice also exhibit enhanced angiogenic properties and increased expression of malignant melanoma markers. Analysis of tumor adjacent normal skin from these mice reveals altered expression of several biomarkers indicative of melanoma susceptibility; including reduced expression of tumor suppressor p53 and PTEN loss with concomitant increase in AKT activation. These results suggest a crucial role of keratinocytic RXRα to suppress formation of UVB-induced melanomas and their progression to malignant, metastatic cancers in the context of tumor-driving mutations such as activated CDK4 ($Cdk4^{R24C/\ R24C}$) or oncogenic $NRAS^{Q61K}$.

2.2 Introduction

Malignant melanoma is the deadliest form of skin cancer, and ultraviolet (UV) radiation plays an important role in most cases. Therefore, understanding the molecular mechanisms behind UV-induced melanoma formation is crucial for determining new pathways that can be manipulated for diagnosis and therapeutic targeting. Retinoid-X-Receptors (RXRs) α, β, and γ are members of the nuclear hormone receptor (NR) superfamily, and have a complex and dynamic role in regulation of cellular processes. RXRs function as a ubiquitous DNA-binding transcription factor via ligand binding [1,2] and promiscuous heterodimerization with other NRs [1,3]; by interacting with several transcriptional coactivators and/or corepressors they can regulate gene expression via multiple signaling pathways [1]. Previously we established that RXRα ablation in keratinocytes (cells comprising skin epidermis) alters paracrine signals to the melanocytes (pigment producing cells in the skin) and can enhance melananomagenesis [4,5]. Mice with epidermis-specific *Rxrα* knockout ($Rxr\alpha^{ep-/-}$) show increased melanocyte proliferation and defective DNA damage repair following acute ultraviolet-B (UVB) irradiation [4]; and have increased melanocytic tumor formation resulting from chemical carcinogenesis [5,6]. Expression of several mitogenic factors are upregulated in keratinocytes lacking RXRα, including Endothelin-1 (EDN1), Stem Cell Factor (SCF), Microphthalmia-associated Transcription Factor (MITF), and Hepatocyte Growth Factor (HGF) [4,5,7]; which stimulate melanocyte activation/proliferation *in vitro* [4,7]. We also found that combining epidermis-specific RXRα knockout with an oncogenic CDK4 mutation

(R24C) in a bigenic mouse model further enhanced chemical carcinogen-induced melanomagenesis [5]. This suggests that keratinocytic RXRα loss cooperates with common oncogenes to enhance melanomagenesis. Analyses performed on human melanomas collected at different stages of disease progression revealed progressive loss of RXRα protein as tumors progress from benign nevi to *in situ* and metastatic lesions [5]; affirming it as a viable biomarker of melanoma progression and potential therapeutic target for melanoma treatment in humans.

UV radiation exposure is a major risk factor for formation of melanomas and other skin cancers (American Cancer Society, 2013). Being a more biologically-relevant model of melanoma than chemical carcinogenesis, in this study we aimed to investigate a mechanistic role for keratinocytic RXRα in UVB-induced melanomagenesis. *Rxrα*$^{ep-/-}$ mice were combined with either oncogenic *NRAS (NRAS*^{Q61K}*)* or activated *Cdk4 (Cdk4*$^{R24C/R24C}$*)* mutations to elucidate the role of RXRα loss in UVB-induced melanomas in combination with aberrant signaling pathways. The CDK4 pathway (p16-cyclin D-CDK4/6-retinoblastoma protein pathway) is reported to be dysregulated in 90% of human melanomas [8], while *NRAS* gene mutations are detected in 15-20% [9].

We observed that keratinocytic *Rxrα* ablation combined with either *Cdk4*$^{R24C/R24C}$ or *NRAS*^{Q61K} mutations resulted in increased number/size of UVB-induced melanocytic tumors compared to control *Cdk4*$^{R24C/R24C}$ or *NRAS*^{Q61K} mice with functional RXRα (*Rxrα*$^{L2/L2}$). Melanomas from bigenic *Rxrα*$^{ep-/-}$ mice were more proliferative and showed increased labeling for malignant conversion and tumor angiogenesis markers. We also observed increased lymph node

metastasis of melanocytic cells in bigenic *Rxrα*$^{ep-/-}$ mice. The tumors also had altered expression of several genes implicated in mouse cancer compared to corresponding *Rxrα*$^{L2/L2}$ control samples. Additionally, the tumor adjacent normal (TAN) skin of UVB-treated bigenic *Rxrα*$^{ep-/-}$ mice showed dysregulated expression of several melanoma biomarkers. Particularly, we observed reduced Phosphatase and Tensin Homolog (PTEN) protein and concomitant increase in the phosphorylated, active form of its downstream effector AKT; in addition to reduced expression of p53. These results suggest that loss of keratinocytic RXRα both promotes and enhances formation of UVB-induced malignant melanomas. Therefore epidermal RXRα expression may represent a new potential biomarker for diagnosis and treatment of UVB-induced melanomas in humans.

2.3 Materials and Methods

Mice

Generation of *Rxrα*$^{ep-/-}$ [10], *Cdk4*$^{R24C/R24C}$ [11], and *Tyr-NRAS*^{Q61K} [12] mice have been described previously. Mice were housed in our approved University Animal Facility with 12-h light cycles, food/water were provided ad libitum, and institutional approval was granted for all experiments via an Animal Care and Use Protocol (ACUP).

UVR treatment of mice

Age- and sex-matched (female) P2 mice were exposed to a single dose of 800 mJ/cm^2 of UVB light from a bank of four Philips FS-40 UV sunlamps [4]. Upon weaning (21 days postnatal), dorsal skin was shaved weekly and exposed to chronic doses of 320 mJ/cm^2, 3X weekly for 30 weeks [13]. For negative controls, parallel groups of mice were shaved but not UVB-treated. At the conclusion of 30 weeks, melanocytic lesions were quantitated, and biopsies of lesions and tumor adjacent normal (TAN) skin were collected for analyses. This experiment was repeated independently twice with at least five mice per group.

Histological analyses

Analyses were performed on 5 μm formalin-fixed paraffin sections. Prior to all procedures, sections were deparaffinized in xylene and rehydrated using graded alcohols. Sections were stained with hematoxylin and eosin (H&E) as previously described [6]. Fontana-Masson and Combined eosinophil/mast cell stain (CEM)

procedures were performed using commercial kits (American MasterTech) according to the manufacturer's protocol. Prior to CEM staining, melanin pigment was removed by treating slides with a 10% H_2O_2 solution in 1X PBS for 25 minutes at 60°C. Slides were cleared in xylene and mounted in DPX mounting medium.

Immunohistochemistry

5 µm thick sections were deparaffinized and rehydrated as described above. All slides were treated with 10% H_2O_2 in 1X PBS for 25 minutes at 60°C to remove melanin pigment. Antigen retrieval was performed in a 95°C-100°C bath for 20 minutes, using either Tris-EDTA buffer (pH 9.0) for metastatic melanoma antibody cocktail HMB45 + MART1, or citrate buffer (pH 6.0) for all other antigens. All sections were then washed three times with 0.05% PBS-Tween (PBST), and blocked with 10% normal goat serum in PBST for 30 minutes to block nonspecific antibody binding. Sections were then incubated overnight with primary antibody at 4°C. Primary antibody incubation was followed by three washes with PBS-Tween before addition of either biotin or fluorophore-conjugated secondary antibodies, which were incubated on the sections for 2 hours at room temperature. For fluorescent IHC, nuclei were counterstained with DAPI (200 ng/mL) for 10 minutes at room temperature. For chromogenic IHC, sections were incubated with streptavidin-horseradish peroxidase (Vector Laboratories) for 30 minutes at room temperature, signal developed with DAB peroxidase substrate kit (Vector Laboratories), and counterstained with

hematoxylin (1:1 in H_20) for 15 minutes at room temperature. Finally, sections were rinsed with PBST (fluorescent IHC) or running tap water (chromogenic IHC), dehydrated through sequential alcohol washes and then cleared in xylene. Slides were mounted with DPX mounting medium. Antibodies used are detailed in Table 2.1. Sections stained without primary antibody was used as negative controls, and all experiments were performed in triplicates.

Imaging and quantitation of histological experiments

Brightfield images were captured with a Leica DME light microscope using the Leica Application Suite software, version 3.3.1. Fluorescent images were captured using a Zeiss AXIO Imager.Z1 with a digital AxioCam HRm and processed using AxioVision 4.8 and Adobe Photoshop. Quantifications of cell labeling were performed using ImageJ software (NIH), multiple fields imaged from several replicate mice in all groups were randomly chosen and 20 fields per group were counted. The slides were analyzed independently in a double-blinded manner by two investigators and significance was determined using a Student's two-tailed t-test as calculated by GraphPad Prism software.

Laser Capture Microdissection (LCM) and RNA isolation from melanoma tissue

Melanocytic lesions embedded in OCT (fresh, not fixed) were sectioned at 14 μm using a cryostat. Blocks were kept on dry ice prior to sectioning. One section was affixed per glass slide, and slides were immediately placed on dry ice, stored at -80°C long term, and kept on dry ice until immediately before LCM. Sections

were dehydrated through sequential washes of cold alcohol followed by cold xylene. LCM was performed using a Zeiss PALM MicroBeam laser microdissection system; tissue was collected from five individual sections from each lesion and pooled. RNA was isolated using an Arcturus Pico Pure RNA Isolation Kit according to manufacturer's protocol.

RT-qPCR analysis of gene expression in melanoma tissue isolated by LCM

Equal amounts of RNA from five distinct lesions from each group (each from a different animal) were pooled and converted to cDNA using a RT^2 PreAMP cDNA Synthesis Kit (SA Biosciences/Qiagen) according to manufacturer's protocol. cDNAs were applied to an SA Biosciences/Qiagen RT^2 Profiler PCR Array (Mouse Cancer, PAMM-033Z). Triplicate arrays were run for each group, and data analyses performed using SA Biosciences web-based software.

Immunoblotting analyses

Protein lysates were obtained by homogenizing tissue in lysis buffer (20 mM HEPES, 250 mM NaCl, 2 mM EDTA, 1% SDS, 10% glycerol, 50 mM NaF, 0.1mM hemin chloride, 5 mM NEM, 1 mM PMSF and 10 mg/mL leupeptin and aproptinin) [4,14,15] followed by sonication. Protein concentration was performed using the BCA assay (Thermo Scientific). Protein lysates were resolved using SDS-PAGE gel electrophoresis and transferred onto a nitrocellulose membrane. The blots were blocked overnight with 5% non-fat dry milk and incubated with specific antibodies (detailed in Table 2.1). After

incubation with appropriate secondary antibody, signals were detected using immunochemiluminescent reagents (GE Healthcare, Piscataway, NJ). Equal protein loading in each lane was confirmed with a β-actin antibody (#A300-491, Bethyl).

2.4 Results

Loss of keratinocytic *Rxrα* expression in cooperation with activated *Cdk4* or oncogenic *NRAS* mutations results in increased UVB-induced melanoma formation

Our previous studies indicated that loss of keratinocytic RXRα protein has a role in melanocyte homeostasis and melanomagenesis, as observed in mouse models with epidermis-specific knockout of *Rxrα* (*Rxrα*$^{ep-/-}$) [4-6] and human melanoma samples [5]. Therefore we hypothesized that loss of keratinocytic *Rxrα* expression would result in enhanced malignant melanoma formation from chronic UVB-irradiation, in combination with activated *Cdk4*$^{R24C/R24C}$ or melanocyte-specific expression of oncogenic human *NRAS* (*Tyr-NRAS*^{Q61K}) in a bigenic mouse model.

To that end, *Rxrα*$^{ep-/-}$ mice were bred to either *Cdk4*$^{R24C/R24C}$ or *Tyr-NRAS*^{Q61K} mice to generate *Rxrα*$^{ep-/-}$ | *Cdk4*$^{R24C/R24C}$ and *Rxrα*$^{ep-/-}$ | *Tyr-NRAS*^{Q61K} bigenic mice, respectively. *Rxrα*$^{L2/L2}$ | *Cdk4*$^{R24C/R24C}$ and *Rxrα*$^{L2/L2}$ | *Tyr-NRAS*^{Q61K} mice (floxed *Rxrα* mice containing LoxP sites flanking exon 4) were used as controls for wild-type *Rxrα* function. Here onwards, homozygous *Cdk4*$^{R24C/R24C}$ mutation will be simply referred to as *Cdk4*^{R24C}. Cohorts of neonatal (P2) mice from each group were irradiated with a single large dose of UVB, followed by 3X weekly doses of UVB (2X minimal erythemal dose) for 30 weeks and monitored periodically for formation of melanocytic tumors (Figure 2.1 A) [13].

Phenotypically, overall skin coloration of adult homozygous *Cdk4*^{R24C} mice was distinct from those expressing oncogenic *Tyr-NRAS*^{Q61K}. The *Tyr-NRAS*^{Q61K} mice have heavily pigmented skin throughout (Figure 2.1 B) compared to skin of

Cdk4^{R24C} mice (Figure 2.1 C), making it difficult to quantitate smaller melanocytic lesions. Only larger (>2 mm) lesions in *Rxrα*$^{ep-/-}$ | *Tyr-NRAS*^{Q61K} mice could be quantitated; as they were raised at that size due to the presence of a follicular cyst underneath. Dermal cysts are another phenotype of epidermal *Rxrα* ablation [10], resulting from degenerate hair follicles, and were also found within the lesions from *Rxrα*$^{ep-/-}$ | *Cdk4*^{R24C} mice.

Both bigenic *Rxrα*$^{ep-/-}$ mouse lines developed higher numbers of melanocytic lesions, most of which were larger in size (>2 mm), compared to mice with functional *Rxrα* expression (Figure 2.1 B, C, F, G). The *Rxrα*$^{ep-/-}$ lesions were also more densely pigmented (Figure 2.1 D, E) and showed enhanced penetration into the epidermal basal layer (Figure 2.1 D, E (inset)). Histological analysis confirmed that the melanocytic lesions (>2 mm) from both bigenic mouse lines are melanomas with hallmarks of round and/or spindle cell tumors. Cohorts of *Rxrα*$^{L2/L2}$ and *Rxrα*$^{ep-/-}$ mice without *Cdk4*^{R24C} or *Tyr-NRAS*^{Q61K} mutations were treated identically with chronic UVB and did not develop any melanocytic lesions after end of treatment (data not shown). Additionally, bigenic mice from each group were shaved weekly without any UVB treatment to monitor spontaneous melanoma formation and did not develop any lesions (data not shown). Altogether, our results suggest that loss of epidermal *Rxrα* expression in combination with oncogenic NRAS or activated CDK4 enhances UVB-induced melanomagenesis.

Increased proliferation, malignant conversion, and enhanced angiogenesis in melanomas from mice lacking keratinocytic *Rxrα* expression

We employed immunohistochemical (IHC) analyses in order to characterize the melanomas formed after chronic UVB exposure. We aimed to elucidate the differences between melanomas from bigenic $Rxr\alpha^{ep-/-}$ | $Tyr\text{-}NRAS^{Q61K}$ and $Rxr\alpha^{ep-/-}$ | $Cdk4^{R24C}$ mice and their corresponding $Rxr\alpha^{L2/L2}$ controls. Fluorescent IHC was performed on sections from melanocytic lesions. To characterize immune cell infiltration, IHC was performed to label MAC1+ macrophages (Figure 2.S1 A-D) and CD4+ T-cells (Figure 2.S1 E-H). A significant increase in infiltration of MAC1+ macrophages was observed specifically in melanomas from $Rxr\alpha^{ep-/-}$ | $Cdk4^{R24C}$ mice compared to their control (Figure 2.S1 C, D). IHC for CD4+ T-cells (Figure 2.S1 E-H) and combined CEM staining for eosinophils/mast cells (Figure 2.S2) did not reveal any changes in either bigenic group. These results suggest specific cooperative effects between epidermal *Rxrα* loss and activated *Cdk4* mutation to alter UVB-induced macrophage response.

Next we co-labeled the lesions for proliferation marker PCNA and melanocyte-specific marker Tyrosinase-Related Protein 1 (TYRP1); an enzyme involved in melanin synthesis [16]. Compared to their controls we observed higher overall proliferation, particularly in PCNA/TYRP1 co-labeled cells, in lesions from bigenic $Rxr\alpha^{ep-/-}$ mice (Figure 2.2 A, B and insets). An antibody cocktail against malignant melanoma antigens (MART1 + HMB45) [17] showed markedly higher staining in melanomas from bigenic $Rxr\alpha^{ep-/-}$ mice (Figure 2.2 C, D). We then labeled for tumor angiogenesis marker CD31 [18]. Although

melanomas from *Rxrα*$^{ep-/-}$ | *Tyr-NRAS*^{Q61K} mice exhibited a similar presence of CD31+ cells compared to controls, there was a higher incidence of larger, more complex CD31+ vasculature (Figure 2.2 E, right panel). Similarly, we observed more intense staining of CD31 in *Rxrα*$^{ep-/-}$ | *Cdk4*^{R24C} melanocytic lesions than in the control group (Figure 2.2 F). Altogether, these results suggest that loss of *Rxrα* expression in the epidermis contributes to enhanced proliferation, malignant conversion, and angiogenesis in UVB-induced melanomas in the context of oncogenic signaling or dysregulated cell-cycle regulators.

Chronic UVB-irradiation results in increased melanoma metastasis to draining lymph nodes in mice lacking keratinocytic *Rxrα* expression

Next we wanted to determine the effects of keratinocytic *Rxrα* loss on metastasis of UVB-induced melanomas. Upon conclusion of the 30 week chronic UVB treatment period, draining inguinal lymph nodes (LNs) were excised from the mice. Fontana-Masson staining for melanin pigment showed increased number of pigment-containing cells in LNs from mice expressing *Tyr-NRAS*^{Q61K} compared to those expressing the activated *Cdk4*^{R24C} gene (Figure 2.3 A). Interestingly, no significant difference in overall pigmentation was observed in *Rxrα*$^{ep-/-}$ LNs compared to their corresponding *Rxrα*$^{L2/L2}$ controls in either group of bigenic mice (Figure 2.3 A). To specifically characterize the presence of melanocytic cells in the LNs, we performed chromogenic IHC for TYRP1 on LN sections from mutant and control mice. While we observed a higher presence of TYRP1+ positive cells in the *Tyr-NRAS*^{Q61K} group compared to the *Cdk4*^{R24C} group, a marked increase in TYRP1+ cells in LNs from both groups was

observed in the *Rxrα*$^{ep-/-}$ mice compared to their *Rxrα*$^{L2/L2}$ controls (Figure 2.3 B). These results suggest that epidermal loss of *Rxrα* expression contributes to formation of UVB-induced melanomas with enhanced metastasis of pigment-producing melanoma cells to distal LNs.

Overlapping and distinct set of genes related to cancer progression are dysregulated in melanomas from *Rxrα*$^{ep-/-}$ | *Tyr-NRAS*^{Q61K} and *Rxrα*$^{ep-/-}$ | *Cdk4*^{R24C} bigenic mice

In order to determine gene signature changes that might cause the observed phenotypic differences between melanomas from bigenic *Rxrα*$^{ep-/-}$ mice compared to *Rxrα*$^{L2/L2}$ controls, we utilized LCM to specifically isolate RNA from pigmented melanoma tissue (Figure 2.4 A). Converted cDNA was then applied to an RT-qPCR array of genes implicated in mouse cancer progression (Qiagen/SA Biosciences PAMM-033Z) (Figures 2.S3, 2.S4). Using a 1.7 fold cutoff, melanomas from both *Rxrα*$^{ep-/-}$|*Tyr-NRAS*^{Q61K} and *Rxrα*$^{ep-/-}$ | *Cdk4*^{R24C} mice exhibited similar upregulation of four gene transcripts relative to corresponding controls (Figure 2.4 B). Three are involved in cell cycle regulation/proliferation: *Mki67* (standard proliferation marker), Aurora Kinase A (*Aurka*, required for G2-M transition [19]) and Cell Division Cycle Protein 20 (*Cdc20*, activates anaphase promoting complex [20]). Additionally, both *Rxrα*$^{ep-/-}$ | *Tyr-NRAS*^{Q61K} and *Rxrα*$^{ep-/-}$ |*Cdk4*^{R24C} melanomas had upregulated angiopoietin 1 (*Angpt1*) expression, which contributes to blood vessel formation/maturation [21]. Interestingly, a single gene was appreciably dysregulated specifically in the *Rxrα*$^{ep-/-}$ | *Tyr-NRAS*^{Q61K} melanomas but not in the *Rxrα*$^{ep-/-}$ | *Cdk4*^{R24C} melanomas; *Tnks2*, associated with

telomere maintenance processes [22], was upregulated (Figure 2.4 B). Additionally, a diverse subset of genes was dysregulated only in *Rxrα*$^{ep-/-}$ | *Cdk4*^{R24C} melanomas but not in the *Rxrα*$^{ep-/-}$ | *Tyr-NRAS*^{Q61K} lesions (Figure 2.4 B, C). They are involved in regulating key cellular processes including microtubule dynamics (*Stmn1* [23]), angiogenesis (*Serpinf1*[24], *Fgf2* [25], and *Pgf* [26]), cell adhesion (*Ocln* [27]), apoptosis (*Bcl2l11* [28], *Casp2* [29], and *Fasl* [30]), chromatin remodeling (*Atrx* [31]), DNA Repair (*Xrcc4* [32]), lipid synthesis/metabolism (*Lpl* [33]), growth factor signaling (*Pgf* [26]) and immune response (*Ccl2* [34], and *Fasl* [30]); as well as ubiquitous transcription factors *Gsc* [35] and *Tbx2* [36] (Figure 2.4 B, C). Overall the above results suggest that epidermal ablation of *Rxrα* expression results in melanomas with altered gene signatures related to promoting proliferation and angiogenesis; and in specific cooperation with activated CDK4 dysregulates an additional set of genes with diverse functions with regard to enhancing melanomagenesis.

Dysregulated melanoma signaling in Tumor Adjacent Normal (TAN) skin from chronic UVB-irradiated mice lacking keratinocytic *Rxrα* expression

Thus far our data suggests that loss of keratinocytic RXRα has a role in enhancing progression of melanocytic tumors to malignant, metastatic lesions. As bigenic *Rxrα*$^{ep-/-}$ mice formed a higher number of chronic UVB-induced melanocytic lesions relative to *Rxrα*$^{L2/L2}$ controls, we next aimed to determine if keratinocytic *Rxrα* loss also leads to phenotypic changes in the skin that enhance susceptibility to UVB-induced melanomas. To that end, we performed IHC and immunoblotting analyses to analyze expression of known biomarkers of

melanoma susceptibility in tumor adjacent normal (TAN) skin from chronic UVB-irradiated bigenic *Rxrα*$^{ep-/-}$ mice and compared them to their controls. We found that ablation of epidermal *Rxrα* expression resulted in reduced protein expression of tumor suppressor Phosphatase and Tensin homolog (PTEN) observed by both chromogenic IHC (Figure 2.5 A-D) and immunoblotting (Figure 2.5 E, F). As expected, we also observed a concomitant increase in Ser473 phosphorylation of its downstream effector AKT without change in total AKT levels (Figure 2.5 G-L). In both bigenic *Rxrα*$^{ep-/-}$ mouse lines we also observed reduced p53 expression in TAN skin; both by IHC (Figure 2.6 A-D) and immunoblotting (Figure 2.6 E-F). Additionally, by immunoblotting we observed upregulation of Cyclin D1 (Figure 2.6 G,H); this protein has been found to be upregulated due to p53 inactivation [37]. IHC revealed that expression of total CDK4 protein in TAN skin was modestly upregulated in both bigenic *Rxrα*$^{ep-/-}$ mouse lines (Figure 2.S5 A-D). Interestingly, phosphorylated-ERK (p-ERK p44/42) was decreased in *Rxrα*$^{ep-/-}$ TAN skin as determined by immunoblotting (Figure 2.S5 E, F), though an increase has been previously correlated with malignant melanoma progression [38]. Expression of transcription factor E2F1, which has been associated with increased melanoma invasiveness [39], was upregulated only in *Rxrα*$^{ep-/-}$|*Cdk4*^{R24C} TAN skin but not in that of *Rxrα*$^{ep-/-}$|*Tyr-NRAS*^{Q61K} mice (Figure 2.S5 G, H). Altogether, these results suggest that loss of keratinocytic *Rxrα* expression and chronic UVB exposure results in altered expression of several key signaling pathways in the melanoma microenvironment that enhance melanoma susceptibility.

2.5 Discussion

We have previously established a role of keratinocytic RXRα in acute UV-induced melanocyte proliferation and in melanomagenesis induced by chemical carcinogenesis [4-6]. As exposure to UV plays a major role in the majority of melanoma cases, we wanted to investigate a mechanism for epidermal RXRα loss in UVB-induced melanomagenesis. Here we used *Rxrα*$^{ep-/-}$ mice combined with oncogenic mutant *NRAS (Q61K)* or activated *Cdk4 (R24C)* to elucidate the role of keratinocytic RXRα protein in promoting chronic UVB-induced melanoma formation and determine cooperativity with oncogenic signaling pathways.

As hypothesized, *Rxrα*$^{ep-/-}$ mice developed more and larger UVB-induced melanocytic tumors in combination with either *Tyr-NRAS*^{Q61K} or *Cdk4*^{R24C} mutations compared to their corresponding *Rxrα*$^{L2/L2}$ controls. Interestingly, we also observed increased penetration of pigmented cells into the epidermal basal layer, possibly due to increased secretion of several mitogenic paracrine growth factors from the keratinocytes as we have reported previously [4,5].

Our LCM gene expression studies corroborate what we observed via immunohistochemistry. mRNA transcripts for several coordinators of cell cycle/proliferation were found to be upregulated in melanocytic tumors from both *Rxrα*$^{ep-/-}$ bigenic mouse lines. We also found enhanced angiogenic properties in tumors from the bigenic *Rxrα*$^{ep-/-}$ mice. Angiogenesis regulator *Angpt1* was upregulated in tumors from both *Rxrα*$^{ep-/-}$ bigenic mouse lines. Three additional genes (*Serpinf1, Fgf, Pgf*) with reported roles in angiogenesis were also altered specifically in *Rxrα*$^{ep-/-}$ | *Cdk4*^{R24C} tumors. We observed a higher degree of

malignancy in melanocytic tumors from both bigenic *Rxrα*$^{ep-/-}$ mouse lines, as well as increased metastasis of TYRP1-expressing melanoma cells to draining lymph nodes. Similar observations of enhanced proliferative, angiogenic, and malignant/metastatic properties were made previously in lesions from DMBA-TPA treated *Rxrα*$^{ep-/-}$ | *Cdk4*^{R24C} mice [5]. All of these results underscore an important role for RXRα in mediating melanocyte proliferation, homeostasis, and angiogenesis and suggest that loss of keratinocytic RXRα contributes to progression of UVB-induced melanocytic lesions to malignant and metastatic tumors. That is further supported by our previous observations in human melanomas that demonstrated progressive loss of RXRα protein levels in adjacent epidermis as lesions progressed from benign nevi to metastatic melanomas [5].

Besides several overlapping observations in *Rxrα*$^{ep-/-}$ | *Tyr-NRAS*^{Q61K} and *Rxrα*$^{ep-/-}$ | *Cdk4*^{R24C} melanocytic tumors, we observed multiple changes specific to the *Rxrα*$^{ep-/-}$ | *Cdk4*^{R24C} group. This suggests that in addition to a general role of keratinocytic RXRα in mediating melanomagenesis, a specific cooperative effect results from combined loss of epidermal RXRα and activated CDK4. CDK4 initiates events leading to accumulation of transcription factor E2F1 and promotes entry into S-phase of the cell cycle [40]. E2F1 has been associated with increased melanoma invasion [39] and used as a biomarker toward sensitivity to MDM2 inhibitors [41]. We observed modest upregulations of total CDK4 protein in *Rxrα*$^{ep-/-}$ TAN skin from both of our bigenic mouse models compared to *Rxrα*$^{L2/L2}$ controls, suggesting that loss of keratinocytic RXRα

contributes to enhanced CDK4 expression. As the *Rxrα*$^{ep-/-}$| *Cdk4*^{R24C} mice are homozygous for the mutant *Cdk4*^{R24C} allele, any upregulated CDK4 expression in these animals is exclusively the mutant, activated CDK4^{R24C} protein; resulting in increased expression levels of activated CDK4 (*Cdk4*^{R24C}) above that of *Rxrα*$^{L2/L2}$| *Cdk4*^{R24C} control mice and potentially further enhancing alterations of downstream targets. Our observation of enhanced E2F1 protein expression in *Rxrα*$^{ep-/-}$ | *Cdk4*^{R24C} TAN skin is unique to that group and not observed in mice expressing oncogenic *NRAS,* supporting this notion. Additionally, we found a diverse set of genes implicated in mouse cancer formation dysregulated only in *Rxrα*$^{ep-/-}$ | *Cdk4*^{R24C} melanocytic lesions and not in the *Tyr-NRAS*^{Q61K} group. Those genes are involved in regulating a multitude of key cellular processes, including ubiquitous transcription factor function; which themselves may control a wide array of downstream processes affecting melanoma formation/progression. Our observation of increased MAC1+ macrophage infiltration exclusively in *Rxrα*$^{ep-/-}$ | *Cdk4*^{R24C} lesions is also supported by the LCM gene expression studies, expression of the macrophage attractant *Ccl2* was upregulated in *Rxrα*$^{ep-/-}$ | *Cdk4*^{R24C} lesions relative to *Rxrα*$^{L2/L2}$ control; this was not observed in melanomas from *Rxrα*$^{ep-/-}$ | *Tyr-NRAS*^{Q61K} mice. CCL2 is a ligand of receptor CCR2, and melanocytes have been reported to secrete CCR2 ligands to attract CCR2+ macrophages into the skin following UVB irradiation [34]. These macrophages secrete interferon-y which promotes post-UV survival of melanocytes [34]. Therefore, a specific cooperative could result from combined loss of epidermal RXRα and activated CDK4, contributing to enhanced

melanoma progression via increased macrophage attraction. More work will need to be undertaken to elucidate the specific cooperative effects of combined epidermal RXRα loss and activated CDK4 in melanomagenesis.

Thus far our results suggest that loss of keratinocytic RXRα can enhance progression of UVB-induced melanocytic lesions to malignant, metastatic tumors in the context of activating *Cdk4*^{R24C} or oncogenic *Tyr-NRAS*^{Q61K} mutations. As chronically UVB-irradiated bigenic *Rxrα*$^{ep-/-}$ mice formed a higher number of melanocytic lesions than their control *Rxrα*$^{L2/L2}$ counterparts, we wanted to determine whether epidermal RXRα loss can also promote melanoma formation in addition to enhance its progression.

We observed reduced expression of tumor suppressor p53 in bigenic *Rxrα*$^{ep-/-}$ TAN skin. p53 has been reported to cooperate with both NRAS [37,42] or CDK4 [43,44] mutations to promote melanoma formation. In both bigenic mouse lines we also observed an upregulation of Cyclin D1 in TAN skin as a result of RXRα ablation. Enhanced expression of Cyclin D1 has been correlated with progression of primary melanoma [38,45] and is upregulated due to p53 inactivation [37].

Functional PTEN expression loss occurs in 30-60% of melanomas [46]. PTEN expression inactivation can occur through deletion/mutation [46]; or alternatively via aberrant epigenetic silencing [46]. This makes it difficult to accurately estimate the impact of PTEN inactivation as no detectable mutation in the gene itself may be present [46]. Indeed, in TAN skin from UVB-irradiated

bigenic *Rxrα*$^{ep-/-}$ mice, we observed reduced PTEN protein levels. PTEN functions as a tumor suppressor by degrading second messenger lipids produced by Phosphoinositide 3-kinase (PI3K). Without functional PTEN these signals result in excessive AKT activation, suppress apoptosis, and promote tumorigenesis [46]. PTEN normally functions in homeostatic balance with AKT, and when functionally suppressed results in excessive AKT phosphorylation [46]. We observed a concomitant increase in levels of activated, phosphorylated AKT protein in *Rxrα*$^{ep-/-}$ TAN skin, corroborating our observation of reduced PTEN. Since the above results are obtained from non-tumorigenic skin, they strongly suggest that loss of epidermal RXRα in combination with chronic UVB exposure creates a microenvironment in the skin that is susceptible to melanoma formation in the context of multiple oncogenic signaling pathways such as NRAS and CDK4 mutations.

Overall, our results suggest that loss of RXRα in the epidermis alters the skin microenvironment in a manner that both promotes formation and enhances progression of malignant and metastatic UVB-induced melanomas when combined with upregulated NRAS and CDK4 signaling pathways. Further studies will need to be undertaken to evaluate RXRα as a clinical diagnostic marker and therapeutic target.

2.6 Acknowledgments

We thank all Indra lab members and the OSU College of Pharmacy; specifically Dr. Mark Zabriskie and Dr. Gary Delander for their continuous support and encouragement. We are grateful for services provided by the Cell and Tissue Analysis Facilities, specifically C. Samuel Bradford for help with LCM, and Services Core of the Environmental Health Sciences Center (EHSC) at OSU, grant number P30 ES00210, National Institute of Environmental Health Sciences (NIEHS), National Institutes of Health (NIH). Research reported in this publication was supported by the NIEHS of the NIH under award numbers ES016629-01A1 as well as the National Cancer Institute (NCI) of the NIH under award number T32CA106195.

2.7 References

1. Chambon P (1996) A decade of molecular biology of retinoic acid receptors. FASEB J 10: 940-954.

2. Heyman RA, Mangelsdorf DJ, Dyck JA, Stein RB, Eichele G, et al. (1992) 9-cis retinoic acid is a high affinity ligand for the retinoid X receptor. Cell 68: 397-406.

3. Leid M, Kastner P, Chambon P (1992) Multiplicity generates diversity in the retinoic acid signalling pathways. Trends Biochem Sci 17: 427-433.

4. Wang Z, Coleman DJ, Bajaj G, Liang X, Ganguli-Indra G, et al. (2011) RXRalpha ablation in epidermal keratinocytes enhances UVR-induced DNA damage, apoptosis, and proliferation of keratinocytes and melanocytes. J Invest Dermatol 131: 177-187.

5. Hyter S, Bajaj G, Liang X, Barbacid M, Ganguli-Indra G, et al. (2010) Loss of nuclear receptor RXRalpha in epidermal keratinocytes promotes the formation of Cdk4-activated invasive melanomas. Pigment Cell Melanoma Res 23: 635-648.

6. Indra AK, Castaneda E, Antal MC, Jiang M, Messaddeq N, et al. (2007) Malignant transformation of DMBA/TPA-induced papillomas and nevi in the skin of mice selectively lacking retinoid-X-receptor alpha in epidermal keratinocytes. J Invest Dermatol 127: 1250-1260.

7. Hyter S, Coleman DJ, Ganguli-Indra G, Merrill GF, Ma S, et al. (2013) Endothelin-1 is a transcriptional target of p53 in epidermal keratinocytes and regulates ultraviolet-induced melanocyte homeostasis. Pigment Cell Melanoma Res 26: 247-258.

8. Sheppard KE, McArthur GA (2013) The cell-cycle regulator CDK4: an emerging therapeutic target in melanoma. Clin Cancer Res 19: 5320-5328.

9. Kwong LN, Costello JC, Liu H, Jiang S, Helms TL, et al. (2012) Oncogenic NRAS signaling differentially regulates survival and proliferation in melanoma. Nat Med 18: 1503-1510.

10. Li M, Chiba H, Warot X, Messaddeq N, Gerard C, et al. (2001) RXR-alpha ablation in skin keratinocytes results in alopecia and epidermal alterations. Development 128: 675-688.

11. Rane SG, Dubus P, Mettus RV, Galbreath EJ, Boden G, et al. (1999) Loss of Cdk4 expression causes insulin-deficient diabetes and Cdk4 activation results in beta-islet cell hyperplasia. Nat Genet 22: 44-52.

12. Ackermann J, Frutschi M, Kaloulis K, McKee T, Trumpp A, et al. (2005) Metastasizing melanoma formation caused by expression of activated N-RasQ61K on an INK4a-deficient background. Cancer Res 65: 4005-4011.

13. Newkirk KM, Parent AE, Fossey SL, Choi C, Chandler HL, et al. (2007) Snai2 expression enhances ultraviolet radiation-induced skin carcinogenesis. Am J Pathol 171: 1629-1639.

14. Wang Z, Kirkwood JS, Taylor AW, Stevens JF, Leid M, et al. (2013) Transcription factor Ctip2 controls epidermal lipid metabolism and regulates expression of genes involved in sphingolipid biosynthesis during skin development. J Invest Dermatol 133: 668-676.

15. Liang X, Bhattacharya S, Bajaj G, Guha G, Wang Z, et al. (2012) Delayed cutaneous wound healing and aberrant expression of hair follicle stem cell markers in mice selectively lacking Ctip2 in epidermis. PLoS One 7: e29999.

16. Kobayashi T, Urabe K, Winder A, Jimenez-Cervantes C, Imokawa G, et al. (1994) Tyrosinase related protein 1 (TRP1) functions as a DHICA oxidase in melanin biosynthesis. EMBO J 13: 5818-5825.

17. Yamazaki F, Okamoto H, Matsumura Y, Tanaka K, Kunisada T, et al. (2005) Development of a new mouse model (xeroderma pigmentosum a-deficient, stem cell factor-transgenic) of ultraviolet B-induced melanoma. J Invest Dermatol 125: 521-525.

18. Wang D, Stockard CR, Harkins L, Lott P, Salih C, et al. (2008) Immunohistochemistry in the evaluation of neovascularization in tumor xenografts. Biotech Histochem 83: 179-189.

19. Dutertre S, Cazales M, Quaranta M, Froment C, Trabut V, et al. (2004) Phosphorylation of CDC25B by Aurora-A at the centrosome contributes to the G2-M transition. J Cell Sci 117: 2523-2531.

20. Fang G, Yu H, Kirschner MW (1998) The checkpoint protein MAD2 and the mitotic regulator CDC20 form a ternary complex with the anaphase-promoting complex to control anaphase initiation. Genes Dev 12: 1871-1883.

21. Yancopoulos GD, Davis S, Gale NW, Rudge JS, Wiegand SJ, et al. (2000) Vascular-specific growth factors and blood vessel formation. Nature 407: 242-248.

22. Sbodio JI, Lodish HF, Chi NW (2002) Tankyrase-2 oligomerizes with tankyrase-1 and binds to both TRF1 (telomere-repeat-binding factor 1) and IRAP (insulin-responsive aminopeptidase). Biochem J 361: 451-459.

23. Karst AM, Levanon K, Duraisamy S, Liu JF, Hirsch MS, et al. (2011) Stathmin 1, a marker of PI3K pathway activation and regulator of microtubule dynamics, is expressed in early pelvic serous carcinomas. Gynecol Oncol 123: 5-12.

24. Ren JG, Jie C, Talbot C (2005) How PEDF prevents angiogenesis: a hypothesized pathway. Med Hypotheses 64: 74-78.

25. Seghezzi G, Patel S, Ren CJ, Gualandris A, Pintucci G, et al. (1998) Fibroblast growth factor-2 (FGF-2) induces vascular endothelial growth factor (VEGF) expression in the endothelial cells of forming capillaries: an autocrine mechanism contributing to angiogenesis. J Cell Biol 141: 1659-1673.

26. Carmeliet P, Moons L, Luttun A, Vincenti V, Compernolle V, et al. (2001) Synergism between vascular endothelial growth factor and placental growth factor contributes to angiogenesis and plasma extravasation in pathological conditions. Nat Med 7: 575-583.

27. Moreno-Bueno G, Portillo F, Cano A (2008) Transcriptional regulation of cell polarity in EMT and cancer. Oncogene 27: 6958-6969.

28. Costa DB, Halmos B, Kumar A, Schumer ST, Huberman MS, et al. (2007) BIM mediates EGFR tyrosine kinase inhibitor-induced apoptosis in lung cancers with oncogenic EGFR mutations. PLoS Med 4: 1669-1679; discussion 1680.

29. Lassus P, Opitz-Araya X, Lazebnik Y (2002) Requirement for caspase-2 in stress-induced apoptosis before mitochondrial permeabilization. Science 297: 1352-1354.

30. Griffith TS, Brunner T, Fletcher SM, Green DR, Ferguson TA (1995) Fas ligand-induced apoptosis as a mechanism of immune privilege. Science 270: 1189-1192.

31. Xue Y, Gibbons R, Yan Z, Yang D, McDowell TL, et al. (2003) The ATRX syndrome protein forms a chromatin-remodeling complex with Daxx and localizes in promyelocytic leukemia nuclear bodies. Proc Natl Acad Sci U S A 100: 10635-10640.

32. Gao Y, Ferguson DO, Xie W, Manis JP, Sekiguchi J, et al. (2000) Interplay of p53 and DNA-repair protein XRCC4 in tumorigenesis, genomic stability and development. Nature 404: 897-900.

33. Merkel M, Eckel RH, Goldberg IJ (2002) Lipoprotein lipase: genetics, lipid uptake, and regulation. J Lipid Res 43: 1997-2006.

34. Zaidi MR, Davis S, Noonan FP, Graff-Cherry C, Hawley TS, et al. (2011) Interferon-gamma links ultraviolet radiation to melanomagenesis in mice. Nature 469: 548-553.

35. Conway SJ (1999) Novel expression of the goosecoid transcription factor in the embryonic mouse heart. Mech Dev 81: 187-191.

36. Christoffels VM, Hoogaars WM, Tessari A, Clout DE, Moorman AF, et al. (2004) T-box transcription factor Tbx2 represses differentiation and formation of the cardiac chambers. Dev Dyn 229: 763-770.

37. Bardeesy N, Bastian BC, Hezel A, Pinkel D, DePinho RA, et al. (2001) Dual inactivation of RB and p53 pathways in RAS-induced melanomas. Mol Cell Biol 21: 2144-2153.

38. Oba J, Nakahara T, Abe T, Hagihara A, Moroi Y, et al. (2011) Expression of c-Kit, p-ERK and cyclin D1 in malignant melanoma: an immunohistochemical study and analysis of prognostic value. J Dermatol Sci 62: 116-123.

39. Alla V, Engelmann D, Niemetz A, Pahnke J, Schmidt A, et al. (2010) E2F1 in melanoma progression and metastasis. J Natl Cancer Inst 102: 127-133.

40. Nevins JR (2001) The Rb/E2F pathway and cancer. Hum Mol Genet 10: 699-703.

41. Verhaegen M, Checinska A, Riblett MB, Wang S, Soengas MS (2012) E2F1-dependent oncogenic addiction of melanoma cells to MDM2. Oncogene 31: 828-841.

42. Dovey M, White RM, Zon LI (2009) Oncogenic NRAS cooperates with p53 loss to generate melanoma in zebrafish. Zebrafish 6: 397-404.

43. Muthusamy V, Hobbs C, Nogueira C, Cordon-Cardo C, McKee PH, et al. (2006) Amplification of CDK4 and MDM2 in malignant melanoma. Genes Chromosomes Cancer 45: 447-454.

44. Yang G, Rajadurai A, Tsao H (2005) Recurrent patterns of dual RB and p53 pathway inactivation in melanoma. J Invest Dermatol 125: 1242-1251.

45. Ramirez JA, Guitart J, Rao MS, Diaz LK (2005) Cyclin D1 expression in melanocytic lesions of the skin. Ann Diagn Pathol 9: 185-188.

46. Stahl JM, Cheung M, Sharma A, Trivedi NR, Shanmugam S, et al. (2003) Loss of PTEN promotes tumor development in malignant melanoma. Cancer Res 63: 2881-2890.

Figure 2.1: Macroscopic and histological characterization of melanocytic tumors from bigenic *Rxrα*$^{ep-/-}$ mice combined with *Tyr-NRAS*^{Q61K} or *Cdk4*^{R24C} mutations.

(A) Scheme for chronic UVB treatment of mice. (B, C) *Tyr-NRAS*^{Q61K} or (F, G) *Cdk4*^{R24C} mice with epidermal-specific knockout of *Rxrα* have more growths than mice with functional Rxrα: *Rxrα*$^{ep-/-}$ | *Cdk4*^{R24C} mice also have an increase in large melanocytic (>2 mm) lesions. Lesions indicated by arrows. (D, E) H&E staining of melanocytic lesions. (D) *Tyr-NRAS*^{Q61K} or (E) *Cdk4*^{R24C} mice with epidermal-specific knockout of *Rxrα* have more densely pigmented lesions with enhanced penetration into epidermal basal layer (inset). Scale bar = 50 μm. *** = $p \leq 0.001$

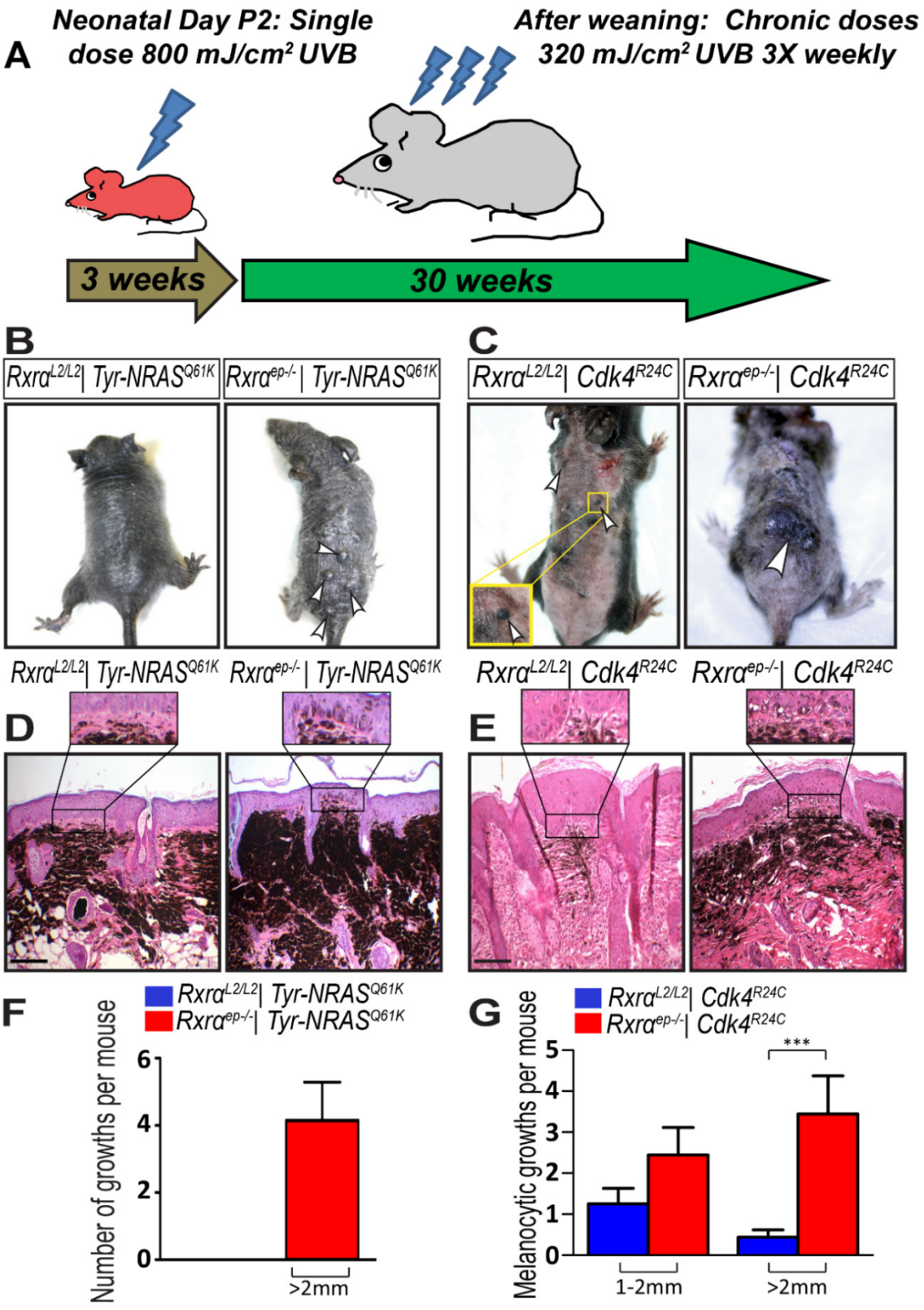
A
Neonatal Day P2: Single dose 800 mJ/cm² UVB
After weaning: Chronic doses 320 mJ/cm² UVB 3X weekly
3 weeks
30 weeks
B
C
Rxrα^L2/L2| Tyr-NRAS^Q61K
Rxrα^ep-/-| Tyr-NRAS^Q61K
Rxrα^L2/L2| Cdk4^R24C
Rxrα^ep-/-| Cdk4^R24C
D
E
F
G
Number of growths per mouse
>2mm
Melanocytic growths per mouse
1-2mm
>2mm
***

Figure 2.1

Figure 2.2: Melanocytic tumors from bigenic *Rxrα*$^{ep-/-}$ mice combined with *Tyr-NRAS*^{Q61K} or *Cdk4*^{R24C} mutations have enhanced proliferative, angiogenic, and malignant properties.

(A, B) Fluorescent IHC for proliferation marker PCNA (red) and melanocyte marker TYRP1 (green). More proliferation was observed in lesions from *Rxrα*$^{ep-/-}$ mice compared to *Rxrα*$^{L2/L2}$ control mice in combination with either *Tyr-NRAS*^{Q61K} (A) or *Cdk4*^{R24C} (B) mutations; particularly an increase in TYRP1+/PCNA+ double positive cells. (C, D) IHC for malignant melanoma antigen HMB45 (red). Overall, more positive staining was observed in lesions from bigenic *Rxrα*$^{ep-/-}$ mice compared to *Rxrα*$^{L2/L2}$ controls. (E, F) IHC for tumor angiogenesis marker CD31 (red). Overall, more prominent staining was observed in lesions from bigenic *Rxrα*$^{ep-/-}$ mice compared to controls. Particularly in mice carrying the *Tyr-NRAS*^{Q61K} mutation, loss of epidermal *Rxrα* results in lesions with large multicellular CD31+ blood vessels (E, right panel). E=Epidermis, D= Dermis. Scale bars = 50 μm.

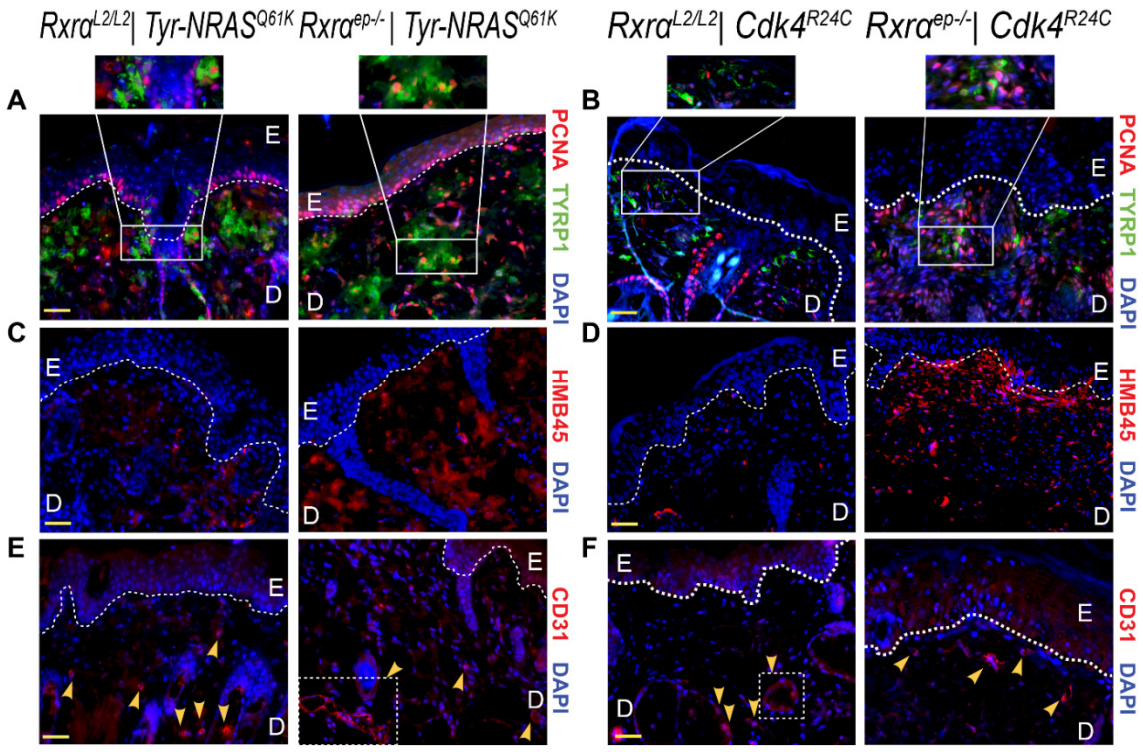
Rxra^L2/L2| Tyr-NRAS^Q61K
Rxra^ep-/-| Tyr-NRAS^Q61K
Rxra^L2/L2| Cdk4^R24C
Rxra^ep-/-| Cdk4^R24C
A
B
C
D
E
F
E
D
PCNA TYRP1 DAPI
HMB45 DAPI
CD31 DAPI

Figure 2.2

Figure 2.3: Enhanced TYRP1+ pigment-producing cells are present in draining lymph nodes of *Tyr-NRAS^{Q61K}* mice compared to *Cdk4^{R24C}* mice, which are further increased in absence of keratinocytic RXRα in both *Tyr-NRAS^{Q61K}* and *Cdk4^{R24C}* groups.

(A) General stain for melanin-containing cells (black staining) as determined by Fontana Masson assay. Nuclear Fast Red (pink) was used as a nuclear counterstain. A higher number of pigment-containing cells are observed in LNs from the *Tyr-NRAS^{Q61K}* background as opposed to those expressing *Cdk4^{R24C}*, but no difference in either background is observed between *Rxrα$^{ep-/-}$* and *Rxrα$^{L2/L2}$* controls. (B) Chromogenic IHC for pigment-producing melanocyte-specific marker TYRP1 (brown). More positive staining overall is observed in *Tyr-NRAS^{Q61K}* LNs as opposed to the *Cdk4^{R24C}* LNs, but an increase in both groups is observed in *Rxrα$^{ep-/-}$* mice relative to *Rxrα$^{L2/L2}$*. Black arrows indicate positive cells in *Rxrα$^{ep-/-}$* | *Cdk4^{R24C}* mice (lower right panel). Hematoxylin (purple) was used as a nuclear counterstain. Scale bars = 100 μm.

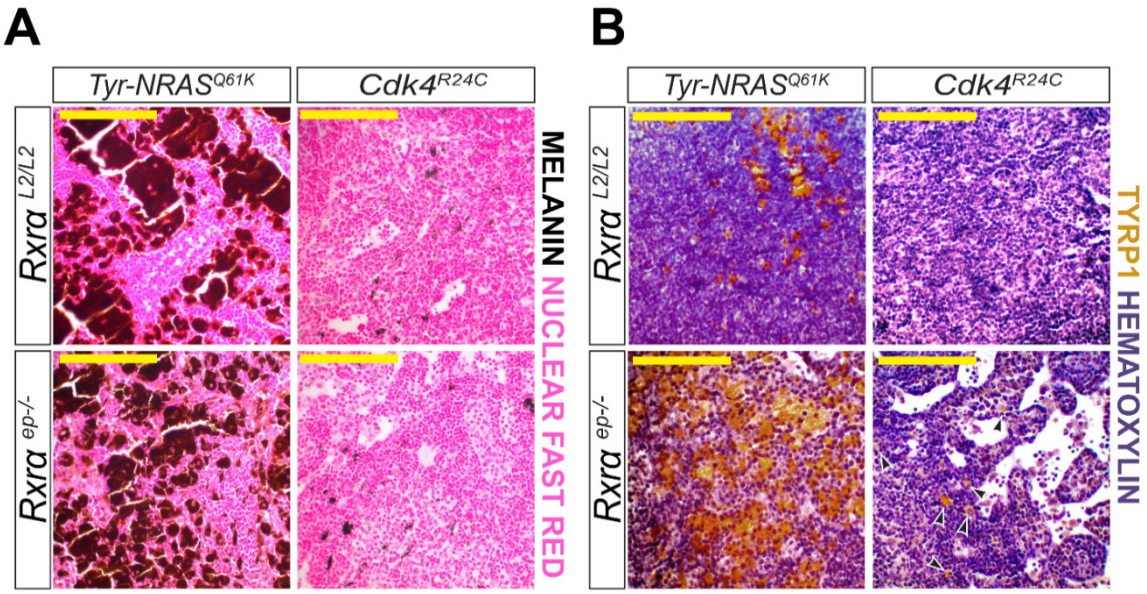
A
B
Tyr-NRASQ61K
Cdk4R24C
Rxrα L2/L2
Rxrα ep-/-
MELANIN NUCLEAR FAST RED
TYRP1 HEMATOXYLIN

Figure 2.3

Figure 2.4: Melanocytic tumors from bigenic *Rxra*$^{ep-/-}$ mice show both overlapping and distinct dysregulated expression of several genes implicated in melanoma progression.

(A) Laser Capture Microdissection (LCM) was performed to isolate RNA from melanoma tissue and analyze gene expression. (B) mRNA expression of several genes implicated in cancer were found to be dysregulated (>1.7 fold) in melanocytic lesions from *Rxra*$^{ep-/-}$ mice compared to *Rxra*$^{L2/L2}$ controls, as determined by an RT-qPCR array (SA Biosciences PAMM-033Z). A subset of these genes were dysregulated in *Rxra*$^{ep-/-}$ mice from both the *Tyr-NRAS*^{Q61K} and *Cdk4*^{R24C} groups, *Tnks2* was dysregulated only in *Rxra*$^{ep-/-}$ | *Tyr-NRAS*^{Q61K} while several others were changed only in the *Rxra*$^{ep-/-}$ | *Cdk4*^{R24C} group. RNA from five mice was pooled and three replicate RT-qPCR arrays were run per group. * = $p \leq 0.05$, ** = $p \leq 0.01$, *** = $p \leq 0.001$, **** = $p \leq 0.0001$. (C) Categories of gene functions represented by significantly dysregulated genes determined by RT-qPCR arrays shown in (B).

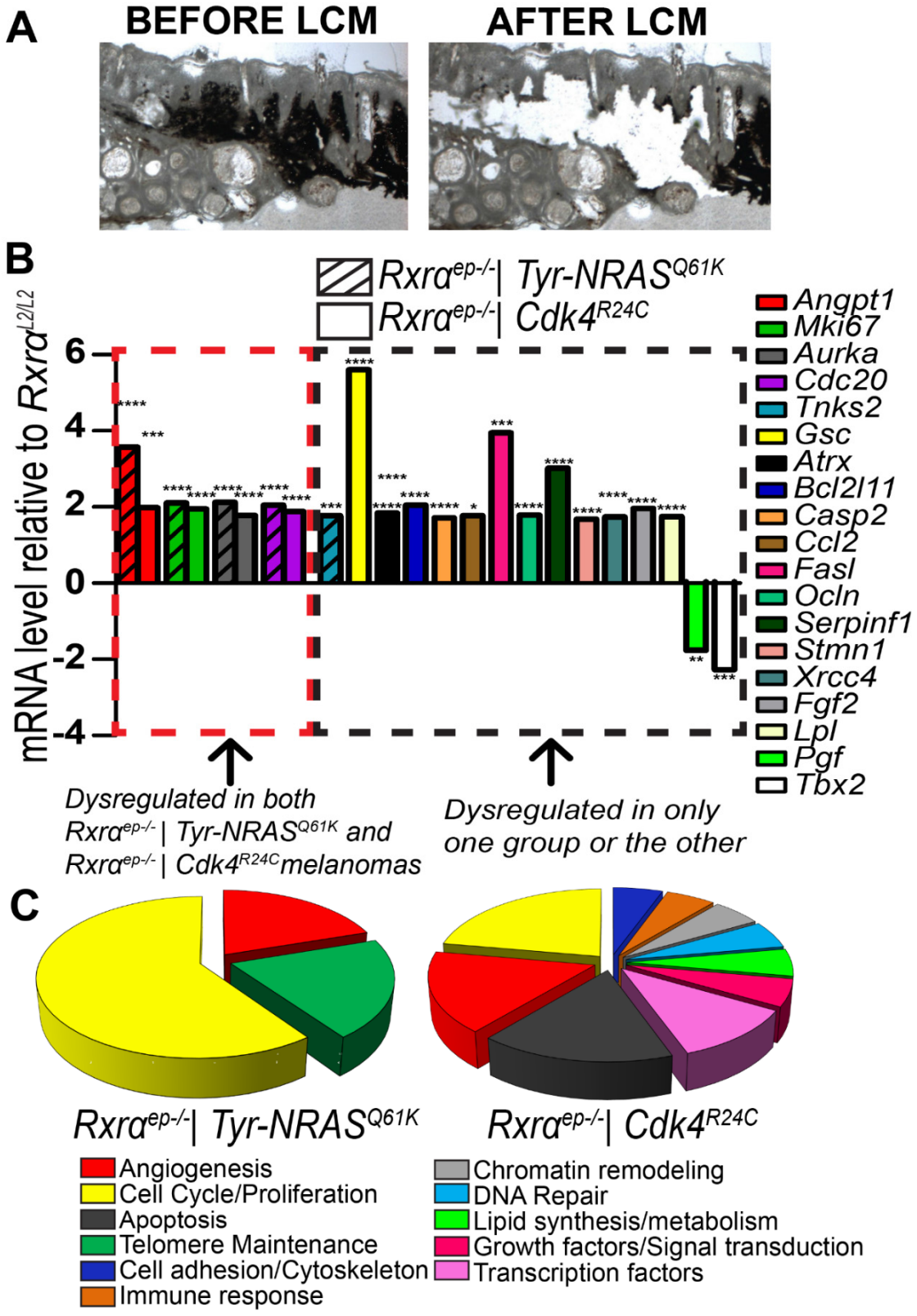
A
BEFORE LCM
AFTER LCM
B
Rxrα^ep-/-| Tyr-NRAS^Q61K
Rxrα^ep-/-| Cdk4^R24C
mRNA level relative to Rxrα^L2/L2
6
4
2
0
-2
-4
Angpt1
Mki67
Aurka
Cdc20
Tnks2
Gsc
Atrx
Bcl2l11
Casp2
Ccl2
Fasl
Ocln
Serpinf1
Stmn1
Xrcc4
Fgf2
Lpl
Pgf
Tbx2
Dysregulated in both Rxrα^ep-/-| Tyr-NRAS^Q61K and Rxrα^ep-/-| Cdk4^R24C melanomas
Dysregulated in only one group or the other
C
Rxrα^ep-/-| Tyr-NRAS^Q61K
Rxrα^ep-/-| Cdk4^R24C
Angiogenesis
Cell Cycle/Proliferation
Apoptosis
Telomere Maintenance
Cell adhesion/Cytoskeleton
Immune response
Chromatin remodeling
DNA Repair
Lipid synthesis/metabolism
Growth factors/Signal transduction
Transcription factors

Figure 2.4

Figure 2.5: Chronically UVB-irradiated tumor-adjacent normal (TAN) skin from bigenic *Rxrα*$^{ep-/-}$ mice exhibit loss of PTEN and increase in phosphorylated AKT.

(A-D) Loss of PTEN expression in TAN skin of bigenic *Rxrα*$^{ep-/-}$ compared to *Rxrα*$^{L2/L2}$ controls, as determined by IHC and (E, F) immunoblotting. (G-L) Increase in phosphorylated AKT (Ser 473) in epidermis and dermis of bigenic *Rxrα*$^{ep-/-}$ mice as determined by (G-J) IHC and (K, L) immunoblotting. Two biological replicates for each group are shown for all immunoblots. E=Epidermis, D= Dermis. Scale bars = 100 μm. # = no statistical significance, * = $p \leq 0.05$, *** = $p \leq 0.001$, **** = $p \leq 0.0001$.

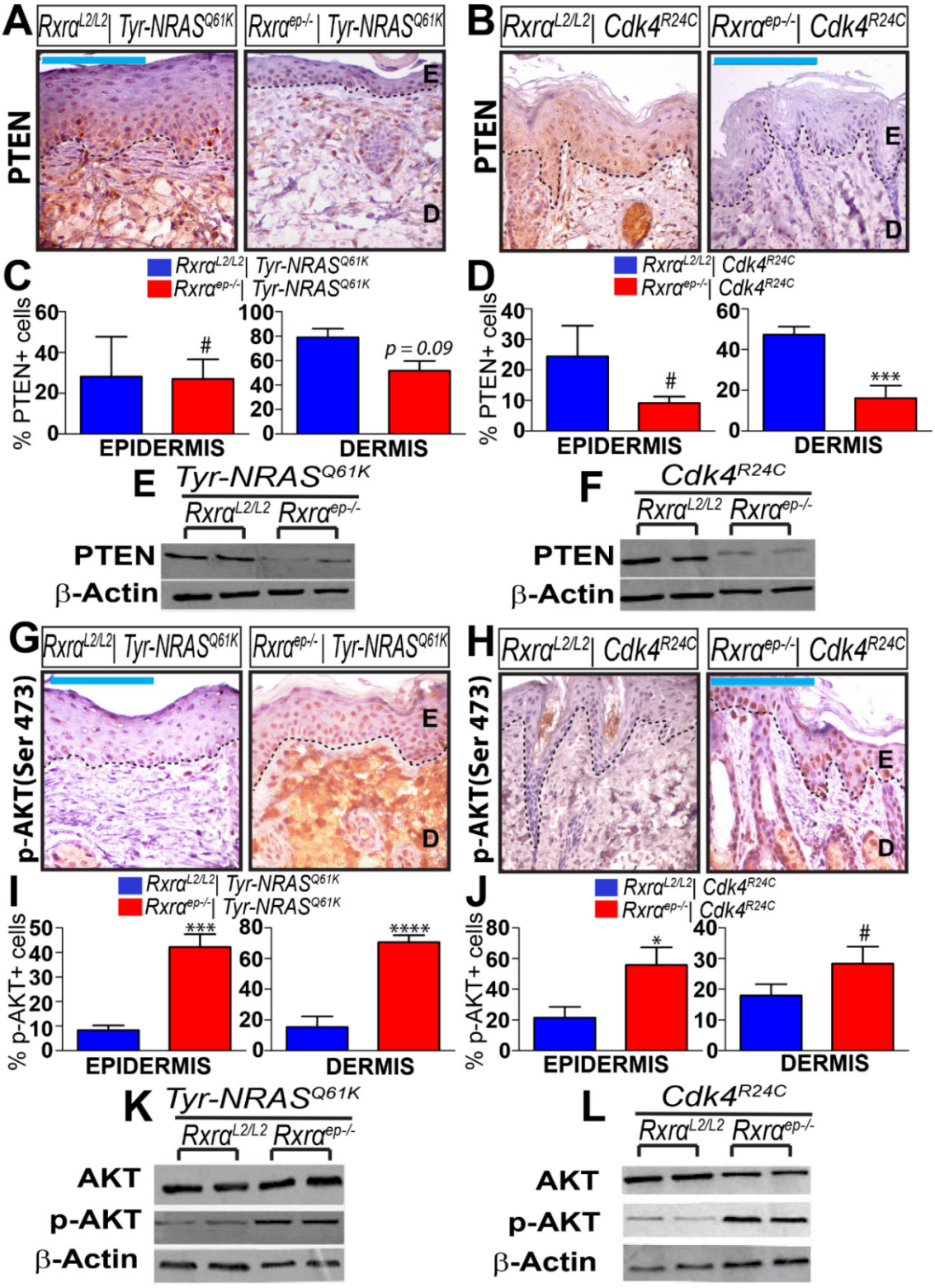
A
Rxrα^L2/L2| Tyr-NRAS^Q61K
Rxrα^ep-/-| Tyr-NRAS^Q61K
PTEN
E
D
B
Rxrα^L2/L2| Cdk4^R24C
Rxrα^ep-/-| Cdk4^R24C
PTEN
E
D
C
Rxrα^L2/L2| Tyr-NRAS^Q61K
Rxrα^ep-/-| Tyr-NRAS^Q61K
% PTEN+ cells
60
40
20
0
#
100
80
60
40
20
0
p = 0.09
EPIDERMIS
DERMIS
D
Rxrα^L2/L2| Cdk4^R24C
Rxrα^ep-/-| Cdk4^R24C
% PTEN+ cells
40
30
20
10
0
#
60
40
20
0
***
EPIDERMIS
DERMIS
E
Tyr-NRAS^Q61K
Rxrα^L2/L2
Rxrα^ep-/-
PTEN
β-Actin
F
Cdk4^R24C
Rxrα^L2/L2
Rxrα^ep-/-
PTEN
β-Actin
G
Rxrα^L2/L2| Tyr-NRAS^Q61K
Rxrα^ep-/-| Tyr-NRAS^Q61K
p-AKT(Ser 473)
E
D
H
Rxrα^L2/L2| Cdk4^R24C
Rxrα^ep-/-| Cdk4^R24C
p-AKT(Ser 473)
E
D
I
Rxrα^L2/L2| Tyr-NRAS^Q61K
Rxrα^ep-/-| Tyr-NRAS^Q61K
% p-AKT+ cells
50
40
30
20
10
0
***
80
60
40
20
0
****
EPIDERMIS
DERMIS
J
Rxrα^L2/L2| Cdk4^R24C
Rxrα^ep-/-| Cdk4^R24C
% p-AKT+ cells
80
60
40
20
0
*
40
30
20
10
0
#
EPIDERMIS
DERMIS
K
Tyr-NRAS^Q61K
Rxrα^L2/L2
Rxrα^ep-/-
AKT
p-AKT
β-Actin
L
Cdk4^R24C
Rxrα^L2/L2
Rxrα^ep-/-
AKT
p-AKT
β-Actin

Figure 2.5

Figure 2.6: Chronically UVB-irradiated tumor-adjacent normal (TAN) skin from bigenic *Rxrα*$^{ep-/-}$ mice exhibit loss of p53 and upregulation of Cyclin D1.

(A-D) Loss of p53 expression in TAN skin of bigenic *Rxrα*$^{ep-/-}$ mice as compared to *Rxrα*$^{L2/L2}$ controls, as determined by IHC and (E,F) immunoblotting. (G,H) Upregulation in Cyclin D1 in TAN skin of bigenic *Rxrα*$^{ep-/-}$ mice; as shown by immunoblotting. Three biological replicates for each group are shown for all immunoblots. E=Epidermis, D= Dermis. Scale bars = 100 μm. # = no statistical significance, *** = $p \leq 0.001$, **** = $p \leq 0.0001$.

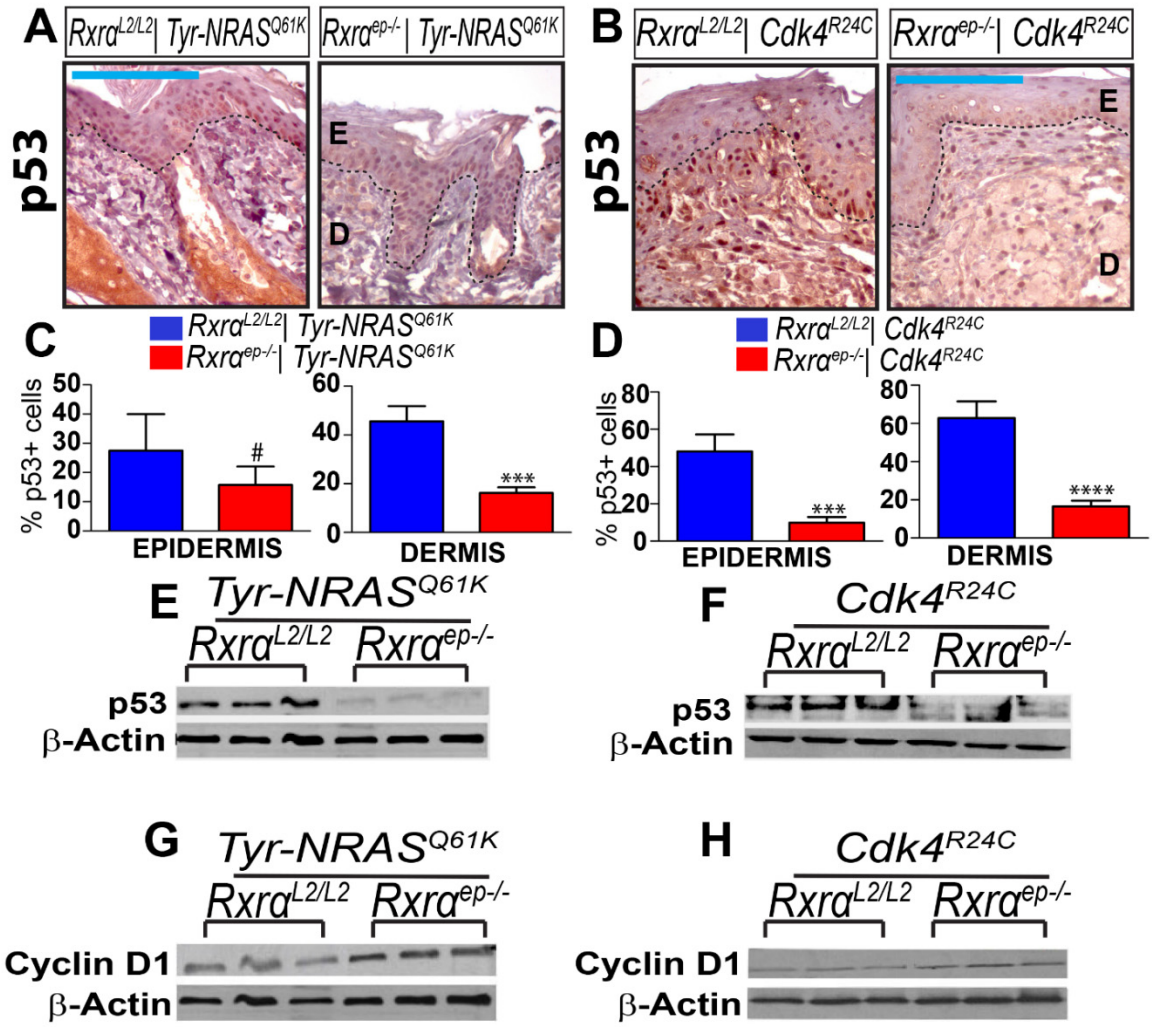
A
Rxra^L2/L2| Tyr-NRAS^Q61K
Rxra^ep-/-| Tyr-NRAS^Q61K
p53
E
D
B
Rxra^L2/L2| Cdk4^R24C
Rxra^ep-/-| Cdk4^R24C
p53
E
D
C
Rxra^L2/L2| Tyr-NRAS^Q61K
Rxra^ep-/-| Tyr-NRAS^Q61K
% p53+ cells
50
40
30
20
10
0
#
60
40
20
0
***
EPIDERMIS
DERMIS
D
Rxra^L2/L2| Cdk4^R24C
Rxra^ep-/-| Cdk4^R24C
% p53+ cells
80
60
40
20
0
***
80
60
40
20
0
****
EPIDERMIS
DERMIS
E
Tyr-NRAS^Q61K
Rxra^L2/L2
Rxra^ep-/-
p53
β-Actin
F
Cdk4^R24C
Rxra^L2/L2
Rxra^ep-/-
p53
β-Actin
G
Tyr-NRAS^Q61K
Rxra^L2/L2
Rxra^ep-/-
Cyclin D1
β-Actin
H
Cdk4^R24C
Rxra^L2/L2
Rxra^ep-/-
Cyclin D1
β-Actin

Figure 2.6

Figure 2.7: Cooperativity between loss of epidermal RXRα expression and activated CDK4 or oncogenic NRAS during UVB induced melanoma progression in bigenic mice.

Illustration representing the results of epidermal RXRα ablation in combination with *Cdk4*^{R24C} or *Tyr-NRAS*^{Q61K} oncogenic mutations and chronic UVB exposure. TAN = "Tumor Adjacent Normal." Similarities/differences between the two bigenic *Rxrα*$^{ep-/-}$ mouse lines are represented by a Venn diagram. Relative to control *Cdk4*^{R24C} or *Tyr-NRAS*^{Q61K} mice with functional *Rxrα* expression, melanomas from bigenic *Rxrα*$^{ep-/-}$ mice have increased proliferation, malignant conversion, angiogenesis, and metastasis to draining lymph nodes (LNs). The TAN skin from the bigenic *Rxrα*$^{ep-/-}$ mice show altered expression of several known melanoma biomarkers relative to *Rxrα*$^{L2/L2}$ controls; including reduced expression of PTEN/concomitant increase in phosphorylated AKT, reduced p53 expression, and upregulation of Cyclin D1. On their own, *Rxrα*$^{ep-/-}$ | *Tyr-NRAS*^{Q61K} mice had heavily pigmented skin overall and higher numbers of melanocytic cells metastasized to draining LNs compared to the *Cdk4*^{R24C} group. Increased macrophage infiltration and a distinct, diverse subset of dysregulated genes were observed specifically in *Rxrα*$^{ep-/-}$ | *Cdk4*^{R24C} lesions.

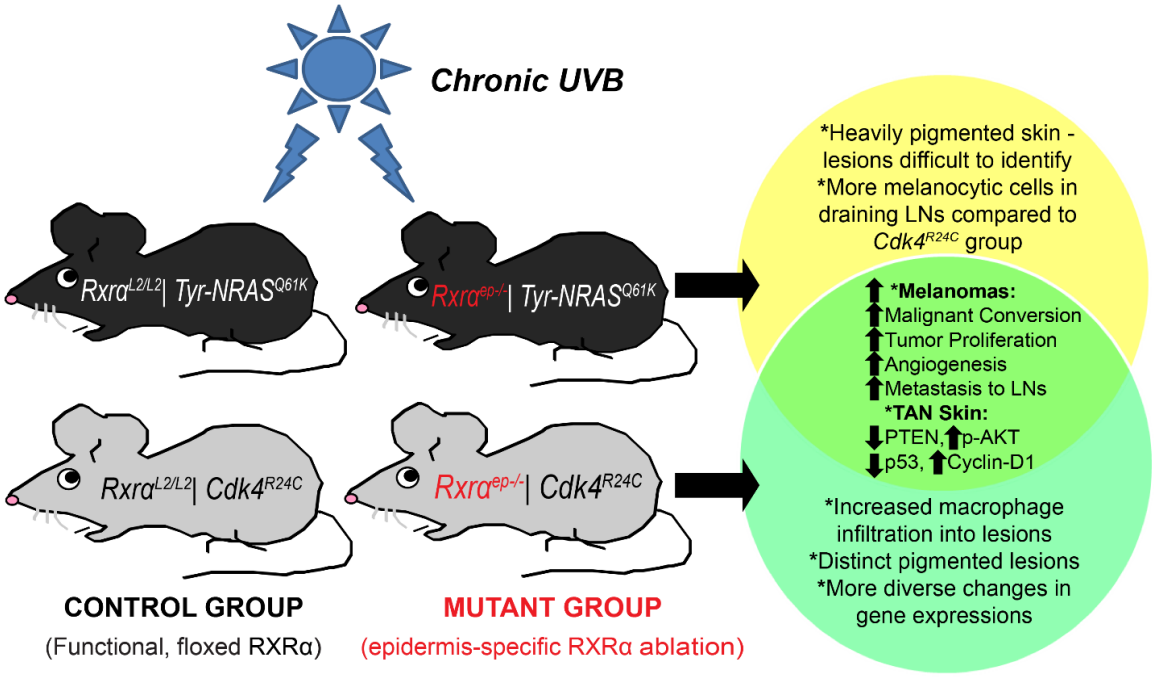
Chronic UVB
Rxrα^L2/L2| Tyr-NRAS^Q61K
Rxrα^ep-/-| Tyr-NRAS^Q61K
Rxrα^L2/L2| Cdk4^R24C
Rxrα^ep-/-| Cdk4^R24C
CONTROL GROUP
(Functional, floxed RXRα)
MUTANT GROUP
(epidermis-specific RXRα ablation)
*Heavily pigmented skin - lesions difficult to identify
*More melanocytic cells in draining LNs compared to Cdk4^R24C group
*Melanomas:
Malignant Conversion
Tumor Proliferation
Angiogenesis
Metastasis to LNs
*TAN Skin:
PTEN, p-AKT
p53, Cyclin-D1
*Increased macrophage infiltration into lesions
*Distinct pigmented lesions
*More diverse changes in gene expressions

Figure 2.7

Figure 2.S1: An increase in infiltrating macrophages is observed in melanocytic lesions from *Cdk4*^{R24C} mice with epidermal-specific knockout of *Rxrα*, but not in *Rxrα*$^{ep-/-}$ | *Tyr-NRAS*^{Q61K} mice. No change in infiltrating CD4+ T-cells observed in melanocytic lesions from either *Cdk4*^{R24C} or *Tyr-NRAS*^{Q61K} mice with epidermal-specific knockout of *Rxrα*.

(A, B) No change in infiltrating macrophages, as determined by fluorescent immunohistochemistry (IHC) for the MAC1 antigen was observed in melanocytic lesions from *Rxrα*$^{ep-/-}$ | *Tyr-NRAS*^{Q61K} mice as compared to *Rxrα*$^{L2/L2}$ controls. (C, D) An increase in infiltrating macrophages was observed in *Rxrα*$^{ep-/-}$ | *Cdk4*^{R24C} lesions as compared to *Rxrα*$^{L2/L2}$ controls. (E-H) No change in infiltrating CD4+ T-cells as determined by fluorescent IHC was observed in *Rxrα*$^{ep-/-}$ | *Tyr-NRAS*^{Q61K} or *Rxrα*$^{ep-/-}$ | *Cdk4*^{R24C} mice as compared to *Rxrα*$^{L2/L2}$ controls. Scale bars = 50 μm. ** = $p \leq 0.01$

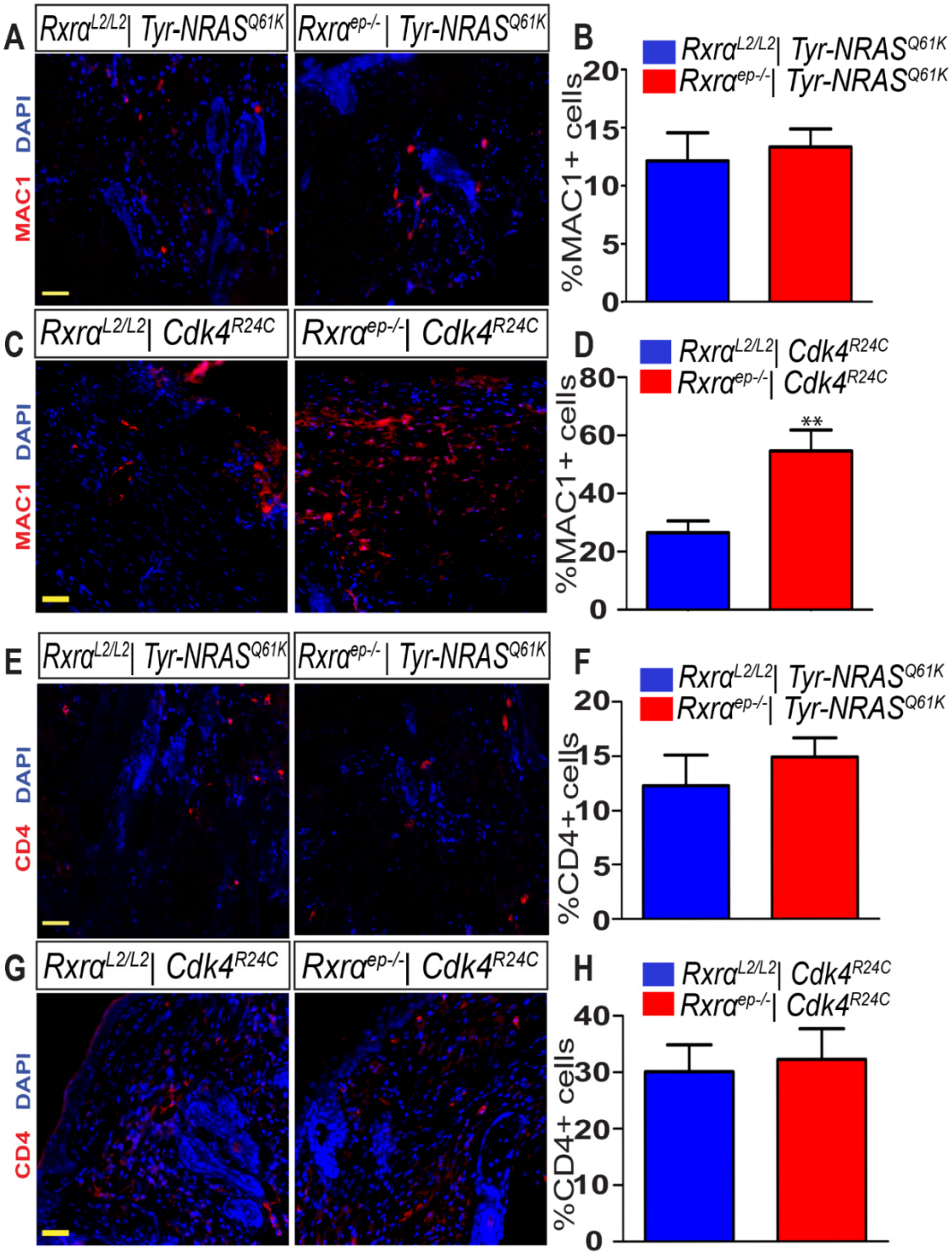
A
Rxrα^L2/L2| Tyr-NRAS^Q61K
Rxrα^ep-/-| Tyr-NRAS^Q61K
DAPI
MAC1
B
Rxrα^L2/L2| Tyr-NRAS^Q61K
Rxrα^ep-/-| Tyr-NRAS^Q61K
%MAC1+ cells
0
5
10
15
20
C
Rxrα^L2/L2| Cdk4^R24C
Rxrα^ep-/-| Cdk4^R24C
DAPI
MAC1
D
Rxrα^L2/L2| Cdk4^R24C
Rxrα^ep-/-| Cdk4^R24C
**
%MAC1+ cells
0
20
40
60
80
E
Rxrα^L2/L2| Tyr-NRAS^Q61K
Rxrα^ep-/-| Tyr-NRAS^Q61K
DAPI
CD4
F
Rxrα^L2/L2| Tyr-NRAS^Q61K
Rxrα^ep-/-| Tyr-NRAS^Q61K
%CD4+ cells
0
5
10
15
20
G
Rxrα^L2/L2| Cdk4^R24C
Rxrα^ep-/-| Cdk4^R24C
DAPI
CD4
H
Rxrα^L2/L2| Cdk4^R24C
Rxrα^ep-/-| Cdk4^R24C
%CD4+ cells
0
10
20
30
40

Figure 2.S1

Figure 2.S2: No change in infiltrating mast cells as determined by CEM staining is observed in melanocytic lesions from either *Cdk4*^{R24C} or *Tyr-NRAS*^{Q61K} mice with epidermis-specific knockout of *Rxrα*.

Infiltrating mast cells are labeled with light blue staining. E=Epidermis, D= Dermis. Scale bars = 50 μm.

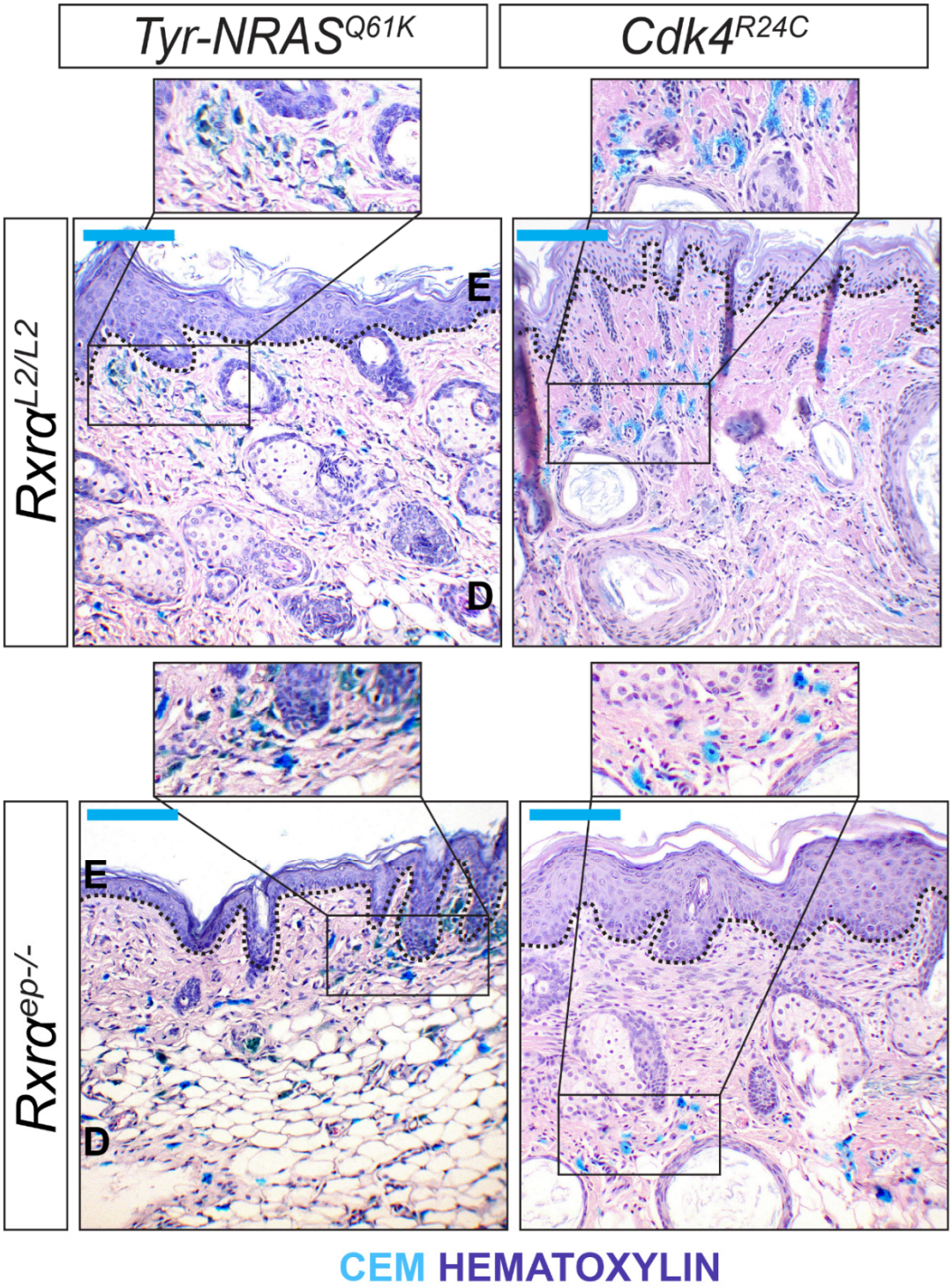
Tyr-NRAS^Q61K
Cdk4^R24C
Rxra^L2/L2
Rxra^ep-/-
E
D
E
D
CEM HEMATOXYLIN

Figure 2.S2

Figure 2.S3: Heat Map and Clustergram of dysregulated genes in melanocytic lesions from *Rxrα*$^{ep-/-}$ | *Tyr-NRAS*^{Q61K} mice.

Tissue from melanocytic lesions was captured using Laser Capture Microdissection (LCM) (See Figure 4 for details). Isolated RNA was converted to cDNA and gene expression in *Rxrα*$^{ep-/-}$ lesions relative to *Rxrα*$^{L2/L2}$ lesions was assayed using an RT-qPCR array (SA Biosciences, PAMM-033Z (Mouse Cancer)). Mean fold change relative to *Rxrα*$^{L2/L2}$ group is represented by the heat map (A). Three replicate arrays were performed for both *Rxrα*$^{L2/L2}$ and *Rxrα*$^{ep-/-}$ groups; magnitude of gene expression for each replicate is shown in the clustergram (B), which correlates genes with similar expression levels.

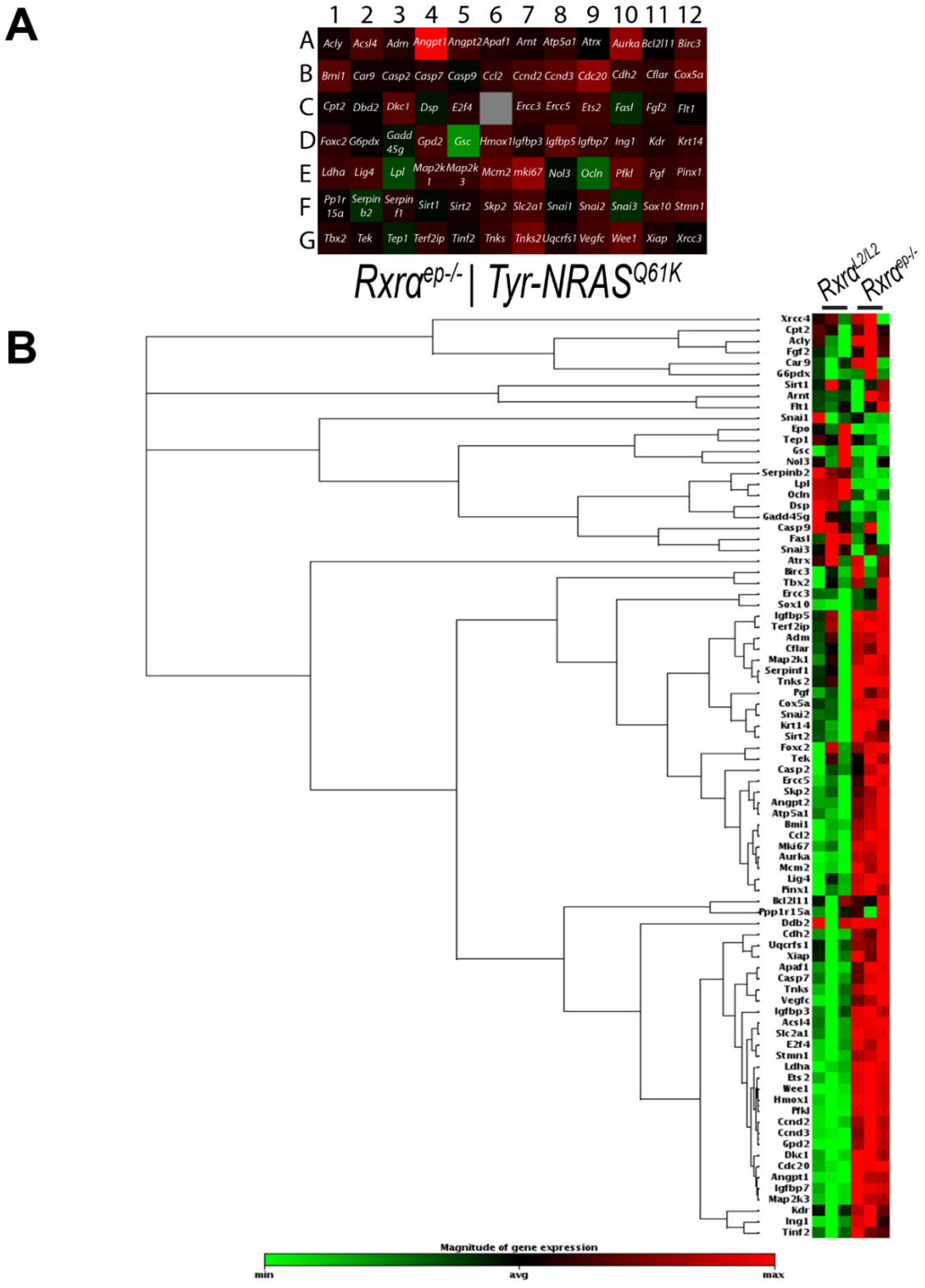
A
1 2 3 4 5 6 7 8 9 10 11 12
A Acly Acsl4 Adm Angpt1 Angpt2 Apaf1 Arnt Atp5a1 Atrx Aurka Bcl2l11 Birc3
B Bmi1 Car9 Casp2 Casp7 Casp9 Ccl2 Ccnd2 Ccnd3 Cdc20 Cdh2 Cflar Cox5a
C Cpt2 Dbd2 Dkc1 Dsp E2f4 Ercc3 Ercc5 Ets2 Fasl Fgf2 Flt1
D Foxc2 G6pdx Gadd 45g Gpd2 Gsc Hmox1 Igfbp3 Igfbp5 Igfbp7 Ing1 Kdr Krt14
E Ldha Lig4 Lpl Map2k 1 Map2k 3 Mcm2 mki67 Nol3 Ocln Pfkl Pgf Pinx1
F Pp1r 15a Serpin b2 Serpin f1 Sirt1 Sirt2 Skp2 Slc2a1 Snai1 Snai2 Snai3 Sox10 Stmn1
G Tbx2 Tek Tep1 Terf2ip Tinf2 Tnks Tnks2 Uqcrfs1 Vegfc Wee1 Xiap Xrcc3
Rxra ep-/- | Tyr-NRAS Q61K
B
Rxra L2/L2
Rxra ep-/-
Xrcc4 Cpt2 Acly Fgf2 Car9 G6pdx Sirt1 Arnt Flt1 Snai1 Epo Tep1 Gsc Nol3 Serpinb2 Lpl Ocln Dsp Gadd45g Casp9 Fasl Snai3 Atrx Birc3 Tbx2 Ercc3 Sox10 Igfbp5 Terf2ip Adm Cflar Map2k1 Serpinf1 Tnks2 Pgf Cox5a Snai2 Krt14 Sirt2 Foxc2 Tek Casp2 Ercc5 Skp2 Angpt2 Atp5a1 Bmi1 Ccl2 Mki67 Aurka Mcm2 Lig4 Pinx1 Bcl2l11 Ppp1r15a Ddb2 Cdh2 Uqcrfs1 Xiap Apaf1 Casp7 Tnks Vegfc Igfbp3 Acsl4 Slc2a1 E2f4 Stmn1 Ldha Ets2 Wee1 Hmox1 Pfkl Ccnd2 Ccnd3 Gpd2 Dkc1 Cdc20 Angpt1 Igfbp7 Map2k3 Kdr Ing1 Tinf2
Magnitude of gene expression
min
avg
max

Figure 2.S3

Figure 2.S4: Heat Map and Clustergram of dysregulated genes in melanocytic lesions from *Rxrα*$^{ep-/-}$ | *Cdk4*^{R24C} mice.

Tissue from melanocytic lesions was captured using Laser Capture Microdissection (LCM) (See Figure 4 for details). Isolated RNA was converted to cDNA and gene expression in *Rxrα*$^{ep-/-}$ lesions relative to *Rxrα*$^{L2/L2}$ lesions was assayed using an RT-qPCR array (SA Biosciences, PAMM-033Z (Mouse Cancer)). Mean fold change relative to *Rxrα*$^{L2/L2}$ group is represented by the heat map (A). Three replicate arrays were performed for both *Rxrα*$^{L2/L2}$ and *Rxrα*$^{ep-/-}$ groups; magnitude of gene expression for each replicate is shown in the clustergram (B), which correlates genes with similar expression levels.

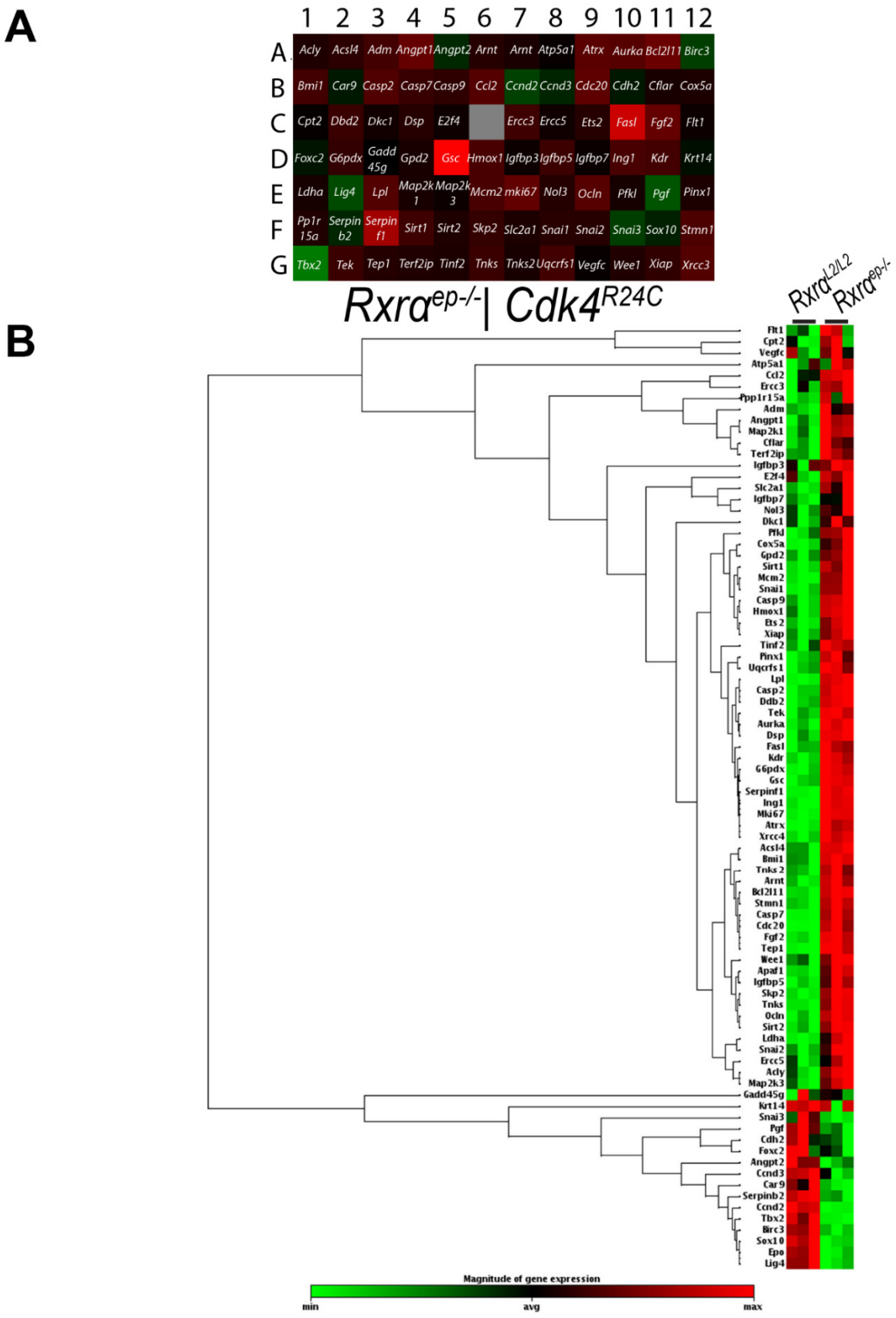
A
1 2 3 4 5 6 7 8 9 10 11 12
A Acly Acsl4 Adm Angpt1 Angpt2 Arnt Arnt Atp5a1 Atrx Aurka Bcl2l11 Birc3
B Bmi1 Car9 Casp2 Casp7 Casp9 Ccl2 Ccnd2 Ccnd3 Cdc20 Cdh2 Cflar Cox5a
C Cpt2 Dbd2 Dkc1 Dsp E2f4 Ercc3 Ercc5 Ets2 Fasl Fgf2 Flt1
D Foxc2 G6pdx Gadd 45g Gpd2 Gsc Hmox1 Igfbp3 Igfbp5 Igfbp7 Ing1 Kdr Krt14
E Ldha Lig4 Lpl Map2k 1 Map2k 3 Mcm2 mki67 Nol3 Ocln Pfkl Pgf Pinx1
F Pp1r 15a Serpin b2 Serpin f1 Sirt1 Sirt2 Skp2 Slc2a1 Snai1 Snai2 Snai3 Sox10 Stmn1
G Tbx2 Tek Tep1 Terf2ip Tinf2 Tnks Tnks2 Uqcrfs1 Vegfc Wee1 Xiap Xrcc3
B
Rxra ep-/- | Cdk4 R24C
Rxra L2/L2
Rxra ep-/-
Flt1
Cpt2
Vegfc
Atp5a1
Ccl2
Ercc3
Ppp1r15a
Adm
Angpt1
Map2k1
Cflar
Terf2ip
Igfbp3
E2f4
Slc2a1
Igfbp7
Nol3
Dkc1
Pfkl
Cox5a
Gpd2
Sirt1
Mcm2
Snai1
Casp9
Hmox1
Ets2
Xiap
Tinf2
Pinx1
Uqcrfs1
Lpl
Casp2
Ddb2
Tek
Aurka
Dsp
Fasl
Kdr
G6pdx
Gsc
Serpinf1
Ing1
Mki67
Atrx
Xrcc4
Acsl4
Bmi1
Tnks2
Arnt
Bcl2l11
Stmn1
Casp7
Cdc20
Fgf2
Tep1
Wee1
Apaf1
Igfbp5
Skp2
Tnks
Ocln
Sirt2
Ldha
Snai2
Ercc5
Acly
Map2k3
Gadd45g
Krt1-4
Snai3
Pgf
Cdh2
Foxc2
Angpt2
Ccnd3
Car9
Serpinb2
Ccnd2
Tbx2
Birc3
Sox10
Epo
Lig4
Magnitude of gene expression
min
avg
max

Figure 2.S4

Figure 2.S5: Chronically UVB-irradiated tumor-adjacent normal skin from *Tyr-NRAS^{Q61K}* or *Cdk4^{R24C}* mice with epidermis-specific knockout of *Rxrα* show modest increase in CDK4 expression; downregulation of phosphorylated ERK, as well as increased E2F1 expression specifically in *Rxrα$^{ep-/-}$* | *Cdk4^{R24C}* mice.

(A-D) Modest increase of CDK4 expression in both epidermis and dermis of *Rxrα$^{ep-/-}$* |*Tyr-NRAS^{Q61K}* and *Rxrα$^{ep-/-}$* | *Cdk4^{R24C}* mice as compared to *Rxrα$^{L2/L2}$* controls, as determined by IHC. E=Epidermis, D= Dermis. Scale bars = 50 μm. # = no statistical significance, * = $p \leq 0.05$, *** = $p \leq 0.001$ (E-H) Immunoblotting studies of protein expression. (E,F) Downregulation in phosphorylated ERK in tumor-adjacent normal skin of *Rxrα$^{ep-/-}$* | *Tyr-NRAS^{Q61K}* and *Rxrα$^{ep-/-}$* | *Cdk4^{R24C}* mice as compared to *Rxrα$^{L2/L2}$* controls (G, H). Analysis of E2F1 protein in tumor-adjacent normal skin of *Rxrα$^{ep-/-}$* | *Tyr-NRAS^{Q61K}* and *Rxrα$^{ep-/-}$* | *Cdk4^{R24C}* mice as compared to *Rxrα$^{L2/L2}$* controls. No difference was observed in the *Tyr-NRAS^{Q61K}* group, while increased E2F1 levels were observed in *Rxrα$^{ep-/-}$* | *Cdk4^{R24C}* mice compared to *Rxrα$^{L2/L2}$* control. Two biological replicates for each group are shown for all immunoblots.

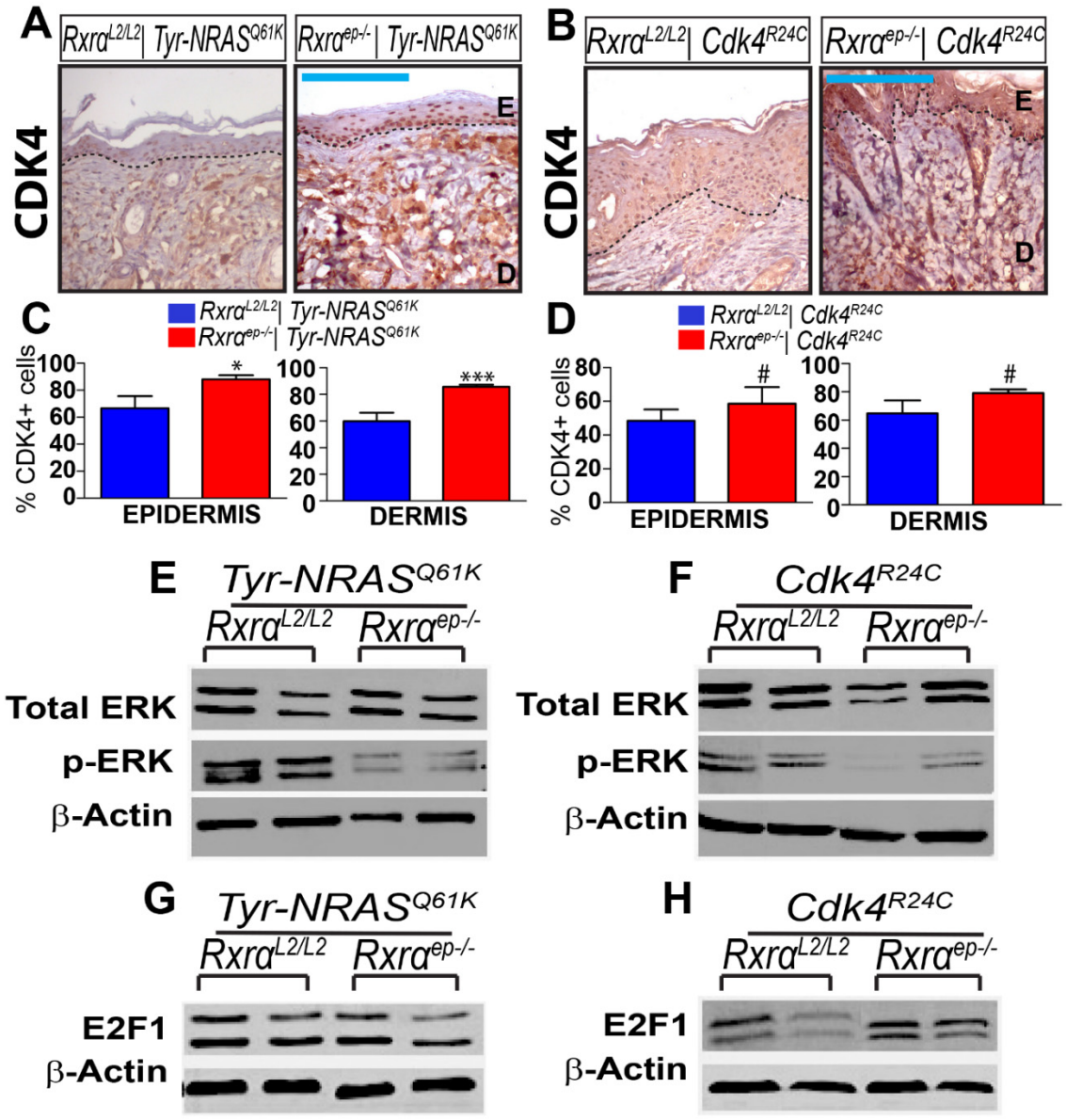
A
Rxra^L2/L2| Tyr-NRAS^Q61K
Rxra^ep-/-| Tyr-NRAS^Q61K
CDK4
E
D
B
Rxra^L2/L2| Cdk4^R24C
Rxra^ep-/-| Cdk4^R24C
CDK4
E
D
C
Rxra^L2/L2| Tyr-NRAS^Q61K
Rxra^ep-/-| Tyr-NRAS^Q61K
% CDK4+ cells
100
80
60
40
20
0
*
***
EPIDERMIS
DERMIS
D
Rxra^L2/L2| Cdk4^R24C
Rxra^ep-/-| Cdk4^R24C
% CDK4+ cells
80
60
40
20
0
100
80
60
40
20
0
#
#
EPIDERMIS
DERMIS
E
Tyr-NRAS^Q61K
Rxra^L2/L2
Rxra^ep-/-
Total ERK
p-ERK
β-Actin
F
Cdk4^R24C
Rxra^L2/L2
Rxra^ep-/-
Total ERK
p-ERK
β-Actin
G
Tyr-NRAS^Q61K
Rxra^L2/L2
Rxra^ep-/-
E2F1
β-Actin
H
Cdk4^R24C
Rxra^L2/L2
Rxra^ep-/-
E2F1
β-Actin

Figure 2.S5

Table 2.1: List of antibodies used during experimental procedures

Antibody	Host	Source	Application	Dilution/Concentration
anti-MAC1	Mouse	Abcam (ab22506)	IHC-P	1:1000
anti-CD4	Mouse	Abcam (ab57312)	IHC-P	1:100
anti-HMB45	Mouse	Abcam (ab732)	IHC-P	1:100
anti-pAKT	Rabbit	Cell Signaling (4060)	WB, IHC-P	1:2000 (WB), 1:50 (IHC)
anti-PTEN	Rabbit	Cell Signaling (9559)	WB, IHC-P	1:1000 (WB), 1:300 (IHC)
anti-CDK4	Mouse	Santa Cruz (sc260)	IHC-P	1:100
anti-p53	Rabbit	Santa Cruz (sc-6243)	WB	1:500
anti-p53	Rabbit	Leica (NCL-p53-CM5p)	IHC-P	1:500
anti-AKT	Rabbit	Cell Signaling (6727)	WB	1:1000
anti-ERK(p44/42 MAPkinase)(137F5)	Rabbit	Cell Signaling (4695)	WB	1:1000
anti-pERK	Rabbit	Abcam (ab50011)	WB	1:1000
anti-cyclinD1	Mouse	Cell Signaling (2926)	WB	1:2000
anti-CD31	Rabbit	Abcam (ab28364)	IHC-P	1:50
anti-PEP1 (TYRP1)	Rabbit	NIH (kindly provided by V. Hearing)	IHC-P	1:1000
anti-PCNA	Mouse	Abcam (ab29)	IHC-P	1:6000
anti-B-actin	Rabbit	Bethyl Lab (A300-491A)	WB	1:5000
IHC-P = Immunohistochemistry - Paraffin Sections WB = Western Blot				

Retinoid-X-Receptors (α/β) in Melanocytes Modulate Innate Immune Responses and Differentially Regulate Cell Survival Following UV Irradiation

Chapter 3

Daniel J. Coleman, Gloria Garcia, Stephen Hyter, Hyo Sang Jang, Sharmeen Chagani, Xiaobo Liang, Lionel Larue, Gitali Ganguli-Indra, Arup K. Indra

PLoS Genetics

Published May 8, 2014

PLoS Genet 10(5): e1004321

doi:10.1371/journal.pgen.1004321

3.1 Abstract

Understanding the molecular mechanisms of ultraviolet (UV) induced melanoma formation is becoming crucial with more reported cases each year. Expression of type II nuclear receptor Retinoid-X-Receptor α (RXRα) is lost during melanoma progression in humans. Here, we observed that in mice with melanocyte-specific ablation of RXRα and RXRβ, melanocytes attract fewer IFN-γ secreting immune cells than in wild-type mice following acute UVR exposure; via altered expression of several chemoattractive and chemorepulsive chemokines/cytokines. Reduced IFN-γ in the microenvironment alters UVR-induced apoptosis, and due to this the survival of surrounding dermal fibroblasts is significantly decreased in mice lacking RXRα/β. Interestingly, post-UVR survival of the melanocytes themselves is enhanced in the absence of RXRα/β. Loss of RXRs α/β specifically in the melanocytes results in an endogenous shift in homeostasis of pro- and anti-apoptotic genes in these cells and enhances their survival compared to the wild type melanocytes. Therefore, RXRs modulate post-UVR survival of dermal fibroblasts in a “non-cell autonomous” manner, underscoring their role in immune surveillance; while independently mediating post-UVR melanocyte survival in a “cell autonomous” manner. Our results emphasize a novel immunomodulatory role of melanocytes in controlling survival of neighboring cell types besides controlling their own; and identifies RXRs as potential targets for therapy against UV induced melanoma.

3.2 Author Summary

Melanoma is the deadliest form of skin cancer. It derives from melanocytes, the melanin-producing cells of our skin, which give our skin its tone in addition to protecting it from harmful effects of ultraviolet radiation (UVR). Changes in the skin microenvironment, such as signaling from other cell types, can influence melanoma progression. While several key genes in melanoma development have been identified, the underlying mechanisms are complex; different combinations of mutations can result in melanoma formation and genetic profiles of tumors can vary greatly among patients. Therefore, identification of novel therapeutic targets is crucial. Our present study uses a tissue-specific gene ablation strategy to characterize a novel role of type II nuclear receptors [Retinoid-X-Receptors (RXRs)] in melanocytes to control UVR-induced skin immune responses and cell survival. Several of these observed changes are risk factors for melanoma progression and identify RXRs as potential drug targets for melanoma diagnosis, prevention, and treatment. This newly-discovered role of retinoid receptor signaling in immune surveillance can be studied in different types of cancer and in other diseases including metabolic syndromes and atherosclerosis. The identified pathway is ideal for targeting using specific ligands or small molecule modulators of RXR signaling in different cell types and tissues.

3.3 Introduction

Malignant melanoma is the deadliest form of skin cancer. Understanding the molecular mechanisms behind melanoma formation is crucial for determining new pathways that can be utilized for therapeutic targeting. Retinoid-X-Receptors (RXRs) α, β, and γ (See Table 3.1 for all gene names, abbreviations, and IDs) are members of the nuclear hormone receptor (NR) superfamily, and act as central coordinators of cell signal transduction in many different tissue types through heterodimerization with several other NRs [1]. RXRs function as a ubiquitous DNA-binding transcription factor via ligand binding [1,2] and heterodimerization with several other NRs [1,3]. RXRs are able to interact with various transcriptional coactivators and/or corepressors [1]; adding an additional layer of complexity to their function. Thus, the role of RXRs in regulation of cellular processes is diverse and dynamic, and much is still unknown.

In malignant human melanomas, loss of RXRα expression has been previously reported both in the melanoma cells themselves [4] and in the adjacent epidermal keratinocytes [5]. Also, epidermis-specific ablation of RXRα in a mouse model was shown to promote melanocyte proliferation after UV radiation (UVR) [6] and increased susceptibility to malignant melanomas after a multi-stage carcinogenesis treatment [5].

Chemokines are a family of small (8±14 kDa) polypeptide signaling molecules [7] that bind to transmembrane G protein-coupled receptors [7]. It has been previously reported that secretion of CCR2 ligands CCL2 and CCL8 from

melanocytes following UVB radiation activates F4/80+ macrophages and results in their recruitment [8]. These macrophages infiltrate into the skin and secrete interferon-y (IFN-y); which mediates signaling that influences cell survival post-UVR [8]. Interferons have a complicated role in immunosurveillance with regard to cancer formation and progression. IFN-y secreted from macrophages recruited post-UVR have been shown to promote activation and survival of melanocytes and melanoma cells, suggesting a pro-tumorigenic role of IFN-y in skin [8]. In contrast, there is also evidence that IFN-y can act as an anti-tumorigenic agent [9-12].

In the present study, we discovered that specific ablation of RXRα and RXRβ in the melanocytes of the skin results in increased apoptosis of non-melanocytic cells in the dermis following UVR. However, the mutant melanocytes themselves exhibit slightly reduced apoptosis, suggesting an enhanced ability to survive UVR-induced DNA damage in the absence of RXRα/β. Interestingly, ablation of melanocytic RXRα and RXRβ results in decreased infiltration of immune cells such as F4/80+ macrophages, CD11B+ monocytes, CD8+ T-cells and mast cells into the dermal layer following UVR, as well as corresponding downregulated expression of IFN-γ, suggesting a defect in secretion of chemokines involved in immunomodulation. RT-qPCR analyses of UVR-exposed melanocytes revealed that loss of *Rxrα/β* results in significantly altered expression of both chemoattractive and chemorepulsive ligands implicated in chemotaxis of IFN-γ secreting immune cells. Treatment of primary melanocytes *in vitro* with either a small molecule agonist or antagonist of RXR

function results in decreased UVR-induced apoptosis, suggesting that RXRs can mediate melanocyte apoptosis via multiple pathways utilizing both its activating and repressive functions. RT-qPCR analyses also revealed several post-UVR changes in expression of pro- and anti-apoptotic genes in melanocytes lacking *Rxrα/β* expression.

Our results suggest that ablation of RXRs α/β results in aberrant expression of several chemokines following UVR, resulting in decreased infiltration of macrophages and other immune cells that secrete IFN-γ. The corresponding decrease in IFN-γ may influence changes in survival of melanocytes, fibroblasts, and other cell types in the skin. It has been found previously that UVR-induced apoptosis in skin can stimulate clonal expansion of tumorigenic cells as the death of surrounding cells allows them room to expand [13]. As RXRα/β ablation exists only in the melanocytes, there is a cell-autonomous shift in homeostasis of pro- and anti-apoptotic gene expression in this cell type, which results in an enhanced survival of these cells post-UVR.

3.4 Results

Selective ablation of RXRα and RXRβ in melanocytes of *Tyr-Cre*$^{tg/0}$| *Rxrα/β*$^{L2/L2}$ mice

In order to selectively ablate RXRα and RXRβ in melanocytes, we bred mice carrying LoxP site-containing (floxed) *Rxrα* and *Rxrβ* alleles (*Rxrα/β*$^{L2/L2}$) with hemizygous *Tyr-Cre* transgenic mice [14]. Macroscopically, *Tyr-Cre*$^{tg/0}$| *Rxrα/β*$^{L2/L2}$ mice were indistinguishable from the control *Rxrα/β*$^{L2/L2}$ floxed mice (Figure 3.S1 A) and no effects on their viability were observed. In order to verify that RXRα and RXRβ were specifically deleted in melanocytes of *Tyr-Cre*$^{tg/0}$| *Rxrα/β*$^{L2/L2}$ mice, we used immunohistochemistry (IHC) to examine skin sections from neonatal control and mutant mice collected after exposure to UVR (800 mJ/cm^2 UVB) (Figure 3.1 A), which dramatically increases numbers of extrafollicular melanocytes (Figure 3.S1 D, E). Tissue sections were co-labeled with antibodies for tyrosinase-related protein 1 (TYRP1), which is localized specifically in the cytoplasm of melanocytes [15,16] (Figure 3.1 B, C), and either RXRα (Figure 3.1 B) or RXRβ (Figure 3.1 C). We observed that in absence of the Cre transgene, cells positive for TYRP1 also show nuclear labeling for both RXRα (Figure 3.1 B) and RXRβ (Figure 3.1 C) in *Rxrα/β*$^{L2/L2}$ floxed mice. In presence of the Cre transgene, none of the TYRP1-labeled melanocytes showed positive staining for either receptor in the *Tyr-Cre*$^{tg/0}$|*Rxrα/β*$^{L2/L2}$ mice, while all other cell types of the skin were positive for RXRα (Figure 3.1 B) and RXRβ (Figure 3.1 C), thereby confirming the generation of the *Rxrα/β*$^{mel-/-}$ mice. Altogether, our results indicate that *Rxrα/β*$^{mel-/-}$ mice constitute a model of

selective ablation of both RXRα and RXRβ in the melanocytes of neonatal murine skin.

Melanocytic ablation of RXRα and RXRβ differentially alters UVR-induced apoptosis in melanocytes and dermal cells of the skin

Histological and IHC characterization of *Rxrα/β*$^{L2/L2}$ (control, CT) and *Rxrα/β*$^{mel-/-}$ (mutant, MT) skin was performed on biopsies collected from neonatal mice at different time points following a single dose of UVR (Figure 3.1 A). Measurement of epidermal thickness on Hematoxylin and Eosin (H&E) stained skin sections did not reveal any significant difference between CT and MT skin (Figure 3.S1 B, C). Also, melanocyte numbers (Figure 3.S1 D, E) and levels of UVR-induced DNA damage in melanocytes (Figure 3.S2) were similar between the two groups.

IHC analysis for proliferation marker PCNA revealed a significant reduction in proliferation of cells in the dermal layer that was most prominent at 48 hours post-UVR (Figure 3.2 A, B). Interestingly, we also observed a marked increase in apoptosis of the dermal cells in the MT skin compared to the CT skin using a TUNEL assay (Figure 3.2 C, D). This difference was significant at 24 and 48 hours post-UVR (Figure 3.2 C, D).

We next employed a hybrid TUNEL-IHC assay (with anti-TYRP1 antibody) to specifically evaluate melanocyte apoptosis (Figure 3.2 E). In contrast to the overall dermal apoptosis, we observed a trend in reduced percentage of apoptotic melanocytes in MT skin compared to the CT skin at each time point post-UVR. The reduction in percent apoptotic melanocytes was significant at 72

hours post-UVR (Figure 3.2 E, F). To corroborate this result we utilized an *in vitro* assay using cultured primary murine melanocytes. Growth medium was supplemented with either a small-molecule agonist (BMS-649) or antagonist (HX-531) of RXRs in order to mimic loss of RXRα/β functions; by simulating relief of transcriptional repression or loss of transcriptional activation functions with addition of an agonist or antagonist, respectively. The treated primary melanocytes were then subjected to a single dose of UVR and given fresh medium supplemented with either agonist or antagonist. 24 hours post-UVR, apoptosis of the melanocytes was quantified using an Annexin V/Propidium Iodide cytometry assay. Compared to vehicle controls, apoptosis of the primary melanocytes was reduced when growth medium was supplemented with either an RXR agonist or antagonist (Figure 3.2 G). The above results suggest a non-cell autonomous role in modulating survival of dermal cells and a cell autonomous role of melanocytic RXRα/β in mediating melanocyte homeostasis post-UVR, possibly via distinct mechanisms.

Altered inflammatory responses in the skin of *Rxrα/β*$^{mel-/-}$ mice following exposure to UV radiation

It has been reported that in response to UVR, melanocytes secrete chemokines that mediate infiltration of macrophages [8], which further secrete interferon-γ (IFN-γ) that influences melanocyte survival [8]. We hypothesized that IFN-γ can also influence survival of other cells post-UVR; and the changes we observed in levels of apoptosis in the skin of *Rxrα/β*$^{mel-/-}$ mice may be due to altered immune responses. To test that, we first performed two-color IHC for

IFN-γ expression and presence of macrophages using anti-IFN-γ and anti-F4/80 (a transmembrane cell surface protein associated with macrophages [17]) antibodies on CT and MT skin at different time points post-UVR. In comparison to control mice, MT skin exhibited moderately decreased IFN-γ expression and reduced F4/80+ labeling at 48 and 72 hours post-UVR, and a marked reduction of staining for both IFN-γ and F4/80+ cells at 96 hours post-UVR (Figure 3.3 A). Western blot for F4/80, using a different antibody than used for IHC (Table 3.2), also revealed decreased F4/80 expression in skin lysates from MT skin compared to controls (Figure 3.3 B). An ELISA assay confirmed a significant decrease in IFN-γ level in skin lysates from *Rxrα/β*$^{mel-/-}$ mice at 72 and 96 h post-UVR compared to controls (Figure 3.3 C). We also observed reductions in CD11B+ monocytes, CD8+ T-cells, and mast cells (Figure 3.S3 A-C). It is of note that F4/80 expression was previously reported to be required for CD8+ T-cell activation [18]. These data indicate that ablation of melanocytic RXRα and RXRβ results in reduced immune cell recruitment, which could result in reduced secretion of IFN-γ after exposure to UV radiation.

As a complementary experiment, we wanted to determine how IFN-γ affects the survival of fibroblasts and melanocytes post-UVR. To that end, we irradiated both fibroblasts and melanocytes *in vitro* and examined the effects 24 h post-UVR. First, we confirmed that both cell types express the primary receptor for IFN-γ (IFNGR1) pre- and 24h post-UVR using Western Blot (Figure 3.3 D). We then analyzed apoptosis in cells cultured with recombinant murine IFN-γ post-UVR, using Annexin V/Propidium Iodide Staining. We observed that

increasing concentration of IFN-γ resulted in a corresponding dose-dependent reduction in apoptosis levels of both fibroblasts and melanocytes following exposure to UVR (Figure 3.3 E). These results suggest that secretion of IFN-γ in the microenvironment, which is reduced in *Rxrα/β*$^{mel-/-}$ mice compared to controls, is a key factor for post-UVR cell survival.

Knockdown of RXRα and RXRβ in primary melanocytes results in alteration of the secretory chemokine/cytokine profile, as well as expression of genes involved in apoptosis

We hypothesized that loss of RXRα/β may result in aberrant expression of chemokine ligands and/or receptors that are involved in immune cell infiltration; which in turn may influence survival of other skin cell types, particularly those in the dermis. We also examined the effects of RXRα/β loss on apoptosis-related genes; as mimicking functional RXR loss using an agonist or antagonist reduces post-UVR apoptosis of melanocytes *in vitro* (Figure 3.2 G). To that end, we employed an RNAi-based knockdown strategy of both RXRα and RXRβ in primary murine melanocytes (Figure 3.4, see Materials and Methods for details). We used plasmids expressing shRNA constructs specifically targeting either *Rxrα* or *Rxrβ* transcripts (See Table 3.3 for details). The plasmid expressing *Rxrα*-targeting shRNA contains a GFP marker gene, while the *Rxrβ*-targeting shRNA plasmid encodes an RFP marker. The two different fluorescent marker genes allowed us to co-transfect both constructs into primary murine melanocytes, isolate the cell population expressing both plasmids by Fluorescence-Activated Cell Sorting (FACS) (Figure 3.4 A) and then re-culture

the isolated double positive cells (Figure 3.4 B). We verified that knockdown was successful at both the RNA level using RT-qPCR (Figure 3.4 C) and at the protein level using Western blot (Figure 3.4 D). We observed a compensatory upregulation of *Rxrβ* expression in cells in which only *Rxrα* was knocked down, but not vice-versa (Figure 3.S4).

The *Rxrα/β* double knockdown primary melanocytes were subjected to UVR (10 mJ/cm^2 UV-B) and RNA isolated 6 hours later. We chose the UVR dose and time interval based on peak mRNA expression of chemokines *Ccl2* and *Ccl8* (Figure 3.S5), two ligands secreted by melanocytes that are reported to influence macrophage infiltration in response to UVR [8]. cDNA synthesized from the RNA template was then applied to RT-qPCR arrays. We employed arrays for mouse chemokines/receptors (SA Biosciences, PAMM-022) and for mouse cancer/apoptosis (PAMM-033). Several mouse chemokines/receptors, as well as genes implicated in apoptosis, were found to be differentially up- or down-regulated compared to wild-type melanocytes (Figure 3.S6 A-D; Figure 3.5 A, B). Expression of several candidate genes, which could contribute to reduced immune cell infiltration and reduced IFN-γ expression, were re-validated in new biological replicates by RT-qPCR using our own primer sets (for details see Table 3.4). In particular, expressions of *Cxcl10, Cxcl12, Slit2, Tnf* and *Cxcr4* were confirmed to be upregulated as determined by the array, while *Ccl19, Cx3Cl1, Ccl4, and Cclr2* were confirmed to be downregulated (Figure 3.5 A). Additionally, several candidate genes which may contribute to the enhanced survival in the melanocytes themselves were found to be dysregulated. In

particular, anti-apoptotic gene *Birc5* was found to be upregulated, while anti-apoptotic genes *Bcl2*, *Fgf1*, and *Ncam1* were downregulated (Figure 3.5 B). Pro-apoptotic genes *Bad*, *Fos*, and *Trp53* were also downregulated (Figure 3.5 B). In order to confirm that these genes were also altered in the mouse model, we performed FACS to isolate CD117+/CD45- melanocytes from mouse skin [19] 96 h post-UVR (Figure 3.S7 A,B). Similar trends in dysregulated mRNA expression was observed for several genes in cells isolated from *Rxrα/β*$^{mel-/-}$ mice compared to *Rxrα/β* double knockdown cells; specifically chemokines/receptors *Cxcl10, Slit2, Ccrl2, Ccl19, Cx3Cl1,* and *Ccl4* (Figure 3.S7 C) and apoptosis-related genes *Fgf1, Bad,* and *Trp53* (Figure 3.S7 D). It is of note that *Slit2* had no detectable expression in cells collected from control mice; expression was only seen in *Rxrα/β*$^{mel-/-}$ cells (Figure 3.S7 C). Altogether, results suggest that melanocytic RXRα and RXRβ regulate expression of genes encoding chemokines and cytokines involved in chemoattraction/chemorepulsion of immune cells such as macrophage; as well as genes involved in melanocyte apoptosis/survival.

We then hypothesized that RXRs, and in particular RXRα, may directly regulate expression of a subset of genes whose expression was dysregulated in melanocytes lacking *Rxrα/Rxrβ* expression described above. To test that, a region of ~5 kilobases upstream of the transcriptional start site (TSS) for each gene was interrogated for possible binding motifs of RXRα/NR heterodimers (RXREs) as reported in the TRANSFAC database. Promoter sequences of the predicted target genes were targeted for further investigation and primers were

designed to capture those regions (for details see Table 3.5). Chromatin Immunoprecipitation (ChIP) [20] was performed on nuclear extracts from primary melanocytes using an antibody against RXRα. A mock ChIP was also performed using an IgG antibody. We discovered that the promoter regions of *Cxcl10* and *Fos* had significant enrichment for RXRα binding over the IgG control, as determined by RT-qPCR (Figure 3.5 C, D). Although *in silico* analyses of the promoter region of other dysregulated genes revealed several potential RXREs, no ChIP enrichment at those sites was found (Figure 3.S8). The above results suggest that RXRα directly regulates a small subset of genes involved in skin inflammation and survival; while other dysregulated genes found in the *Rxrα/β*$^{mel-/-}$ melanocytes may be regulated either indirectly or *in trans* via DNA binding elements present beyond 5 kb from the TSS.

3.5 Discussion

Loss of expression of RXRα has been previously reported during melanoma progression in humans [4,5]. The present study provides a mechanistic role of RXRs α/β in differentially regulating survival of melanocytes and fibroblasts. We show that RXRs in melanocytes modulate survival of dermal fibroblasts in a non-cell autonomous manner through secretion of paracrine factors and mediate survival of the melanocytes themselves in a cell autonomous manner (Figure 3.6). Furthermore, our results underscore a novel immunomodulatory role of RXRα/β-mediated nuclear receptor signaling to regulate UVR-induced macrophage activation and cell survival.

RXRα is the predominant RXR isotype expressed in skin [21]; however we also chose to ablate RXRβ due to a compensatory upregulation of *Rxrβ* expression in primary murine melanocytes (Figure 3.S4 A). We did not observe a similar compensatory upregulation of *Rxrα* expression following knockdown of *Rxrβ* (Figure 3.S4 B). Previously, a functional redundancy was shown to exist between RXRα and RXRβ in epidermal keratinocytes, although RXRα function was clearly dominant [21].

The dermis of the skin is comprised largely of fibroblasts, which maintain the structure of the skin via forming an extracellular matrix comprised of collagen and other ECM proteins. IFN-γ has been previously speculated to have a role in regulating fibroblast apoptosis. Human fibroblasts exposed to gamma radiation exhibited decreased apoptosis 24 and 48 h post-radiation when treated with IFN-γ *in vitro* [22], and IFN-γ was reported to inhibit TRAIL-induced apoptosis in

fibroblast-like synovial cells [23]. Indeed, we found that murine dermal fibroblasts express IFNGR1 pre- and post-UVR; and supplementation of the culture medium with IFN-γ following UVR exposure enhances a dose dependent survival of those cells.

The role of interferons in cancer immunosurveillance is complex and at times oppositional. Macrophages recruited after UVR promote survival of melanoma cells, and systemic antibody blockade experiments has established the importance of physiologically relevant IFN-γ in UVR-induced melanocyte activation and melanoma cell survival; underscoring a pro-tumorigenic role of IFN-γ in skin [8]. In contrast, overexpression of SOCS1, a negative regulator of IFN-y mediated signaling, has been previously observed in human melanoma [9,24]. Neutralization of IFN-γ in a mouse model has been demonstrated to abrogate rejection of transplanted fibrosarcoma cells [10] and increase aggressiveness of MCA-induced tumors arising from these transplanted cells [10]. Furthermore, blockage of the IFN-γ pathway either through knockout of IFNGR1 [9,11], signal transducer Stat1 [9,11], or IFN-γ [9,12] develop higher number of spontaneous or chemical carcinogen-induced tumors; supporting its anti-tumorigenic activity [9]. Altogether, these findings and our data support the notion that melanocytic ablation of RXR α/β may increase susceptibility to intermittent or chronic UVR-induced melanomas. The correlation between fibroblast apoptosis and melanoma susceptibility has never been thoroughly investigated. It is possible that together with enhanced post-UVR melanocyte survival in absence of RXRα/β, the decreased post-UVR survival of fibroblasts

we observe may encourage proliferation and propagation of dermal melanomas. It has been found previously that clonal expansion of epidermal cells expressing a mutant p53 is driven by chronic UVB-induced apoptosis of the surrounding cells in the skin [13]; leading to enhanced formation of primary papillomas [13]. Future studies are needed to explore the effects of melanocytic RXR α/β ablation on formation of UVR-induced tumors in adult mice.

Our observation that melanocytic ablation of RXR α/β results in decreased infiltration of F4/80+ macrophages, CD11B+ monocytes, CD8+ T-cells and mast cells suggests defects in expression of paracrine chemokine factors secreted by the melanocytes to mediate immune cell infiltration. Secretion of CCR2 ligands CCL2 and CCL8 from melanocytes following UVR irradiation activates F4/80+ macrophages and enhances their recruitment [8]. Although we did not observe changes in *Ccl2* or *Ccl8* expression after *in vitro* knock-down of *Rxrα/β* in melanocytes, we identified dysregulated post-UVR expression of several genes involved in chemoattraction/chemorepulsion of immune cells. In particular, blockage of chemoattractant CX3CL1 has been previously reported to be reduce macrophage infiltration in experimental autoimmune myositis (EAM) mice [25], indicating that its downregulation in our model could contribute to the reduced macrophage infiltration we observe. Similarly, CCL19 has been reported to be a chemoattractant for several different immune cell types, including lymphocytes [26-28], dendritic cells [28,29], natural killer cells [28,30], and macrophage progenitors [28,31]. CCL4 is also reported to be a chemoattractant of macrophages, monocytes, dendritic cells, natural killer cells, and eosinophils

[32]. Likewise, *Ccrl2*$^{-/-}$ mice have been reported to have a reduced inflammatory response in lung tissue following OVA-induced airway inflammation [33].

Regarding chemorepulsive factors, *Slit2* has a role in regulating axon guidance and neuronal migration through chemorepulsion [34]. SLIT2 has been found to inhibit migration of Langerhans cells [34], leukocytes [35], neutrophils [36], and most interestingly, *Slit2*$^{-/-}$ mice were shown to have increased numbers of F4/80+ macrophages [37], underscoring its chemorepulsive properties. Expression of *Slit2* in skin has been reported to be upregulated at both 4 hours and 48 hours following hapten sensitization [34], suggesting *Slit2* can have a role both early and late in an inflammatory response. Likewise, CXCL10 has been shown to repulse plasmacytoid dendritic cells [38]; interestingly CXCL10 has also been shown to inhibit angiogenesis [39-41] and overexpression or mutation of CXCL10 in melanoma cells results in slower growth of xenografts [41,42]. Our results suggest recruitment of RXRα protein on the proximal promoter region of *Cxcl10*, mRNA expression of which is upregulated in our model. Based on our data, CXCL10 may have a significant role in RXR-mediated immune cell recruitment by melanocytes via direct transcriptional regulation.

We did not observe evidence of RXR recruitment on the promoter regions of several genes dysregulated in our model (Figure 3.S8). These results can be reconciled by the fact that expression of these genes may be regulated via alternative mechanisms such as (1) by downstream effectors of RXR, (2) by RXR binding to distal promoter/enhancer regions, and/or (3) regulated *in trans* via enhancer RNAs (eRNAs) [43].

While melanocyte-specific ablation of RXRα/β results in a paracrine effect, altering chemotaxis of immune cells which ultimately affect survival of the dermal fibroblasts, the melanocytes themselves were able to overcome this effect and have enhanced post-UVR survival over controls despite reduced presence of IFN-γ in the microenvironment that modulates UVR-induced melanocyte survival just as in fibroblasts. Our studies utilizing RXR agonist and antagonist suggested that RXRs can independently mediate apoptosis in melanocytes post-UVR via multiple pathways, by transcriptional activation and/or repression of genes. RT-qPCR analyses of pro- and anti-apoptotic genes in isolated *Rxrα/β* double knockdown melanocytes revealed altered expression of several anti-apoptotic and pro-apoptotic genes. In particular, pro-apoptotic genes *Bad* and *Trp53* and anti-apoptotic gene *Fgf1* were found to be dysregulated in a similar fashion in both UVR-exposed *Rxrα/β* double knockdown melanocytes *in vitro* and in FACS-sorted CD117+/CD45- cells from UVR-exposed *Rxrα/β*$^{mel-/-}$ skin *in vivo.* Our results suggest that RXRα binds directly to the promoter of *Fos*, the product of which (c-FOS) makes up a subunit of the AP1 transcription factor and when activated can induce apoptosis [44]. Interestingly, *Fos* was found to be downregulated in the *Rxrα/β* double knockdown melanocytes but upregulated in the *in vivo* FACS-sorted cells. However, these two models are not fully homologous as there is cell-cell signaling at play *in vivo*; and different parameters with regard to UVR-dose and time points are required to elicit similar responses in a homogenous cell monolayer versus a multicellular organ. This could well be the case for why some other genes are dysregulated differently in *Rxrα/β* double

knockdown melanocytes than in the *in vivo* CD117+/CD45- cells. As our results suggest the promoter of *Fos* is bound by RXRα, it is likely that it is indeed a player in regulating melanocyte apoptosis post-UVR, but in a context-dependent manner. We believe that a shift in homeostasis of pro- and anti-apoptotic signals within the melanocytes themselves in absence of the RXRs might contribute to overcome the negative effects of reduced IFN-γ on cell survival seen in the fibroblasts.

Altogether, ablation of RXRα/β expression in melanocytes appears to have two distinct independent effects induced by UVR: (1) A paracrine immunomodulatory effect reducing infiltrating immune cells and hence survival of dermal fibroblasts owing to reduced available IFN-γ in the microenvironment; and, (2) an independent cell-autonomous effect on survival of the melanocytes themselves due to alteration in the expression level of pro- and anti-apoptotic genes (shift in apoptotic signals) selectively in those cells, allowing them to overcome the negative-effects of reduced IFN-γ on cell survival. Whether these changes enhance susceptibility to melanoma and other types of skin cancer in the long-term, need to be further examined in future using chronic or intermittent UV exposure of the *Rxrα/β*$^{mel-/-}$ mice.

3.6 Materials and Methods

Mice

Generation of *Rxrα/β*$^{L2/L2}$ mice has previously been described [45]. To selectively ablate RXRα and RXRβ in melanocytes, mice carrying LoxP-site-containing (floxed) *Rxrα* and *Rxrβ* alleles were bred with hemizygous Tyr-Cre transgenic mice [14] to produce *Rxrα/β*$^{mel-/-}$ mice in Mendelian ratios, following Cre-mediated recombination selectively in melanocytes. A semi-quantitative PCR was performed in an Eppendorf thermal cycler using primers to amplify the Cre, L2 and L- RXR alleles [21,45] as described. Mice were housed in our approved University Animal Facility with 12 h light cycles, food and water were provided ad libitum, and institutional approval was granted for all animal experiments by the Institutional Animal Care and Users Committee (IACUC).

UVR treatment of mice

Neonatal mice (P4 for data in Figure 3.S7, P2 for all other experiments) were exposed to a single dose of 800 mJ/cm^2 of UV-B light from a bank of four Philips FS-40 UV sunlamps as described [6]. The irradiance of the sunlamps was measured with an IL-1400A radiometer with an SEE240 UVB detector (International Light). Mice were euthanized 24, 48, 72 and 96 h after UVR and skin samples retrieved. 0 h samples were taken from P2 mice not exposed to UVR.

Histological analyses

All analyses were performed on 5 μm formalin-fixed paraffin sections. Prior to all procedures, sections were deparaffinized in xylene and rehydrated using graded alcohols. Sections were stained with hematoxylin and eosin (H&E) as previously described [46]. Fontana-Masson staining was performed according to manufacturer's instructions (American MasterTech). Toluidine Blue staining was performed by immersing slides in a solution of 0.1% Toluidine Blue in 1% Sodium Chloride, pH 2.3 for 2 minutes. Slides were then washed/dehydrated by dipping 10 times in 95% EtOH, followed by 10 dips each in 2 changes of 100% EtOH. Slides were cleared in xylene and mounted in DPX mounting medium.

Immunohistochemistry

For immunohistochemistry (IHC) staining studies, paraffin sections from mouse skin (5 μm thick) were deparaffinized in xylene and rehydrated through graded alcohols. Antigen retrieval was performed in a hot water bath (95°C-100°C) using citrate buffer (pH 6.0) for 20 minutes. Frozen sections from mouse skin (8 μm thick) were post-fixed in cold acetone at -20°C for 10 minutes then air dried at room temperature for 20 minutes. All sections were then washed three times with 0.05% PBS-Tween (PBST); then nonspecific antibody binding was blocked using 10% Normal Goat Serum in PBST at room temperature for 30 minutes. Sections were then incubated overnight at 4°C with primary antibody. Primary antibody incubation was followed by three washes with PBST before addition of the secondary antibodies, which were incubated on the sections for 2 hours at

room temperature. Nuclei were counterstained with DAPI (200 ng/mL) for 10 minutes at room temperature. Finally, sections were rinsed with PBST, dehydrated through sequential alcohol washes and then cleared in xylene. Slides were mounted with DPX mounting medium. Antibodies used in IHC are detailed in Table 3.2. For dual TUNEL-IHC staining, the DeadEnd TUNEL System (Promega) was combined with the above protocol. Sections stained without primary antibody was used as a negative control, and all experiments were performed in triplicates.

Imaging and Quantitation of Histological and IHC Experiments

Brightfield images were captured with a Leica DME light microscope using the Leica Application Suite software, version 3.3.1. Fluorescent images were captured using a Zeiss AXIO Imager.Z1 with a digital AxioCam HRm and processed using AxioVision 4.8 and Adobe Photoshop. Epidermal thickness was measured using the Leica Application Suite, taking random measurements across 20 image fields per animal; which were then averaged to calculate an average value per animal. Quantifications of cell labeling were performed by randomly choosing multiple fields imaged from several replicate animals in each group and counting cells using ImageJ software (NIH). All slides were analyzed independently in a double-blinded manner by two investigators and significance was determined using a Student's two-tailed t-test as calculated by GraphPad Prism software.

Primary Melanocyte Culture

Primary C57BL/6 murine melanocytes were obtained from the Yale University Cell Culture Core. Cells were maintained in a complete growth medium consisting of F-12 nutrient mixture (Ham), 8% FBS, bovine pituitary extract (25 µg/mL), TPA (10 ng/mL), 3-isobutyl-1-methylxanthine (22 µg/mL) and 1X antibiotic/antimycotic. Melanocytes were starved into a quiescent state using a minimal culture medium containing F-12 nutrient mixture (Ham), 8% FBS and 1X antibiotic/antimycotic for 48-72 h prior to all experiments. All cell culture/assays were performed at 37°C, 5% CO_2.

Primary Fibroblast Culture

Primary skin fibroblasts were cultured by removing dorsal and ventral skin from newborn mouse pups and incubating in growth medium containing 5 mg/mL dispase at 4°C overnight with rocking. The next day, the skins were washed in sterile PBS and the epidermis separated and discarded. The dermis was incubated in TrypLE Express (Invitrogen) for 30 minutes at 37°C. The dermis was shredded using forceps, suspended in growth medium (F-12 nutrient mixture (Ham), 8% FBS and 1X antibiotic/antimycotic), and vortexed for 2-3 minutes to shed individual cells. The cell suspension was centrifuged (300 x *g*, 3 minutes) and the pellet resuspended in fresh growth medium and plated. Medium was changed the day after plating, and cells were split at a 1:5 ratio once confluency was reached. Cells were maintained for several passages by culturing in aforementioned growth medium and using a 1:5 split ratio. All cell culture/assays

were performed at 37°C, 5% CO_2.

Transfection and sorting of primary melanocytes with shRNA plasmids

Primary melanocytes cultured in complete growth medium (detailed above) were transfected with a 1:1 mixture of *Rxrα* and *Rxrβ* shRNA-containing plasmids (OriGene, pGFP-V-RS for *Rxrα*, pRFP-C-VS for *Rxrβ*) using the Neon Transfection System (Invitrogen) according to manufacturer's instructions. shRNA targeting sequences are detailed in Table 3.3. Cells were incubated post-transfection for 2 days, then detached from plates using TrypLE Express (Invitrogen) and centrifuged (300 *x g*, 3 minutes). Cell pellets were resuspended in minimal growth medium (detailed above) and placed on ice. Fluorescence-activated cell sorting (FACS) of GFP-positive, RFP-positive, or GFP/RFP double-positive cells was accomplished using a Beckman Coulter MoFlo XDP high-speed cell sorter. Cells were sorted into collection tubes containing a high-serum sorting medium (F-12 nutrient mixture (Ham), 16% FBS and 2X antibiotic/antimycotic) to maximize survival of sorted cells. For UVR studies, sorted cells were re-plated, and medium changed for fresh minimal growth medium once cells had fully adhered (3-4 hours post-plating). Cells were incubated in minimal growth medium for 48 hours prior to use for sample collections or experiments.

FACS sorting of CD117+/CD45- melanocytes from neonatal mouse skin

P4 neonatal mice were irradiated with UVR as described above. 96 hours post-

UVR, mice were sacrificed and dorsal skin was collected. Skin was placed in growth medium [F-12 nutrient mixture (Ham)] containing 5 mg/ml dispase and incubated overnight at 4°C. Skin was then diced using forceps and incubated in TrypLE Select (Invitrogen) for 30 mins at 37°C. Individual cells were shed by physical agitation and suspended in growth medium [(F-12 nutrient mixture (Ham)), 8% FBS]. Cell suspensions were filtered (50 μm), pelleted by centrifugation (300 x *g*, 3 minutes) and resuspended in labeling buffer (PBS + 2% FBS). Non-specific cell-surface binding was blocked by adding Fc Block (BD Pharmingen) at a concentration of 1 μg/10^6 cells and incubating on ice for 10 minutes [19]. PE-CD117 and FITC-CD45 antibodies were added at a concentration of 0.2 μg/10^6 cells [19] and incubated at 4°C for 1 hour with rocking. Two-color FACS sorting was accomplished using a Beckman Coulter MoFlo XDP high-speed cell sorter. Non-labeled and single-labeled samples were used to calibrate the sorter. Cells were sorted directly into Trizol reagent (Invitrogen) for RNA isolation.

UVR treatment of cells *in vitro*

Prior to UVR, growth medium was removed from culture dishes by aspiration. Cells were washed briefly with sterile PBS, which was then removed by aspiration. Lids from culture dishes were removed, and cell monolayers were exposed a single dose of 10 mJ/cm^2 of UV-B light from a bank of four Philips FS-40 UV sunlamps as described above. Immediately after UVR, fresh growth medium was added back to the cells and were returned to the growth incubator.

Immunoblotting analyses

Protein lysates were obtained by collecting cells in a lysis buffer (20 mM HEPES, 250 mM NaCl, 2 mM EDTA, 1% SDS, 10% glycerol, 50 mM NaF, 0.1 mM hemin chloride, 5 mM NEM, 1 mM PMSF and 10 mg/mL leupeptin and aproptinin) [6,47,48] followed by sonication. Protein concentration was performed using the BCA assay (Thermo Scientific). Equal amounts of protein extract (9-15 µg depending on experiment) from each lysate were resolved using sodium dodecyl sulfate polyacrylamide gel electrophoresis and transferred onto a nitrocellulose membrane as described. The blots were blocked overnight with 5% nonfat dry milk and incubated with specific antibodies. The antibodies used are detailed in Table 3.2. After incubation with the appropriate secondary antibody, signals were detected using immunochemiluminescent reagents (GE Healthcare, Piscataway, NJ). Equal protein loading in each lane was confirmed with a β-actin antibody (#A300-491, Bethyl).

ELISA Assays

Protein lysates were prepared as described above. Assays were performed using the eBioscience 'Mouse IFNg 'Femto-HS' High Sensitivity ELISA Ready-Set-Go!' kit according to manufacturer's protocol. 25 µg of protein was loaded per well. Lysates from three mice per group were used and assays performed in triplicate wells. Student's two-tailed t-test was performed using GraphPad Prism software.

Annexin V/Propidium Iodide Assay of Apoptosis in Cultured Cells

Cultured primary melanocytes or fibroblasts were irradiated with UVR as described above. Following UVR, fresh growth medium was added to cells supplemented with treatment, such as 1 μM BMS-649 (A gift from Hinrich Gronemeyer; IGBMC, France) or 100 nM HX-531 (Tocris Bioscience) (Figure 3.2 G); recombinant IFN-y (Millipore) (Figure 3.3 E), or appropriate vehicles. Additionally, cells treated with BMS-649 or HX-531 were pre-treated for 24 h prior to UVR. 24 h post-UVR, cells were harvested and assayed for apoptosis using an Annexin V/Propidium Iodide assay. The assay was performed using a Tali Image-Based Cytometer (Invitrogen) and Tali Apoptosis Kit (Invitrogen) according to manufacturer's protocol. 9 or 20 Tali image fields for each sample were analyzed depending on experiment. All assays were performed in triplicate. Student's two-tailed t-test was performed using GraphPad Prism software.

Reverse transcription–quantitative PCR (RT-qPCR) Analyses of Transcriptional Changes

Total RNA was extracted from cell monolayers using Trizol (Invitrogen), followed by purification using RNEasy spin columns (Qiagen). cDNA was synthesized using SuperScript III RT (Invitrogen). Amplification was performed on an ABI Real Time PCR machine using a QuantiTect SYBR Green PCR kit (Qiagen), and all targets were normalized to the housekeeping gene *Hprt*. All reactions were performed in quadruplicates or sextuplicates. Melting curve analyses were performed to ensure specificity of amplification. Student's two-tailed t-test was performed using GraphPad Prism software.

In silico discovery of RXREs and Chromatin Immunoprecipitation RT-qPCR (ChIP-RT-qPCR) Analyses

In silico discovery of consensus RXR response elements (RXREs) was performed on a 5kb region upstream from the transcription start site, using the Fuzznuc utility (EMBOSS). Primers were designed to capture regions containing potential RXREs. Cultured primary melanocytes were crosslinked using formaldehyde. $3x10^6$ cells were used for each ChIP. Chromatin was sheared using 10 sonication cycles of 10 s with 20% amplitude. ChIP was performed using either 2 µg of an RXRα antibody (Santa Cruz Biotechnology, see Table 3.2) or non-specific IgG (Santa Cruz Biotechnology). RT-qPCR amplification was performed on an ABI Real Time PCR machine using a QuantiTect SYBR Green PCR kit (Qiagen). All reactions were performed in quadruplicates, and average Ct values were used for calculating percent input. Melting curve analyses were performed to ensure specificity of amplification. Each assay was performed in replicate three times. Student's two-tailed t-test was performed using GraphPad Prism software.

3.7 Acknowledgments

We thank members of the Indra lab and the OSU College of Pharmacy, specifically Dr. Mark Zabriskie and Dr. Gary Delander for their continuous support and encouragement. We would also like thank the OSU Environmental Health Sciences Center (EHSC). We are grateful for services provided by the Cell and Tissue Analysis Facilities and Services Core of the EHSC at OSU; specifically C. Samuel Bradford for help with flow cytometry. We would also like to thank the OHSU Knight Cancer Institute.

3.8 References

1. Chambon P (1996) A decade of molecular biology of retinoic acid receptors. FASEB J 10: 940-954.

2. Heyman RA, Mangelsdorf DJ, Dyck JA, Stein RB, Eichele G, et al. (1992) 9-cis retinoic acid is a high affinity ligand for the retinoid X receptor. Cell 68: 397-406.

3. Leid M, Kastner P, Chambon P (1992) Multiplicity generates diversity in the retinoic acid signalling pathways. Trends Biochem Sci 17: 427-433.

4. Chakravarti N, Lotan R, Diwan AH, Warneke CL, Johnson MM, et al. (2007) Decreased expression of retinoid receptors in melanoma: entailment in tumorigenesis and prognosis. Clin Cancer Res 13: 4817-4824.

5. Hyter S, Bajaj G, Liang X, Barbacid M, Ganguli-Indra G, et al. (2010) Loss of nuclear receptor RXRalpha in epidermal keratinocytes promotes the formation of Cdk4-activated invasive melanomas. Pigment Cell Melanoma Res 23: 635-648.

6. Wang Z, Coleman DJ, Bajaj G, Liang X, Ganguli-Indra G, et al. (2011) RXRalpha ablation in epidermal keratinocytes enhances UVR-induced DNA damage, apoptosis, and proliferation of keratinocytes and melanocytes. J Invest Dermatol 131: 177-187.

7. Payne AS, Cornelius LA (2002) The role of chemokines in melanoma tumor growth and metastasis. J Invest Dermatol 118: 915-922.

8. Zaidi MR, Davis S, Noonan FP, Graff-Cherry C, Hawley TS, et al. (2011) Interferon-gamma links ultraviolet radiation to melanomagenesis in mice. Nature 469: 548-553.

9. Dunn GP, Koebel CM, Schreiber RD (2006) Interferons, immunity and cancer immunoediting. Nat Rev Immunol 6: 836-848.

10. Dighe AS, Richards E, Old LJ, Schreiber RD (1994) Enhanced in vivo growth and resistance to rejection of tumor cells expressing dominant negative IFN gamma receptors. Immunity 1: 447-456.

11. Kaplan DH, Shankaran V, Dighe AS, Stockert E, Aguet M, et al. (1998) Demonstration of an interferon gamma-dependent tumor surveillance system in immunocompetent mice. Proc Natl Acad Sci U S A 95: 7556-7561.

12. Street SE, Cretney E, Smyth MJ (2001) Perforin and interferon-gamma activities independently control tumor initiation, growth, and metastasis. Blood 97: 192-197.

13. Zhang W, Hanks AN, Boucher K, Florell SR, Allen SM, et al. (2005) UVB-induced apoptosis drives clonal expansion during skin tumor development. Carcinogenesis 26: 249-257.

14. Delmas V, Martinozzi S, Bourgeois Y, Holzenberger M, Larue L (2003) Cre-mediated recombination in the skin melanocyte lineage. Genesis 36: 73-80.

15. Nissan X, Larribere L, Saidani M, Hurbain I, Delevoye C, et al. (2011) Functional melanocytes derived from human pluripotent stem cells engraft into pluristratified epidermis. Proc Natl Acad Sci U S A 108: 14861-14866.

16. Baxter LL, Pavan WJ (2002) The oculocutaneous albinism type IV gene Matp is a new marker of pigment cell precursors during mouse embryonic development. Mech Dev 116: 209-212.

17. Martinez-Pomares L, Platt N, McKnight AJ, da Silva RP, Gordon S (1996) Macrophage membrane molecules: markers of tissue differentiation and heterogeneity. Immunobiology 195: 407-416.

18. Lin HH, Faunce DE, Stacey M, Terajewicz A, Nakamura T, et al. (2005) The macrophage F4/80 receptor is required for the induction of antigen-specific efferent regulatory T cells in peripheral tolerance. J Exp Med 201: 1615-1625.

19. Diwakar G, Zhang D, Jiang S, Hornyak TJ (2008) Neurofibromin as a regulator of melanocyte development and differentiation. J Cell Sci 121: 167-177.

20. Wang Z, Zhang LJ, Guha G, Li S, Kyrylkova K, et al. (2012) Selective ablation of Ctip2/Bcl11b in epidermal keratinocytes triggers atopic dermatitis-like skin inflammatory responses in adult mice. PLoS One 7: e51262.

21. Li M, Indra AK, Warot X, Brocard J, Messaddeq N, et al. (2000) Skin abnormalities generated by temporally controlled RXRalpha mutations in mouse epidermis. Nature 407: 633-636.

22. Savoldi-Barbosa M, Sakamoto-Hojo ET (2001) Influence of interferon-gamma on radiation-induced apoptosis in normal and ataxia-telangiectasia fibroblast cell lines. Teratog Carcinog Mutagen 21: 417-429.

23. Tamai M, Kawakami A, Tanaka F, Miyashita T, Nakamura H, et al. (2006) Significant inhibition of TRAIL-mediated fibroblast-like synovial cell apoptosis by IFN-gamma through JAK/STAT pathway by translational regulation. J Lab Clin Med 147: 182-190.

24. Li Z, Metze D, Nashan D, Muller-Tidow C, Serve HL, et al. (2004) Expression of SOCS-1, suppressor of cytokine signalling-1, in human melanoma. J Invest Dermatol 123: 737-745.

25. Suzuki F, Nanki T, Imai T, Kikuchi H, Hirohata S, et al. (2005) Inhibition of CX3CL1 (fractalkine) improves experimental autoimmune myositis in SJL/J mice. J Immunol 175: 6987-6996.

26. Kim CH, Pelus LM, White JR, Applebaum E, Johanson K, et al. (1998) CK beta-11/macrophage inflammatory protein-3 beta/EBI1-ligand chemokine is an efficacious chemoattractant for T and B cells. J Immunol 160: 2418-2424.

27. Ngo VN, Tang HL, Cyster JG (1998) Epstein-Barr virus-induced molecule 1 ligand chemokine is expressed by dendritic cells in lymphoid tissues and strongly attracts naive T cells and activated B cells. J Exp Med 188: 181-191.

28. Gibejova A, Mrazek F, Subrtova D, Sekerova V, Szotkowska J, et al. (2003) Expression of macrophage inflammatory protein-3 beta/CCL19 in pulmonary sarcoidosis. Am J Respir Crit Care Med 167: 1695-1703.

29. Dieu MC, Vanbervliet B, Vicari A, Bridon JM, Oldham E, et al. (1998) Selective recruitment of immature and mature dendritic cells by distinct chemokines expressed in different anatomic sites. J Exp Med 188: 373-386.

30. Kim CH, Pelus LM, Appelbaum E, Johanson K, Anzai N, et al. (1999) CCR7 ligands, SLC/6Ckine/Exodus2/TCA4 and CKbeta-11/MIP-3beta/ELC, are chemoattractants for CD56(+)CD16(-) NK cells and late stage lymphoid progenitors. Cell Immunol 193: 226-235.

31. Kim CH, Pelus LM, White JR, Broxmeyer HE (1998) Macrophage-inflammatory protein-3 beta/EBI1-ligand chemokine/CK beta-11, a CC chemokine, is a chemoattractant with a specificity for macrophage progenitors among myeloid progenitor cells. J Immunol 161: 2580-2585.

32. Jing H, Vassiliou E, Ganea D (2003) Prostaglandin E2 inhibits production of the inflammatory chemokines CCL3 and CCL4 in dendritic cells. J Leukoc Biol 74: 868-879.

33. Otero K, Vecchi A, Hirsch E, Kearley J, Vermi W, et al. (2010) Nonredundant role of CCRL2 in lung dendritic cell trafficking. Blood 116: 2942-2949.

34. Guan H, Zu G, Xie Y, Tang H, Johnson M, et al. (2003) Neuronal repellent Slit2 inhibits dendritic cell migration and the development of immune responses. J Immunol 171: 6519-6526.

35. Wu JY, Feng L, Park HT, Havlioglu N, Wen L, et al. (2001) The neuronal repellent Slit inhibits leukocyte chemotaxis induced by chemotactic factors. Nature 410: 948-952.

36. Tole S, Mukovozov IM, Huang YW, Magalhaes MA, Yan M, et al. (2009) The axonal repellent, Slit2, inhibits directional migration of circulating neutrophils. J Leukoc Biol 86: 1403-1415.

37. Marlow R, Strickland P, Lee JS, Wu X, Pebenito M, et al. (2008) SLITs suppress tumor growth in vivo by silencing Sdf1/Cxcr4 within breast epithelium. Cancer Res 68: 7819-7827.

38. Kohrgruber N, Groger M, Meraner P, Kriehuber E, Petzelbauer P, et al. (2004) Plasmacytoid dendritic cell recruitment by immobilized CXCR3 ligands. J Immunol 173: 6592-6602.

39. Keeley EC, Mehrad B, Strieter RM (2008) Chemokines as mediators of neovascularization. Arterioscler Thromb Vasc Biol 28: 1928-1936.

40. Mehrad B, Keane MP, Strieter RM (2007) Chemokines as mediators of angiogenesis. Thromb Haemost 97: 755-762.

41. Richmond A, Yang J, Su Y (2009) The good and the bad of chemokines/chemokine receptors in melanoma. Pigment Cell Melanoma Res 22: 175-186.

42. Yang J, Richmond A (2004) The angiostatic activity of interferon-inducible protein-10/CXCL10 in human melanoma depends on binding to CXCR3 but not to glycosaminoglycan. Mol Ther 9: 846-855.

43. Melo CA, Drost J, Wijchers PJ, van de Werken H, de Wit E, et al. (2013) eRNAs are required for p53-dependent enhancer activity and gene transcription. Mol Cell 49: 524-535.

44. Na HK, Kim EH, Choi MA, Park JM, Kim DH, et al. (2012) Diallyl trisulfide induces apoptosis in human breast cancer cells through ROS-mediated activation of JNK and AP-1. Biochem Pharmacol 84: 1241-1250.

45. Li M, Messaddeq N, Teletin M, Pasquali JL, Metzger D, et al. (2005) Retinoid X receptor ablation in adult mouse keratinocytes generates an atopic dermatitis triggered by thymic stromal lymphopoietin. Proc Natl Acad Sci U S A 102: 14795-14800.

46. Indra AK, Castaneda E, Antal MC, Jiang M, Messaddeq N, et al. (2007) Malignant transformation of DMBA/TPA-induced papillomas and nevi in the skin of mice selectively lacking retinoid-X-receptor alpha in epidermal keratinocytes. J Invest Dermatol 127: 1250-1260.

47. Wang Z, Kirkwood JS, Taylor AW, Stevens JF, Leid M, et al. (2013) Transcription factor Ctip2 controls epidermal lipid metabolism and regulates expression of genes involved in sphingolipid biosynthesis during skin development. J Invest Dermatol 133: 668-676.

48. Liang X, Bhattacharya S, Bajaj G, Guha G, Wang Z, et al. (2012) Delayed cutaneous wound healing and aberrant expression of hair follicle stem cell markers in mice selectively lacking Ctip2 in epidermis. PLoS One 7: e29999.

Figure 3.1: Loss of RXRs α and β are restricted to melanocytes in *Rxrα/β*$^{mel-/-}$ mice.

(A) Experimental scheme for *in vivo* experiments. Floxed *Rxrα/β*$^{L2/L2}$ (controls) and *Rxrα/β*$^{mel-/-}$ mice are irradiated with UVR at Day 2 post-natal (P2) and samples collected at the indicated time points. (B, C) IHC for (B) RXRα or (C) RXRβ (red) co-labeled with melanocyte-specific marker TYRP1 (green) on skin sections collected from mice 96 hours post-UVR. Melanocytes are indicated by yellow arrows. Floxed *Rxrα/β*$^{L2/L2}$ control mice show melanocytes labeled for the RXRs, *Rxrα/β*$^{mel-/-}$ mice show melanocytes that are negative, as it is excised specifically in that cell type. E=epidermis, D=dermis, HF= hair follicle, M=melanocyte. Scale bar = 50 μm.

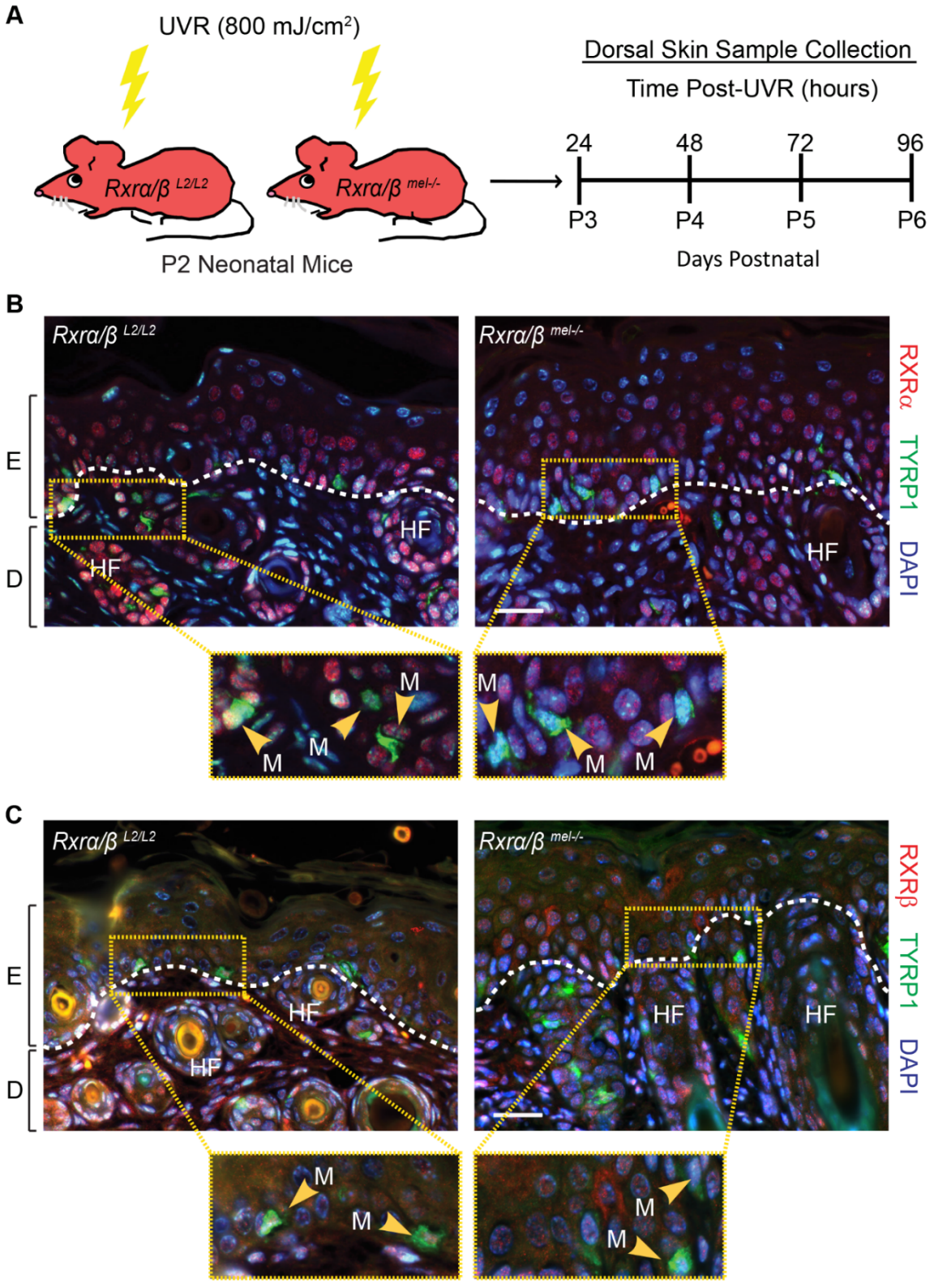
A
UVR (800 mJ/cm²)
Rxrα/β L2/L2
Rxrα/β mel-/-
P2 Neonatal Mice
Dorsal Skin Sample Collection
Time Post-UVR (hours)
24
48
72
96
P3
P4
P5
P6
Days Postnatal
B
Rxrα/β L2/L2
Rxrα/β mel-/-
E
D
HF
M
RXRα
TYRP1
DAPI
C
RXRβ

Figure 3.1

Figure 3.2: Loss of melanocytic RXRs α and β results in contrasting changes in cell survival in dermal skin cells and melanocytes following UV radiation.

(A-F) Histological analyses of skin sections following a single dose of UVR. (A, B) IHC for the proliferation marker PCNA. Proliferating cells are indicated by red staining. ** = p≤ 0.01. (C, D) TUNEL assay to label apoptotic cells. Apoptotic cells are indicated by green staining. * = p≤ 0.05, ** = p≤ 0.01. (E, F) Hybrid TUNEL-IHC to analyze apoptosis specifically in melanocytes. Apoptotic cells are indicated by green staining, cells positive for the melanocyte-specific marker TYRP1 are indicated by red staining. White arrows indicate normal melanocytes, yellow arrows indicate apoptotic melanocytes. * = p≤ 0.1. (G) Apoptosis of cultured melanocytes 24 h post-UVR as a percentage of total cells as measured using Annexin V/Propidium Iodide staining. Cells were treated pre- and post-UVR with RXR agonist BMS-649, antagonist HX-531, or their vehicles as controls (EtOH and DMSO, respectively). *** = p≤ 0.001. For all images: DAPI (blue) was used to counterstain nuclei. E=epidermis, D=dermis, HF= hair follicle. Scale bars = 50 μm.

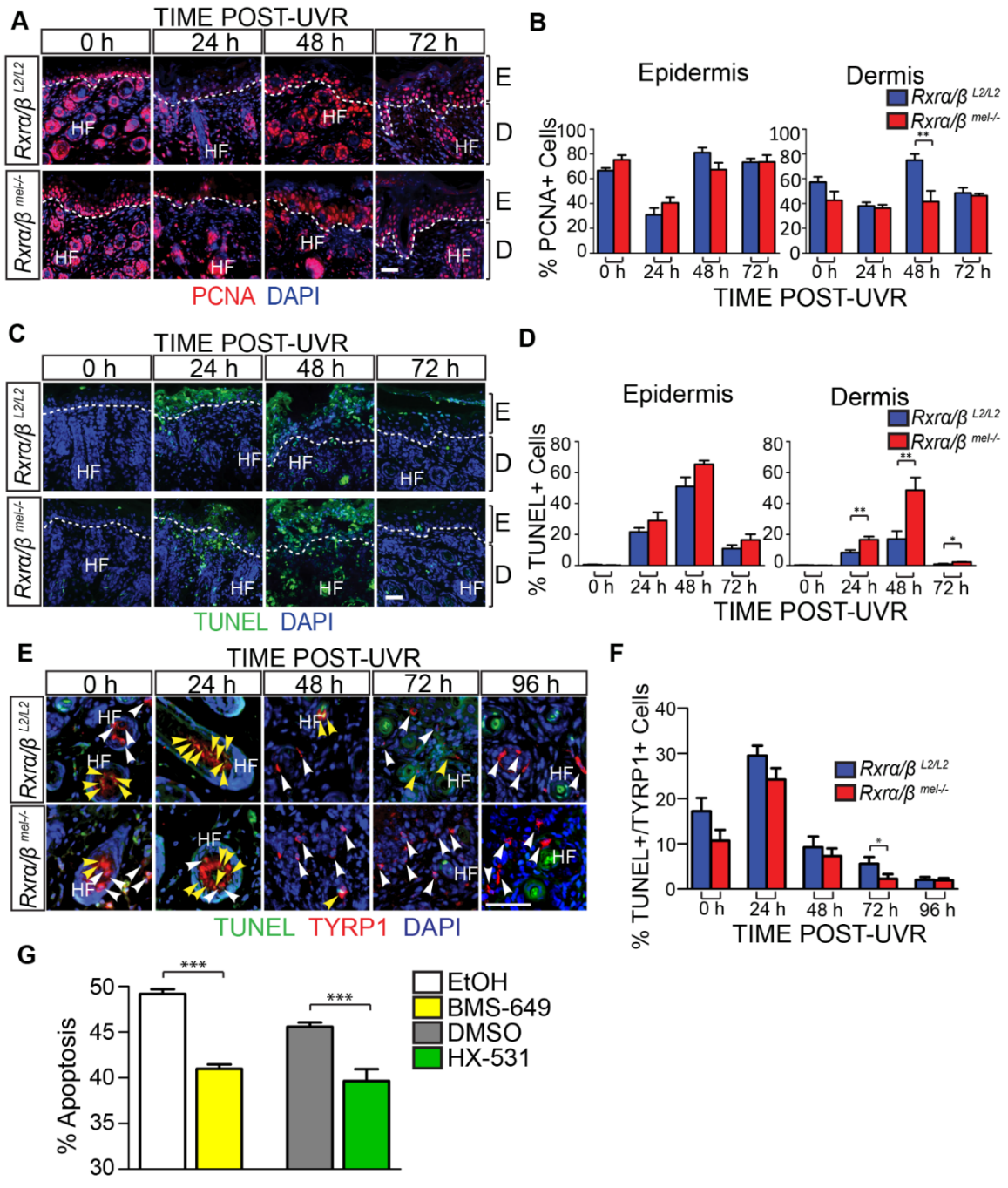
A
TIME POST-UVR
0 h
24 h
48 h
72 h
Rxrα/β L2/L2
Rxrα/β mel-/-
HF
E
D
PCNA DAPI
B
Epidermis
Dermis
Rxrα/β L2/L2
Rxrα/β mel-/-
% PCNA+ Cells
TIME POST-UVR
C
TUNEL DAPI
D
% TUNEL+ Cells
E
96 h
TUNEL TYRP1 DAPI
F
% TUNEL+/TYRP1+ Cells
G
% Apoptosis
EtOH
BMS-649
DMSO
HX-531

Figure 3.2

Figure 3.3: Loss of melanocytic RXRs α and β results in reduced monocyte/macrophage infiltration and corresponding reduced interferon-γ (IFN- γ) expression following UV radiation. IFN-γ influences cell survival post-UVR *in vitro.*

(A) IHC using antibodies specific for IFN- γ (green) and macrophage antigen F4/80 (red) on skin sections collected from mice post-UVR. DAPI (blue) was used to counterstain nuclei. E=epidermis, D=dermis, HF= hair follicle. Scale bars = 50 μm. (B) Western Blot for macrophage antigen F4/80 in skin lysates collected post-UVR. (C) ELISA assay for IFN- γ in skin lysates collected post-UVR. ** = p≤ 0.01. (D, E) IFN- γ acts as a positive effector of post-UV survival in both melanocytes and fibroblasts. (D) Western blot of Interferon-γ receptor 1 (INFGR1) expression in cultured primary melanocytes and fibroblasts pre- and 24 h post-UVR. (E) Apoptosis of cultured fibroblasts and melanocytes 24 h post-UVR as a percentage of total cells as measured using Annexin V/Propidium Iodide. Immediately after UV treatment, culture medium was replaced with fresh medium containing several concentrations of recombinant IFN- γ. * = p≤ 0.05, ** = p≤ 0.01, **** = p≤ 0.0001.

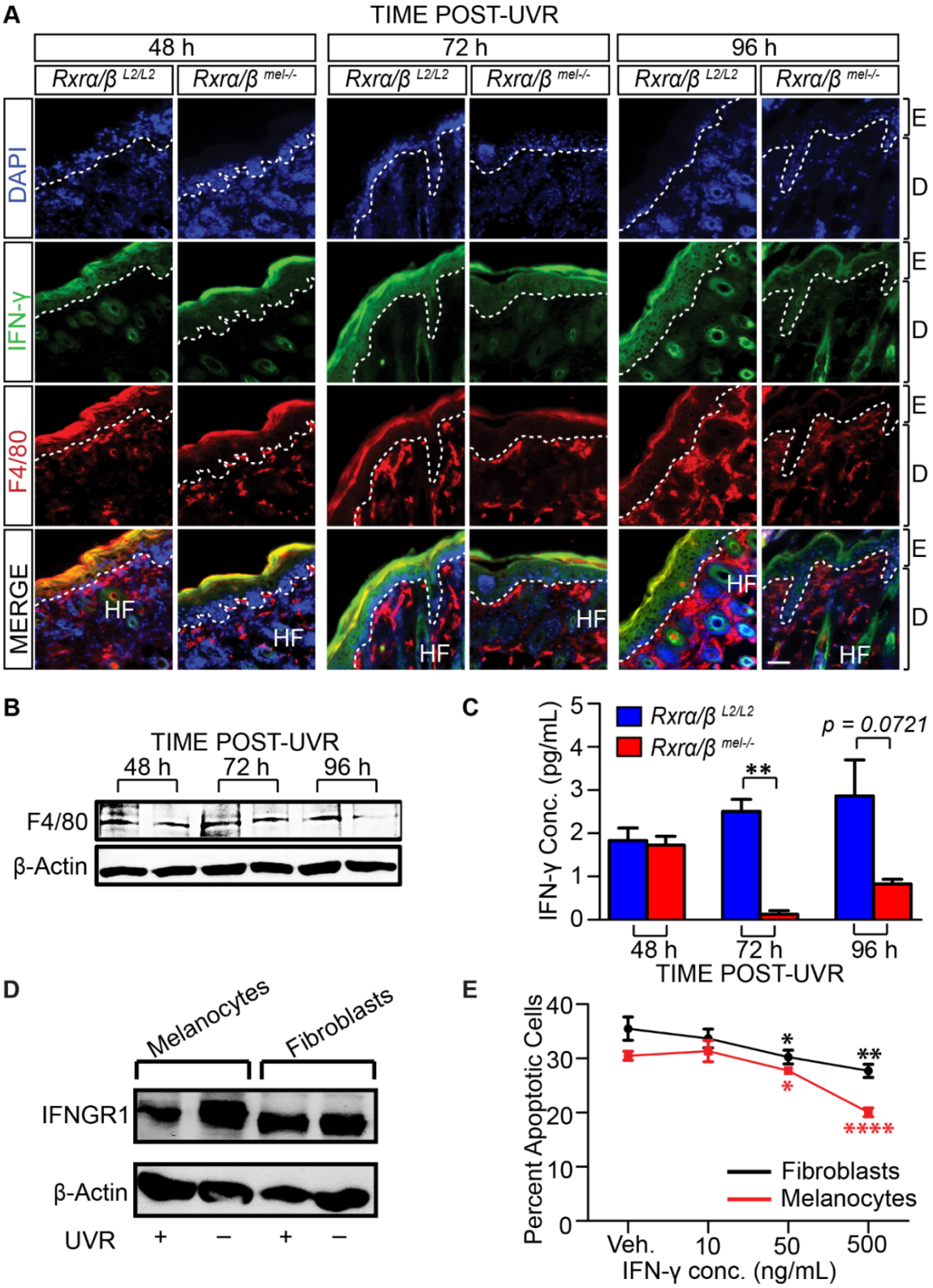
A
TIME POST-UVR
48 h
72 h
96 h
Rxrα/β L2/L2
Rxrα/β mel-/-
DAPI
IFN-γ
F4/80
MERGE
E
D
HF
B
TIME POST-UVR
48 h
72 h
96 h
F4/80
β-Actin
C
Rxrα/β L2/L2
Rxrα/β mel-/-
p = 0.0721
**
IFN-γ Conc. (pg/mL)
0
1
2
3
4
5
48 h
72 h
96 h
TIME POST-UVR
D
Melanocytes
Fibroblasts
IFNGR1
β-Actin
UVR + − + −
E
Percent Apoptotic Cells
0
10
20
30
40
*
**
*
****
Fibroblasts
Melanocytes
Veh.
10
50
500
IFN-γ conc. (ng/mL)

Figure 3.3

Figure 3.4: Generation of *Rxrα/Rxrβ* double knockdown murine melanocytes.

(A) Primary murine melanocytes were transfected using a mixture of two shRNA-expressing plasmids targeting either *Rxrα* or *Rxrβ*. The *Rxrα* shRNA plasmid contains a GFP marker gene; *Rxrβ* shRNA contains a RFP marker gene. Cells positive for both GFP and RFP were sorted using FACS and re-cultured. (B) Re-cultured melanocytes following FACS express both GFP and RFP, indicating expression of both *Rxrα* and *Rxrβ* shRNA constructs. (C) RT-qPCR for measurement of *Rxrα/β* mRNA expression ****= p≤ 0.0001. (D) Western Blot for protein expression of RXRα in FACS-sorted cells.

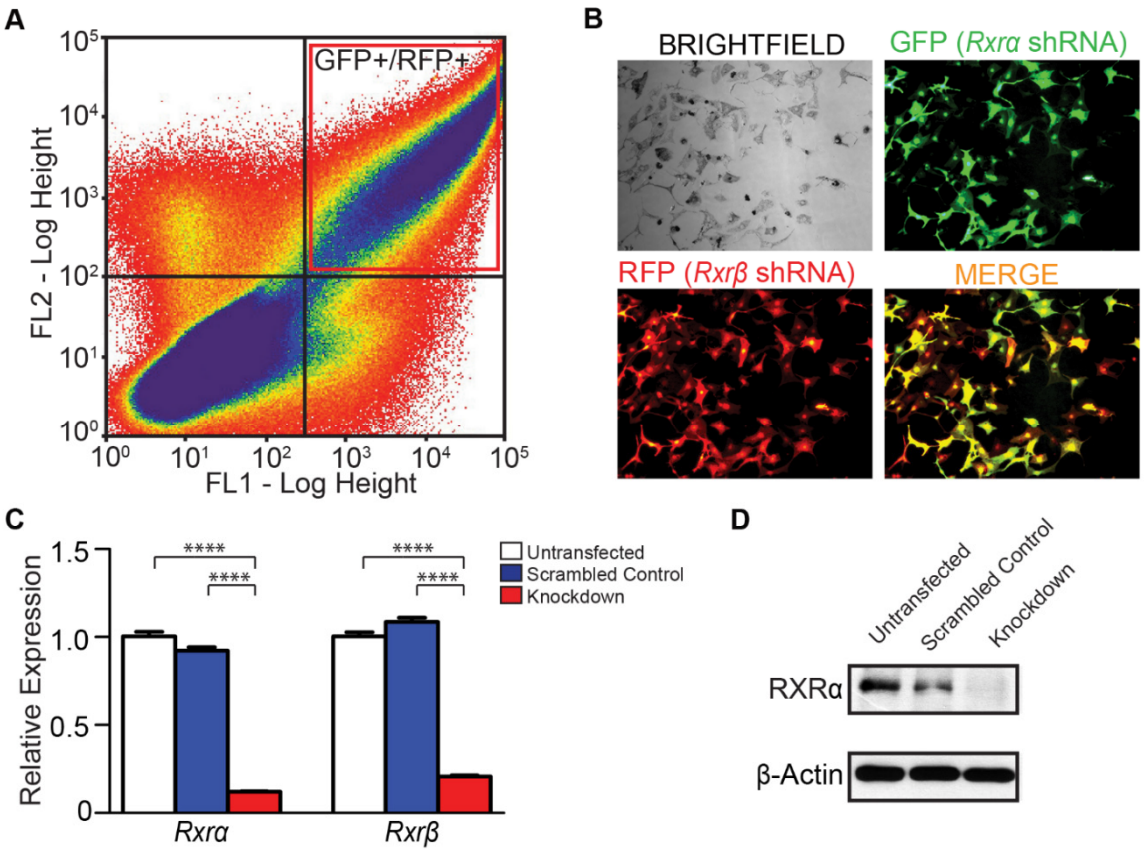
A
GFP+/RFP+
FL2 - Log Height
FL1 - Log Height
B
BRIGHTFIELD
GFP (Rxrα shRNA)
RFP (Rxrβ shRNA)
MERGE
C
Relative Expression
Untransfected
Scrambled Control
Knockdown
Rxrα
Rxrβ
D
Untransfected
Scrambled Control
Knockdown
RXRα
β-Actin

Figure 3.4

Figure 3.5: Ablation of RXR α and β in melanocytes results in altered expression of several chemokines post-UVR, as well as pro- and anti-apoptotic genes, some of which may be direct binding targets of RXRα.

(A, B) Expression of genes found changed in RXRα/β double knockdown melanocytes post-UVR via RT-qPCR arrays (Figure S6). Expression of several chemokines (A) and apoptosis-related genes (B) were then re-verified by RT-qPCR using new primer sets. Primers spanning exon junctions were designed independently, and assays were performed on biological replicates of the sample used in the array. *= p≤ 0.05 **, = p≤ 0.01, *** = p≤ 0.001, **** = p≤ 0.0001. (C, D) *In silico* analysis was used to find potential RXR response elements using Fuzznuc motif finder. These candidate binding sites were verified for enrichment in primary melanocytes using ChIP-RT-qPCR. A mock ChIP using a control IgG antibody was also performed. Arrows indicate targeting regions for primers. Genes negative for enrichment can be found in Figure S8. ** = p≤ 0.01.

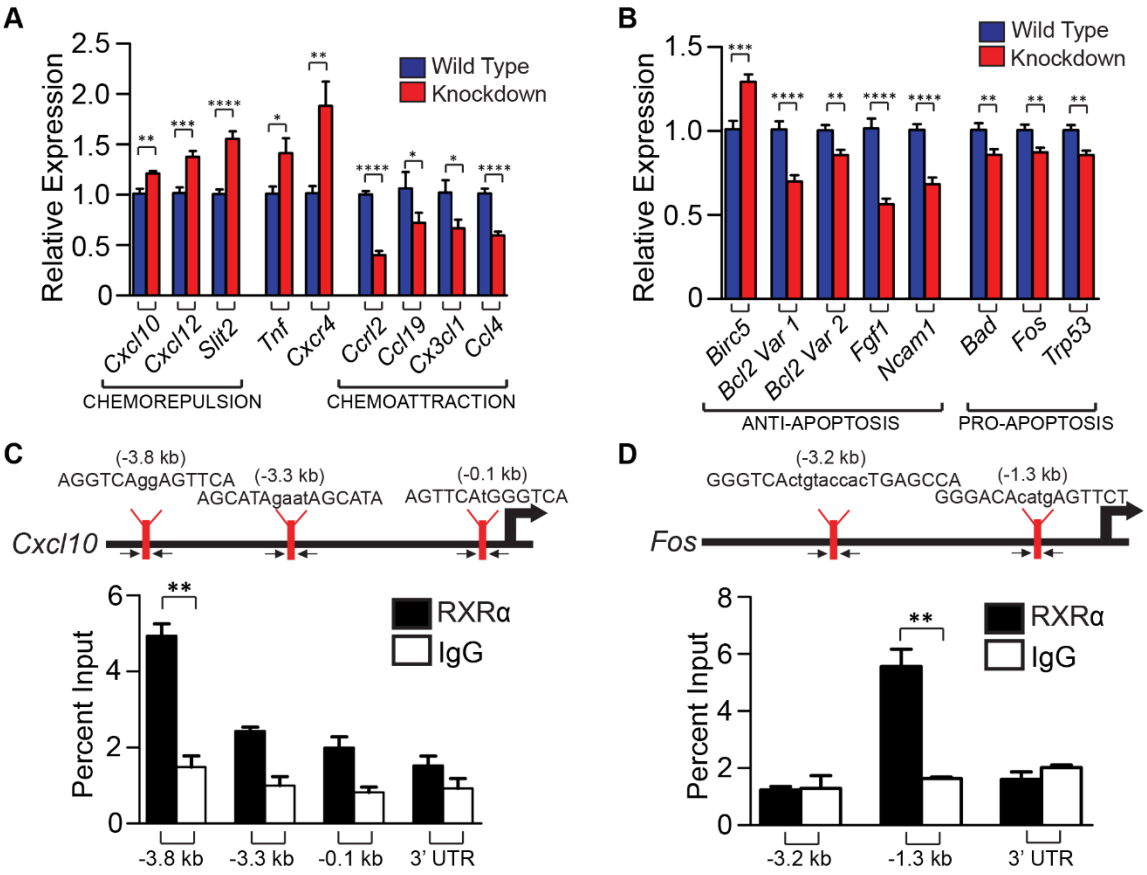
A
Relative Expression
Wild Type
Knockdown
Cxcl10
Cxcl12
Slit2
Tnf
Cxcr4
Ccrl2
Ccl19
Cx3cl1
Ccl4
CHEMOREPULSION
CHEMOATTRACTION
B
Relative Expression
Wild Type
Knockdown
Birc5
Bcl2 Var 1
Bcl2 Var 2
Fgf1
Ncam1
Bad
Fos
Trp53
ANTI-APOPTOSIS
PRO-APOPTOSIS
C
(-3.8 kb)
AGGTCAggAGTTCA
(-3.3 kb)
AGCATAgaatAGCATA
(-0.1 kb)
AGTTCAtGGGTCA
Cxcl10
Percent Input
RXRα
IgG
-3.8 kb
-3.3 kb
-0.1 kb
3' UTR
D
(-3.2 kb)
GGGTCActgtaccacTGAGCCA
(-1.3 kb)
GGGACAcatgAGTTCT
Fos
Percent Input
RXRα
IgG
-3.2 kb
-1.3 kb
3' UTR

Figure 3.5

Figure 3.6: Mechanistic representation of post-UVR defects in *Rxrα/β*$^{mel-/-}$ mice compared to control mice.

In *Rxrα/β*$^{L2/L2}$ control mice post-UVR, melanocytes recruit immune cells via secretion of chemoattractive and repulsive ligands (A). The recruited immune cells secrete IFN-y, which promotes survival of melanocytes/fibroblasts and stimulates additional chemokine secretion from melanocytes via a feedback loop (B). In *Rxrα/β*$^{mel-/-}$ mice, there is less secretion of chemoattractive and more secretion of chemorepulsive ligands from the melanocytes (C). As a result, fewer immune cells are recruited as a result of shift in the chemoattractive/repulsive ligands, resulting in reduced available IFN-y (D), negatively influencing fibroblast survival (E). (F) As RXRs α and β are ablated specifically in melanocytes, an endogenous shift in pro- and anti- apoptotic signals results in enhanced survival of melanocytes in *Rxrα/β*$^{mel-/-}$ mice relative to controls.

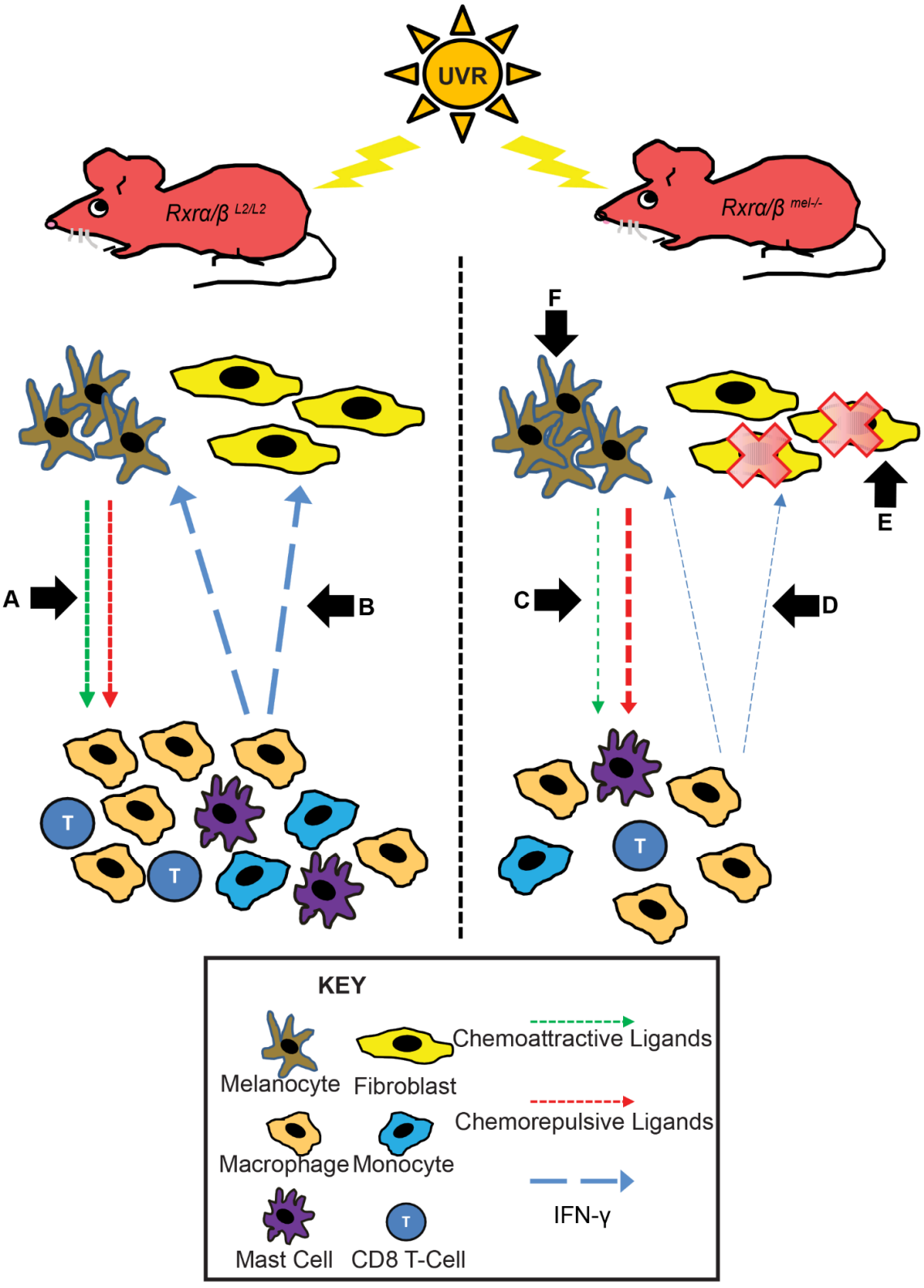
UVR
Rxrα/β L2/L2
Rxrα/β mel-/-
A
B
C
D
E
F
T
T
T
KEY
Melanocyte
Fibroblast
Chemoattractive Ligands
Macrophage
Monocyte
Chemorepulsive Ligands
IFN-γ
Mast Cell
CD8 T-Cell

Figure 3.6

Figure 3.S1: No phenotypic changes observed in adult *Rxrα/β*$^{mel-/-}$ mice compared to controls; post-UVR epidermal thickness and melanocyte numbers are unchanged following ablation of RXR α and β in melanocytes.

(A) Comparison of adult *Rxrα/β*$^{mel-/-}$ to their *Rxrα/β*$^{L2/L2}$ controls. No phenotypic differences or effects on viability are observed. (B, C) H&E staining of skin sections following a single dose of UVR. At least five individual measurements of epidermal thickness were made on 20 different fields. (D, E) Fontana-Masson staining of skin sections following a single dose of UVR. Black staining indicates melanin. Nuclei were counter-stained with Nuclear Fast Red. Black-stained cells were presumed to be melanocytes and quantitated. Yellow arrows indicate epidermal extrafollicular melanocytes; green arrows indicate extrafollicular dermal melanocytes. For all images: E=epidermis, D=dermis, HF=Hair Follicle. Scale bar = 50 μm.

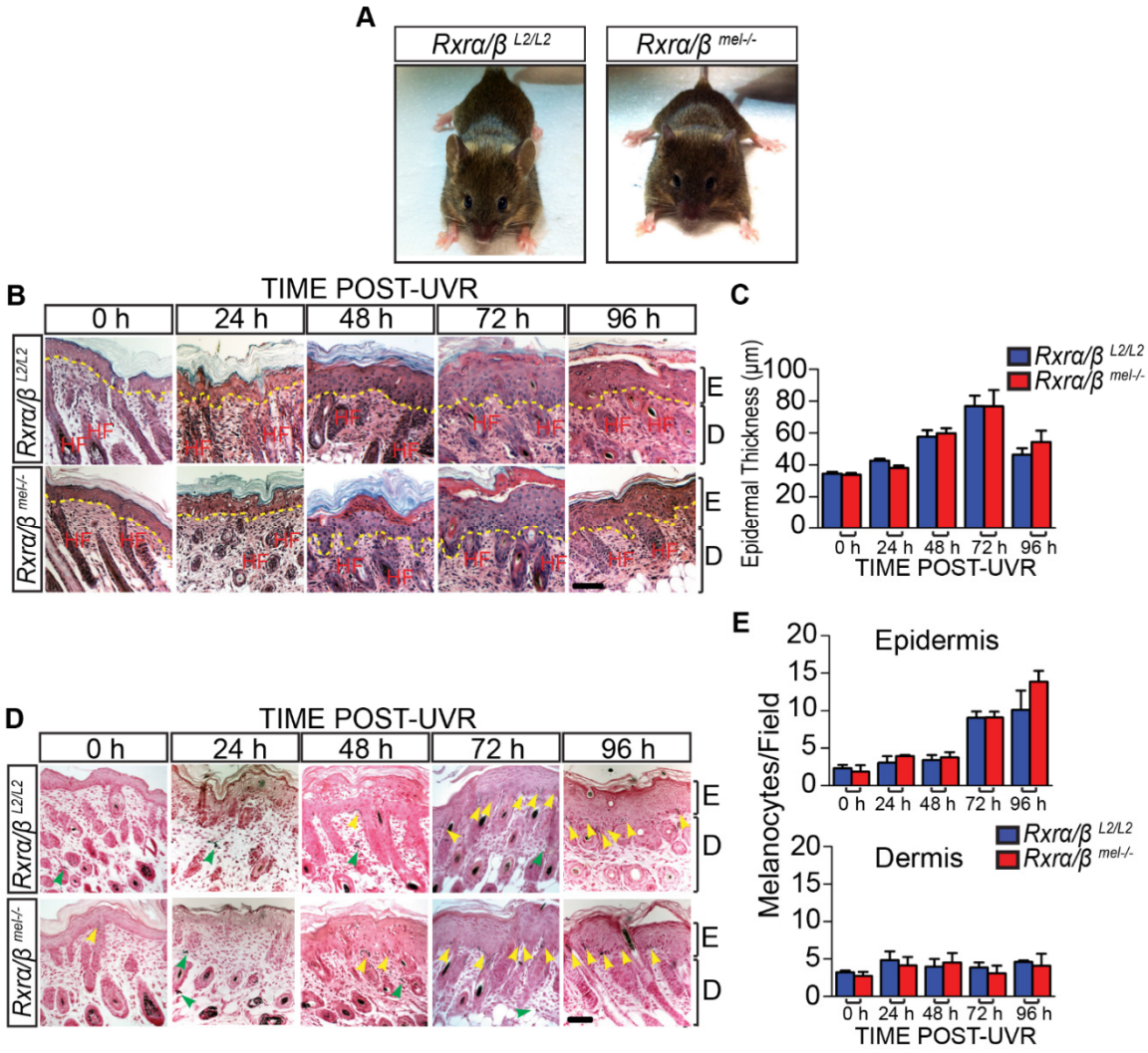
A
Rxrα/β L2/L2
Rxrα/β mel-/-
B
TIME POST-UVR
0 h
24 h
48 h
72 h
96 h
Rxrα/β L2/L2
Rxrα/β mel-/-
E
D
HF
C
Epidermal Thickness (μm)
100
80
60
40
20
0
0 h 24 h 48 h 72 h 96 h
TIME POST-UVR
Rxrα/β L2/L2
Rxrα/β mel-/-
D
TIME POST-UVR
0 h
24 h
48 h
72 h
96 h
Rxrα/β L2/L2
Rxrα/β mel-/-
E
D
E
Epidermis
Melanocytes/Field
20
15
10
5
0
0 h 24 h 48 h 72 h 96 h
Rxrα/β L2/L2
Rxrα/β mel-/-
Dermis
20
15
10
5
0
0 h 24 h 48 h 72 h 96 h
TIME POST-UVR

Figure 3.S1

Figure 3.S2: Levels of post-UVR cyclopyrimidine dimer (CPD) formation and oxidative DNA damage (8-oxo-dG) across all skin compartments is unchanged as a result of ablating RXR α and β from melanocytes.

IHC of skin sections following a single dose of UVR. (A, B) CPD+ cells are indicated by red staining. CPD formation in melanocytes was assessed by co-labeling for the melanocyte-specific protein TYRP1, indicated by green staining. DAPI (blue) was used to counter-stain nuclei. (C, D) 8-oxo-dG+ cells are indicated by red staining. CPD formation in melanocytes was assessed by co-labeling for TYRP1, indicated by green staining. DAPI (blue) was used to counterstain nuclei for all images. E=epidermis, D=dermis, HF= hair follicle. Scale bars = 50 μm.

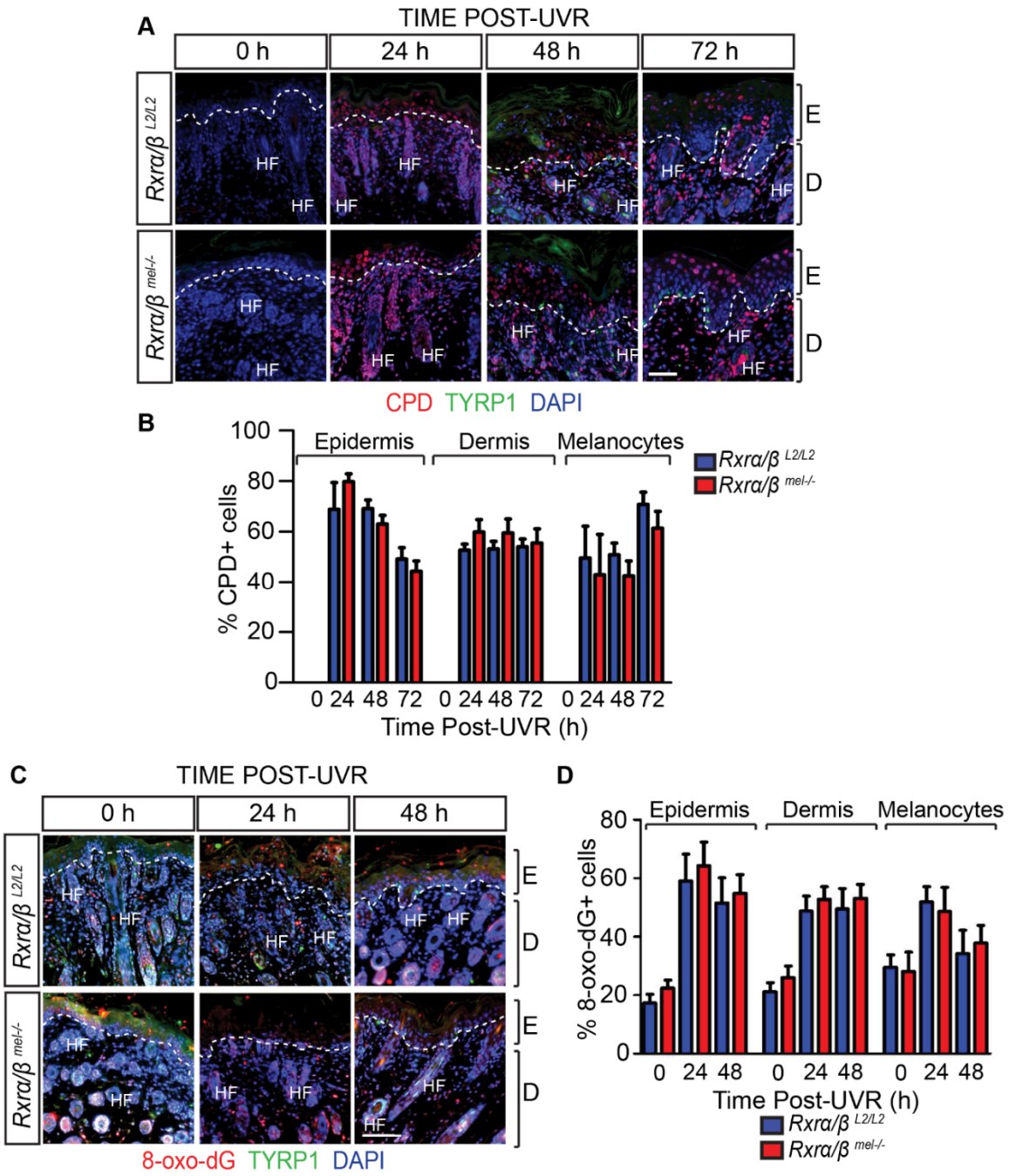
A
TIME POST-UVR
0 h
24 h
48 h
72 h
Rxrα/β L2/L2
Rxrα/β mel-/-
HF
E
D
CPD TYRP1 DAPI
B
100
80
60
40
20
0
% CPD+ cells
Epidermis
Dermis
Melanocytes
Rxrα/β L2/L2
Rxrα/β mel-/-
0 24 48 72 0 24 48 72 0 24 48 72
Time Post-UVR (h)
C
TIME POST-UVR
0 h
24 h
48 h
8-oxo-dG TYRP1 DAPI
D
80
60
40
20
0
% 8-oxo-dG+ cells
Epidermis
Dermis
Melanocytes
0 24 48 0 24 48 0 24 48
Time Post-UVR (h)
Rxrα/β L2/L2
Rxrα/β mel-/-

Figure 3.S2

Figure 3.S3: Loss of melanocytic RXRs α and β also alters profile of infiltrating immune cells other than macrophage following UV radiation.

(A-D) Histological characterizations of skin sections following a single dose of UVR. (A) Monocytes are labeled by red staining, indicating cells positive for the monocyte marker CD11B by IHC. Yellow arrows designate positive cells; boxes indicate clusters of positive cells. ** = p≤ 0.01. (B) IHC labeling for CD8-positive T-Cells, as indicated by red immunofluorescence. Yellow arrows designate positive cells. *** = p≤ 0.001. (C) Toluidine Blue staining of skin sections. Mast cells are indicated by purple staining. ** = p≤ 0.01. (D) IHC labeling for CD3-positive T-Cells, as indicated by red immunofluorescence. Yellow arrows designate positive cells. DAPI (blue) was used to counterstain nuclei in all fluorescent images. E=epidermis, D=dermis, HF= hair follicle. Scale bars = 50 μm.

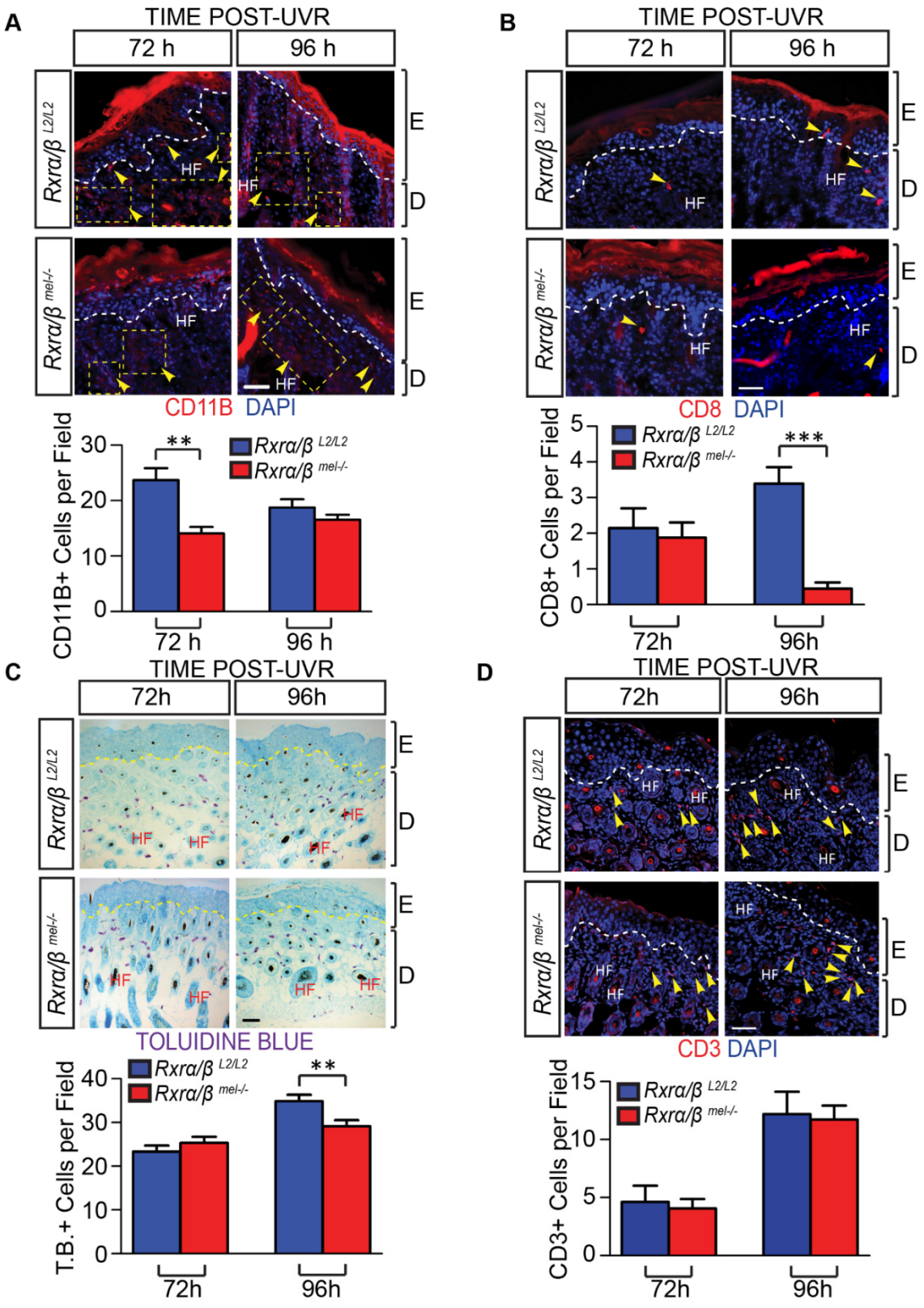
A
TIME POST-UVR
72 h
96 h
Rxrα/β L2/L2
Rxrα/β mel-/-
E
D
HF
CD11B DAPI
CD11B+ Cells per Field
**
Rxrα/β L2/L2
Rxrα/β mel-/-
72 h
96 h
B
TIME POST-UVR
72 h
96 h
CD8 DAPI
CD8+ Cells per Field
***
72h
96h
C
TIME POST-UVR
72h
96h
TOLUIDINE BLUE
T.B.+ Cells per Field
**
D
TIME POST-UVR
72h
96h
CD3 DAPI
CD3+ Cells per Field

Figure 3.S3

Figure 3.S4: Compensatory upregulation of *Rxrβ* expression when *Rxrα* is knocked down in melanocytes.

Expression of each *Rxr* mRNA transcript (*α* or *β*) when the other is knocked down using shRNA, measured by RT-qPCR. (A) *Rxrβ* is upregulated when *Rxrα* is knocked down in primary murine melanocytes; (B) there is not a similar compensatory upregulation of *Rxrα* when *Rxrβ* is knocked down. All cells were sorted for shRNA plasmid transfection by FACS, using either a GFP or RFP marker gene. # = No Statistically Significant Difference, *** = p≤ 0.001, **** = p≤ 0.0001.

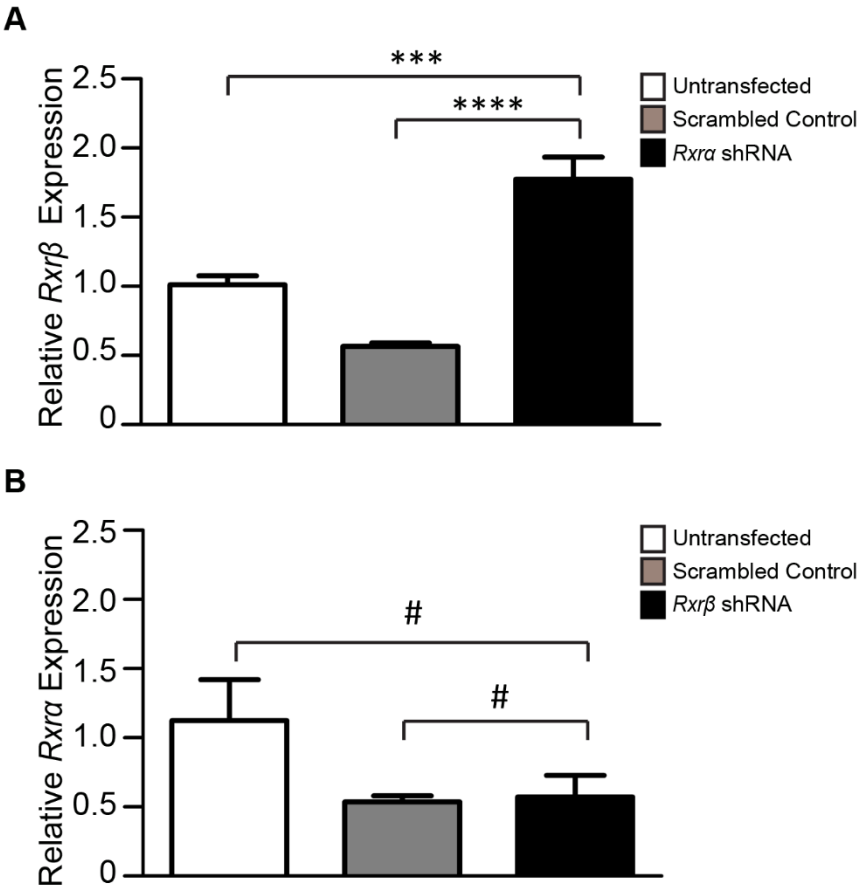
A
***
****
Untransfected
Scrambled Control
Rxrα shRNA
Relative Rxrβ Expression
2.5
2.0
1.5
1.0
0.5
0
B
Untransfected
Scrambled Control
Rxrβ shRNA
#
#
Relative Rxrα Expression
2.5
2.0
1.5
1.0
0.5
0

Figure 3.S4

Figure 3.S5: Analysis of peak mRNA expression of chemokines *Ccl2* and *Ccl8* post-UV in cultured wild-type melanocytes.

Expression of mRNA transcripts for *Ccl2* and *Ccl8* following UV-B radiation of cultured melanocytes was measured using RT-PCR. (A) *Ccl2* expression was highest 6 hours following treatment of cells with 10 mJ/cm^2 UV-B. Similarly, expression of *Ccl8* (B) also peaked at the same time point and UVR dose. In both cases lower UVR doses resulted in a reduced response, and all elevated expression was attenuated 24 hours post-UVR.

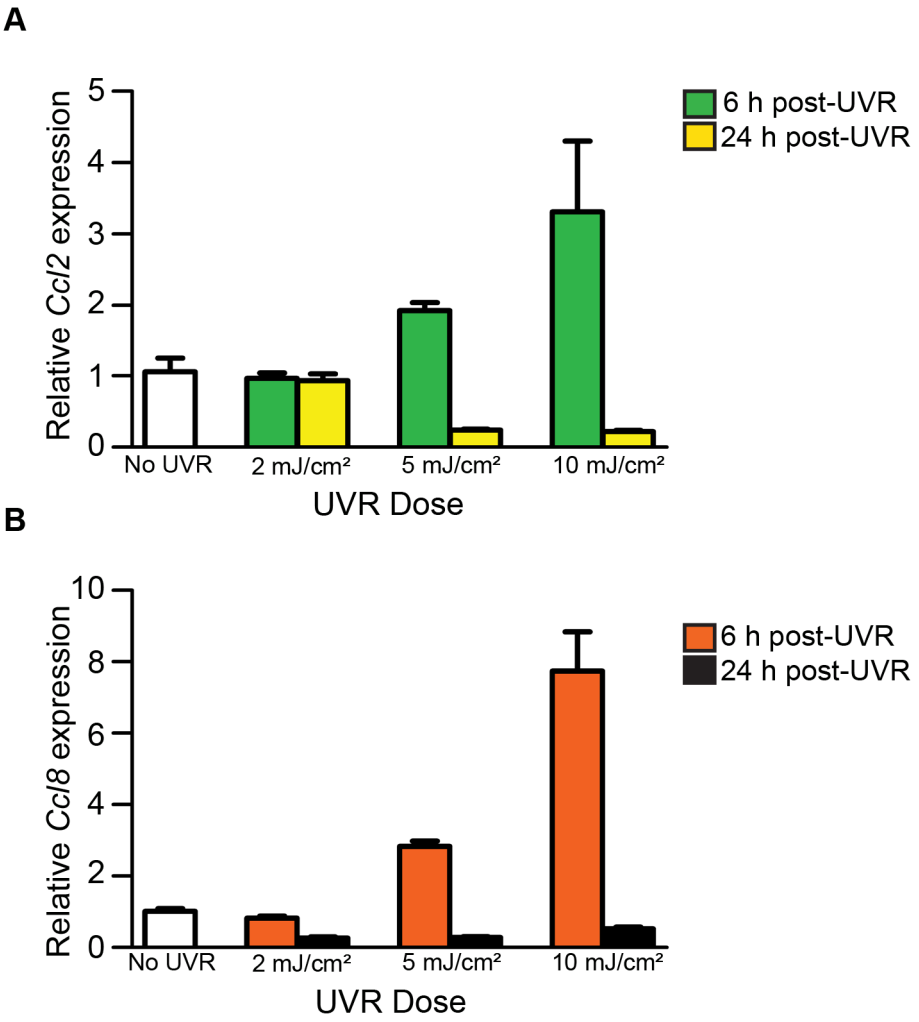
A
Relative Ccl2 expression
0
1
2
3
4
5
No UVR
2 mJ/cm²
5 mJ/cm²
10 mJ/cm²
UVR Dose
6 h post-UVR
24 h post-UVR
B
Relative Ccl8 expression
0
2
4
6
8
10
No UVR
2 mJ/cm²
5 mJ/cm²
10 mJ/cm²
UVR Dose
6 h post-UVR
24 h post-UVR

Figure 3.S5

Figure 3.S6: RT-qPCR arrays to determine altered expression of chemokines/receptors and apoptosis-related genes in RXR knockdown melanocytes post-UVR; and re-validation of results.

(A, B) Heat maps generated by RT-qPCR arrays (SA Biosciences) for mouse chemokines (PAMM-022) (A) and mouse cancer (PAMM-033) (B). Heat maps reflect changes in gene expression in UVR-treated primary melanocytes with *Rxr α* and *β* knocked down using shRNA. (C, D) Several genes of interest found to be altered in RXR knockdown melanocytes were verified in biological replicates using our own primer sets. Primers spanning exon junctions were designed independently, and assays were performed on biological replicates of the sample used in the array. # = no statistical significance, ** = $p \leq 0.01$, *** = $p \leq 0.001$, **** = $p \leq 0.0001$. Re-validations of several other genes are shown in Figure 5. (E, F) BioTapestry representation of fold changes as determined by RT-qPCR arrays.

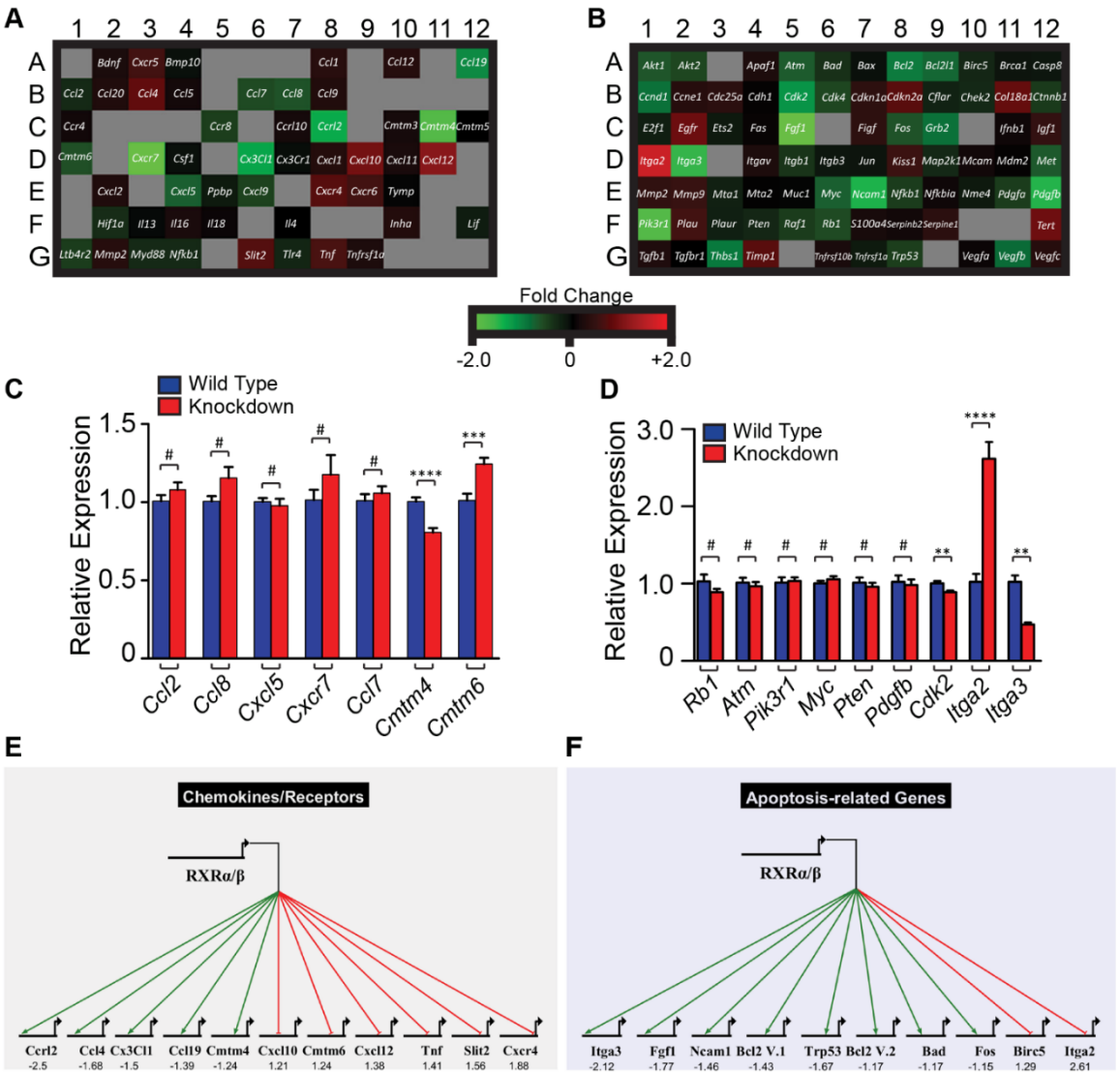
A
B
Fold Change
-2.0
0
+2.0
C
Wild Type
Knockdown
Relative Expression
Ccl2
Ccl8
Cxcl5
Cxcr7
Ccl7
Cmtm4
Cmtm6
D
Rb1
Atm
Pik3r1
Myc
Pten
Pdgfb
Cdk2
Itga2
Itga3
E
Chemokines/Receptors
RXRα/β
Ccrl2 -2.5
Ccl4 -1.68
Cx3Cl1 -1.5
Ccl19 -1.39
Cmtm4 -1.24
Cxcl10 1.21
Cmtm6 1.24
Cxcl12 1.38
Tnf 1.41
Slit2 1.56
Cxcr4 1.88
F
Apoptosis-related Genes
RXRα/β
Itga3 -2.12
Fgf1 -1.77
Ncam1 -1.46
Bcl2 V.1 -1.43
Trp53 -1.67
Bcl2 V.2 -1.17
Bad -1.17
Fos -1.15
Birc5 1.29
Itga2 2.61

Figure 3.S6

Figure 3.S7: Melanocytes isolated by FACS from UVR-treated *Rxrα/β*$^{mel-/-}$ mouse skin show similar gene dysregulation to cultured *Rxrα/β* double shRNA knockdown melanocytes.

(A) Live cells were collected from neonatal mouse skin (96 hours post-UVR) and dual-labeled with fluorescent-conjugated antibodies to cell surface antigens CD117 and CD45 in order to isolate CD117+/CD45- melanocytes. (B) The FACS-isolated CD117+/CD45- cells show upregulated mRNA expression of several melanocyte markers compared to CD117+/CD45+ control cells (non-melanocytes), confirming the success of the sort. (C, D) mRNA expression of several chemokines (C) and apoptosis-related genes (D) previously found dysregulated in irradiated cultured *Rxrα/β* double shRNA knockdown melanocytes (Figure 5) showed similar dysregulations in the isolated CD117+/CD45- cells from *Rxrα/β*$^{mel-/-}$ mice compared to cells isolated from control mice. In particular, chemokines *Cxcl10, Slit2, Ccl19, Cx3Cl1, Ccl4* and apoptosis-related genes *Fgf1, Bad* and *Trp53* were dysregulated in a similar trend to cultured Rxrα/β double shRNA knockdown melanocytes. ψ = no detectable expression in *Rxrα/β*$^{L2/L2}$, only in *Rxrα/β*$^{mel-/-}$. * = $p \leq 0.05$, ** = ≤ 0.01, *** = $p \leq 0.001$.

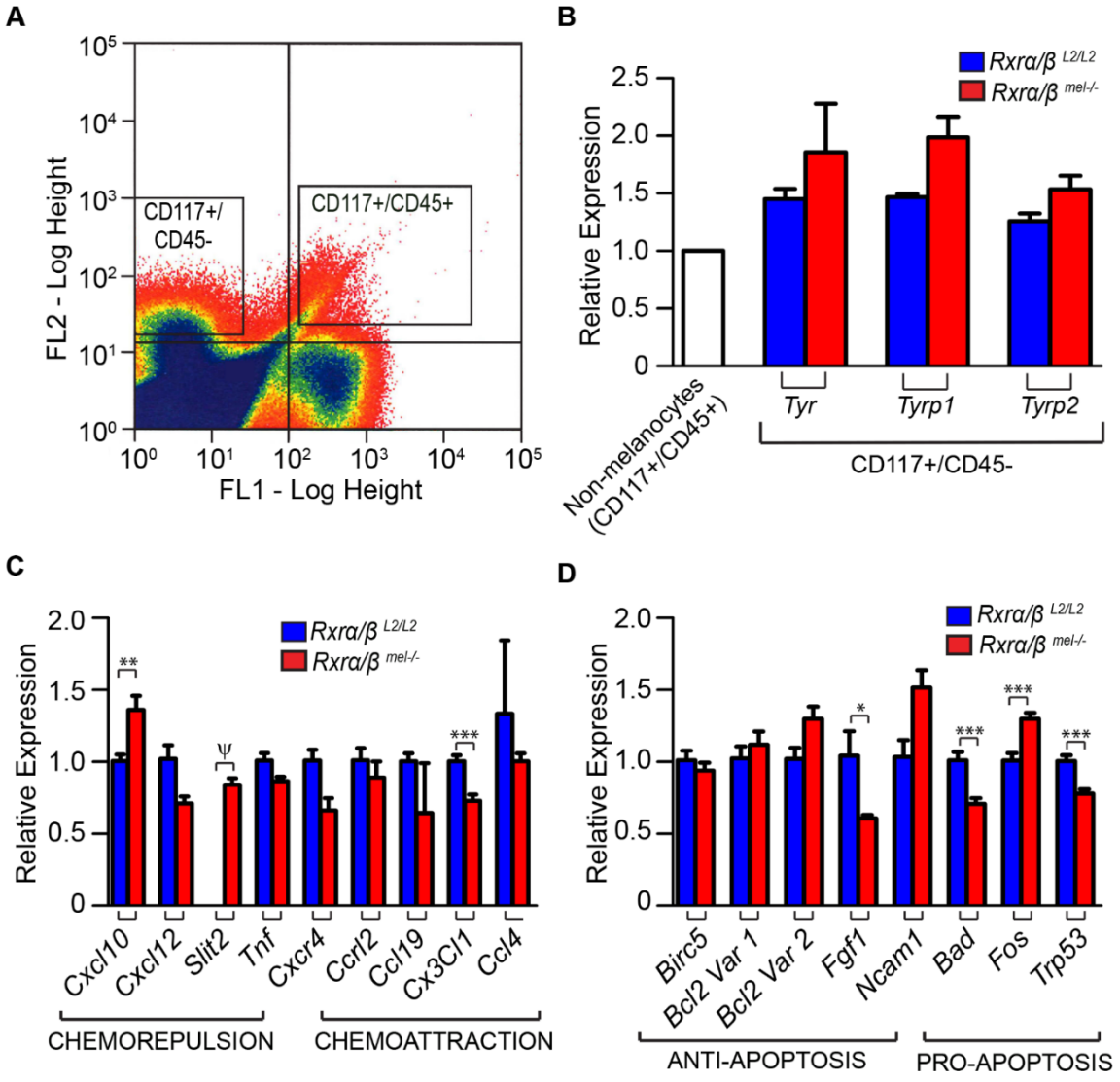
A
FL2 - Log Height
FL1 - Log Height
CD117+/
CD45-
CD117+/CD45+
B
Relative Expression
Rxrα/β L2/L2
Rxrα/β mel-/-
Non-melanocytes
(CD117+/CD45+)
Tyr
Tyrp1
Tyrp2
CD117+/CD45-
C
Relative Expression
Cxcl10
Cxcl12
Slit2
Tnf
Cxcr4
Ccrl2
Ccl19
Cx3Cl1
Ccl4
CHEMOREPULSION
CHEMOATTRACTION
D
Relative Expression
Birc5
Bcl2 Var 1
Bcl2 Var 2
Fgf1
Ncam1
Bad
Fos
Trp53
ANTI-APOPTOSIS
PRO-APOPTOSIS

Figure 3.S7

Figure 3.S8: *In silico* analysis was used to find potential RXR response elements using Fuzznuc motif finder.

(A-H) These candidate binding sites were tested for enrichment using ChIP-RT-qPCR. A mock ChIP using a control IgG antibody was also performed. Arrows indicate targeting regions for primers. No significant enrichment was found for these genes. For significantly enriched genes, see Figure 5.

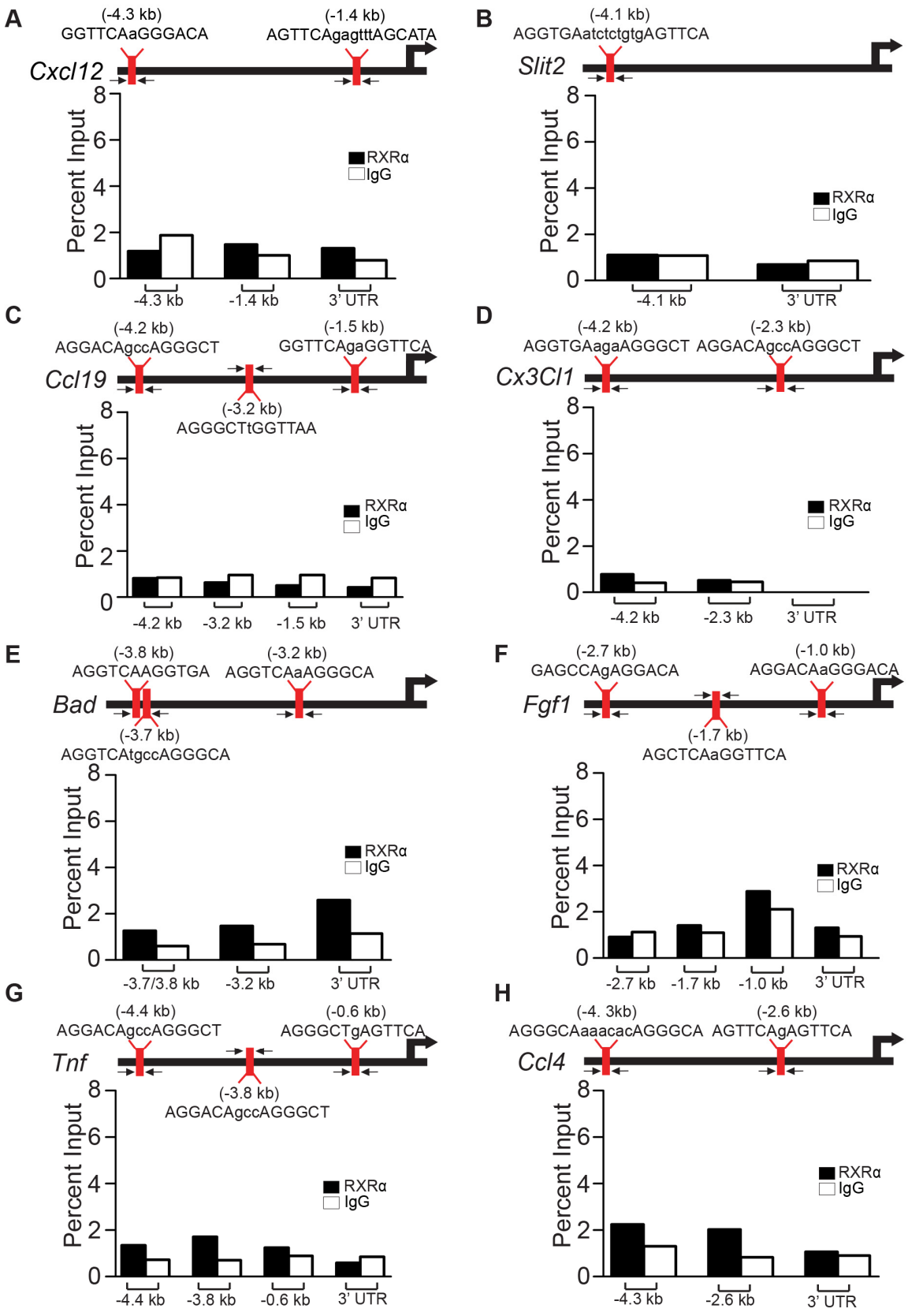
A
(-4.3 kb)
GGTTCAaGGGACA
(-1.4 kb)
AGTTCAgagtttAGCATA
Cxcl12
Percent Input
RXRα
IgG
-4.3 kb
-1.4 kb
3' UTR
B
(-4.1 kb)
AGGTGAatctctgtgAGTTCA
Slit2
C
(-4.2 kb)
AGGACAgccAGGGCT
(-1.5 kb)
GGTTCAgaGGTTCA
Ccl19
(-3.2 kb)
AGGGCTtGGTTAA
-4.2 kb
-3.2 kb
-1.5 kb
D
(-4.2 kb)
AGGTGAagaAGGGCT
(-2.3 kb)
AGGACAgccAGGGCT
Cx3Cl1
E
(-3.8 kb)
AGGTCAAGGTGA
(-3.2 kb)
AGGTCAaAGGGCA
Bad
(-3.7 kb)
AGGTCAtgccAGGGCA
-3.7/3.8 kb
F
(-2.7 kb)
GAGCCAgAGGACA
(-1.0 kb)
AGGACAaGGGACA
Fgf1
(-1.7 kb)
AGCTCAaGGTTCA
G
(-4.4 kb)
AGGACAgccAGGGCT
(-0.6 kb)
AGGGCTgAGTTCA
Tnf
(-3.8 kb)
AGGACAgccAGGGCT
H
(-4. 3kb)
AGGGCAaaacacAGGGCA
(-2.6 kb)
AGTTCAgAGTTCA
Ccl4

Figure 3.S8

Table 3.1: IDs of all genes mentioned in text

Gene Name	Gene Symbol	Species	Ensembl ID
Retinoid-X-Receptor α	*RXRα*	Human	ENSG00000186350
Retinoid-X-Receptor β	*RXRβ*	Human	ENSG00000204231
Retinoid-X-Receptor y	*RXRy*	Human	ENSG00000143171
Suppressor of Cytokine Signaling 1	*SOCS1*	Human	ENSG00000185338
Retinoid-X-Receptor α	*Rxrα*	Mouse	ENSMUSG00000015846
Retinoid-X-Receptor β	*Rxrβ*	Mouse	ENSMUSG00000039656
Retinoid-X-Receptor y	*Rxry*	Mouse	ENSMUSG00000015843
chemokine (C-C motif) receptor 2	*Ccr2*	Mouse	ENSMUSG00000049103
chemokine (C-C motif) ligand 2	*Ccl2*	Mouse	ENSMUSG00000035385
Chemokine (C-C motif) ligand 8	*Ccl8*	Mouse	ENSMUSG00000009185
EGF-like module containing, mucin-like, hormone receptor-like sequence 1	*Emr1* (common name F4/80)	Mouse	ENSMUSG00000004730
Interferon-y	*Ifng*	Mouse	ENSMUSG00000055170
Suppressor of Cytokine Signaling 1	*Socs1*	Mouse	ENSMUSG00000038037
Interferon gamma receptor 1	*Ifngr1*	Mouse	ENSMUSG00000020009
Integrin alpha M	*Itgam* (common name CD11B)	Mouse	ENSMUSG00000030786
CD8 antigen, beta chain 1	*Cd8b1* (common name CD8)	Mouse	ENSMUSG00000053044
Tyrosinase-related protein 1	*Tyrp1*	Mouse	ENSMUSG00000005994
Proliferating cell nuclear antigen	*Pcna*	Mouse	ENSMUSG00000027342
Chemokine (C-X-C motif) ligand 10	*Cxcl10*	Mouse	ENSMUSG00000034855
Chemokine (C-X-C motif) ligand 12	*Cxcl12*	Mouse	ENSMUSG00000061353
Slit homolog 2	*Slit2*	Mouse	ENSMUSG00000031558
Tumor necrosis factor	*Tnf*	Mouse	ENSMUSG00000024401
Chemokine (C-X-C motif) receptor 4	*Cxcr4*	Mouse	ENSMUSG00000045382
C-C motif chemokine 19	*Ccl19*	Mouse	ENSMUSG00000094661
Chemokine (C-X3-C motif) ligand 1	*Cx3Cl1*	Mouse	ENSMUSG00000031778
Chemokine (C-C motif) ligand 4	*Ccl4*	Mouse	ENSMUSG00000018930
Chemokine (C-C motif) receptor-like 2	*Ccrl2*	Mouse	ENSMUSG00000043953
Baculoviral IAP repeat-containing 5	*Birc5*	Mouse	ENSMUSG00000017716
B cell leukemia/lymphoma 2	*Bcl2*	Mouse	ENSMUSG00000057329
Fibroblast growth factor 1	*Fgf1*	Mouse	ENSMUSG00000036585
Neural cell adhesion molecule 1	*Ncam1*	Mouse	ENSMUSG00000039542
BCL2-associated agonist of cell death	*Bad*	Mouse	ENSMUSG00000024959
FBJ osteosarcoma oncogene	*Fos*	Mouse	ENSMUSG00000021250
Transformation related protein 53	*Trp53* (common name p53)	Mouse	ENSMUSG00000059552

Table 3.2: List of antibodies used during experimental procedures

Antibody	Host	Source	Application	Dilution/Conc.
anti-PEP1 (TYRP1)	Rabbit	NIH (kindly provided by V. Hearing)	IHC-P	1:1000
anti-PCNA	Mouse	Abcam (ab29)	IHC-P	1:6000
anti-RXRα	Mouse	Millipore (MAB5478)	IHC-P	1:1000
anti-RXRα	Rabbit	Santa Cruz (sc553)	WB, ChIP	1:250, 2.0 µg/ChIP
anti-RXRβ	Mouse	Abcam (ab2815)	IHC-P	1:500
anti-F4/80	Rabbit	Abcam (ab74383)	WB	1:750
anti-F4/80	Rat	BioLegend (122602)	IHC-Fr	1:200
anti-IFN-γ	Rabbit	LSBio (C85867)	IHC-Fr	1:200
anti-CPD	Mouse	(KB: MC-062)	IHC-P	1:1000
anti-8-OHdG	Mouse	JaICA (MOG-020P)	IHC-P	7.5 µg/mL
anti-CD3	Rabbit	Abcam (ab16669)	IHC-P	1:1000
anti-CD8	Rat	Abcam (ab22378)	IHC-Fr	1:100
anti-CD11B	Rat	Abcam (ab8878)	IHC-Fr	1:50
anti-IFN-γ R1	Armenian Hamster	R&D Systems (MAB10261)	WB	1.0 µg/mL
normal Rabbit IgG	Rabbit	Santa Cruz (sc2027)	ChIP	2.0 µg/ChIP
FITC-anti-CD45	Rat	BD Pharmingen (553079)	FACS	0.2 µg/10^6 cells
PE-anti-CD117	Mouse	eBioscience (12-1172-81)	FACS	0.2 µg/10^6 cells

IHC-P = Immunohistochemistry - Paraffin Sections,
IHC-Fr = Immunohistochemistry - Frozen Sections, WB = Western Blot,
ChIP = Chromatin IP FACS = Fluorescence-activated cell sorting

Table 3.3: 29mer shRNA constructs used for gene knockdown studies

Gene	29mer shRNA Construct (5'-3')
Rxrα	TGCCTGTAGAGAAGATTCTGGAAGCCGAG
Rxrβ	TTGCTGTGGAGCAGAAGAGTGACCAAGGC
Scrambled Control	GCACTACCAGAGCTAACTCAGATAGTACT

Table 3.4: List of primer sets used for RT-qPCR analysis of mRNA expression

Gene	Ensembl ID (mouse)	Forward Primer (5'-3')	Reverse Primer (5'-3')
Atm	ENSMUSG00000034218	GATCTGCTCATTTGCTGCCG	GTGTGGTGGCTGATACATTTGAT
Bad	ENSMUSG00000024959	AAGTCCGATCCCGGAATCC	GCTCACTCGGCTCAAACTCT
Bcl2 Var. 1	ENSMUSG00000057329	ATGCCTTTGTGGAACTATATGGC	GGTATGCACCCAGAGTGATGC
Bcl2 Var. 2	ENSMUSG00000057329	GCTACCGTCGTGACTTCGC	CCCCACCGAACTCAAAGAAGG
Birc5	ENSMUSG00000017716	GAGGCTGGCTTCATCCACTG	CTTTTTGCTTGTTGTTGGTCTCC
Ccl19	ENSMUSG00000094661	AGACTGCTGCCTGTCTGTGA	TCTTCAGTCTTCGGATGATGC
Ccl2	ENSMUSG00000035385	TAAAAACCTGGATCGGAACCAAA	GCATTAGCTTCAGATTTACGGGT
Ccl4	ENSMUSG00000018930	TTCCTGCTGTTTCTCTTACACCT	CTGTCTGCCTCTTTTGGTCAG
Ccl7	ENSMUSG00000035373	GCTGCTTTCAGCATCCAAGTG	CCAGGGACACCGACTACTG
Ccl8	ENSMUSG00000009185	CTGGGCCAGATAAGGCTCC	CATGGGGCACTGGATATTGTT
Ccrl2	ENSMUSG00000043953	GCCCCGGACGATGAATATGAT	CACCAAGATAAACACCGCCAG
Cdk2	ENSMUSG00000025358	ATGGAGAACTTCCAAAAGGTGG	CAGTCTCAGTGTCGAGCCG
Cmtm4	ENSMUSG00000096188	CAAGGTCGCCCAAGTGATTCT	GATTCCAGTTGATCTGGGGGA
Cmtm6	ENSMUSG00000032434	ATGGAGAACGGAGCGGTCTA	CACACTCGGACACAACCTCT
Cx3Cl1	ENSMUSG00000031778	CGCGTTCTTCCATTTGTGTA	TAGCTGATAGCGGATGAGCA
Cxcl10	ENSMUSG00000034855	CCAAGTGCTGCCGTCATTTTC	TCCCTATGGCCCTCATTCTCA
Cxcl12	ENSMUSG00000061353	TGCATCAGTGACGGTAAACCA	CACAGTTTGGAGTGTTGAGGAT
Cxcl5	ENSMUSG00000029371	ATCCCCAGCGGTTCCATCT	GCGGCTATGACTGAGGAAGG
Cxcr4	ENSMUSG00000045382	GACTGGCATAGTCGGCAATG	AGAAGGGGAGTGTGATGACAAA
Cxcr5	ENSMUSG00000047880	ATGAACTACCCACTAACCCTGG	TGTAGGGGAATCTCCGTGCT
Cxcr7	ENSMUSG00000044337	GCAAGAGATGGCCAAGAGAC	GTGTCCACCACAATGCAGTC
Fgf1	ENSMUSG00000036585	CAGCTCAGTGCGGAAAGTG	TGTCTGCGAGCCGTATAAAAG
Fos	ENSMUSG00000021250	CGGGTTTCAACGCCGACTA	TTGGCACTAGAGACGGACAGA
Itga2	ENSMUSG00000015533	GGGGACCGGAGGCTTTCTA	GGCCTGTCACAAACTTTACCAAA
Itga3	ENSMUSG00000001507	CCTCTTCGGCTACTCGGTC	CCAGTCCGGTTGGTATAGTCATC
Myc	ENSMUSG00000022346	ATGCCCCTCAACGTGAACTTC	CGCAACATAGGATGGAGAGCA
Ncam1	ENSMUSG00000039542	GGGGAGGATGCTGTGATTGTC	GCGGTAAGTACCCTCATCTGT
Pdgfb	ENSMUSG00000000489	CATCCGCTCCTTTGATGATCTT	GTGCTCGGGTCATGTTCAAGT
Pik3r1	ENSMUSG00000041417	GCAGAGGGCTACCAGTACAGA	CTGAATCCAAGTGCCACTAAGG
Pten	ENSMUSG00000013663	TGGATTCGACTTAGACTTGACCT	GCGGTGTCATAATGTCTCTCAG
Rb1	ENSMUSG00000022105	TTGGAGTCCGATTGTATTACCGT	AGCACAGGCCAGTAAAGACAT
Rxrα	ENSMUSG00000015846	GATATCAAGCCGCCACTAGG	TGTTGTCTCGGCAGGTGTAG
Rxrβ	ENSMUSG00000039656	CACCTCTTACCCCTTCAGCA	GAGCGACACTGTGGAGTTGA
Slit2	ENSMUSG00000031558	GGCAGACACTGTCCCTATCG	ATCTATCTTCGTGATCCTCGTGA
Thbs2	ENSMUSG00000031558	CTGGGCATAGGGCCAAGAG	GTCTTCCGGTTAATGTTGCTGAT
Tnf	ENSMUSG00000024401	CCTGTAGCCCACGTCGTAG	GGGAGTAGACAAGGTACAACCC
Trp53	ENSMUSG00000059552	CACAGCACATGACGGAGGTC	TCCTTCCACCCGGATAAGATG
Tyr	ENSMUSG00000004651	TTACTCAGCCCAGCATCCTT	TCAGGTGTTCCATCGCATAA
Tyrp1	ENSMUSG00000005994	TCTGGCCTCCAGTTACCAAC	GGCTTCATTCTTGGTGCTTC
Tyrp2	ENSMUSG00000022129	AACAACCCTTCCACAGATGC	TAGTCACCGGTGGGAAGAAG
Hprt	ENSMUSG00000025630	GTTAAGCAGTACAGCCCC	AGGGCATATCCAACAACA

Table 3.5: List of primer sets used for ChIP-RT-qPCR analysis

Gene (distance from TSS)	Forward Primer (5'-3')	Reverse Primer (5'-3')
Cxcl10 (-3.8 kb)	TCAGGGCAAGCTTAACAAGG	TGGGATTTGAACTCCTGACC
Cxcl10 (-3.3 kb)	GGTTTGTGGTTTGAGGAGGA	GGCCAGGTGAGGATTTCATA
Cxcl10 (-0.1 kb)	TCCAAGTTCATGGGTCACAA	GAGTTTCCCTCCCTGAGTCC
Cxcl10 (3' UTR)	CCAACGTGTGAACAAGGAGA	GCGTGCAGTGAGTTGAGGTA
Fos (-3.2 kb)	ACACCCGGCATCATTTCTT	CGCCTGGGTAAACAACACAT
Fos (-1.3 kb)	GACCCTCAGAATGGAGACGA	AAGAGGTCAGGTGCTTCAGTG
Fos (3' UTR)	TGCAAGGATGTGCTTTTCTG	TCTGGTTTGCAGTGTGGAAG
Cxcl12 (-4.3 kb)	GGATGCCCAAGTCCTACAGA	GTTGCTGTCCCTTGAACCAT
Cxcl12 (-1.4 kb)	CAGGCATCAGGTATCCCAAG	TCCATTTCTACCGGCTTTTG
Cxcl12 (3' UTR)	CCATTCTCTCTGCCCACATT	GCCGTAGGCTGTTTGAGAAG
Slit2 (-4.1 kb)	GAAAGCAGAGGCAGGTGAAT	CCATGTTAGGTGGTAGGAATCG
Slit2 (3' UTR)	CTGCATCAGGAAACTGGACA	CCTCCTGAAGGAAATGTTGC
Cx3Cl1 (-4.2 kb)	GGAATGAGTGGGAAAGGTGA	CACGGAATCCTCTGGAGAAA
Cx3Cl1 (-2.3 kb)	TCTGAGTTCAAGGCCAGCTT	CCCACTTGGGCAGGTTACTA
Cx3Cl1 (3' UTR)	ATAGGGCTAAAACCCCAGGA	GGTTGAAGGCAGGAGGACTA
Ccl19 (-4.2 kb)	GCGGATTTCTGAGTTCAAGG	TTAGTCAGGGGCCAGAAATG
Ccl19 (-3.2 kb)	CATTCATTGAGGGCTTGGTT	GAGTGGGCTTTGAGGTTTCA
Ccl19 (-1.5 kb)	CCACAACCAAGGCAACTTTT	CCTCATCCTAGCAGCCTTCA
Ccl19 (3' UTR)	GCCATCTTCTATTCCGTCCA	CCTCACGGTTCTTTCTTCCA
Bad (-3.7/3.8 kb)	AGCGTCTGATTATCCCGATG	GGATACCAGATGCCCACAGT
Bad (-3.2 kb)	AAGGTGAGTCCCAGGCAGT	TGGGAACCAGTCTGTTCTGAG
Bad (3' UTR)	GAGCGTGGCTAGACCCTTG	TGACCCAAATAGGAGCAAATG
Fgf1 (-2.7 kb)	AATGTGGCAGAAGAGGCTGT	GTTGTCAGGCCCAGTCTTGT
Fgf1 (-1.7 kb)	CTAAGCACGGTGGGAGAAAG	GGGCTTGTCAGGTGTCTACC
Fgf1 (-1.0 kb)	AAGCGGTTGACTGCTACCTC	TGTCCCTTGTCCTTGGAGAC
Fgf1 (3' UTR)	TAATTGGGGCTGGCTTACAG	ATGTGGCCCTGTTGGAGTAG
Tnf (-4.4 kb)	GATGTCCTTTGTTGGGCAGT	CAGGCTTCCAATGCTCTGTA
Tnf (-3.8 kb)	GCCAGCCTGGTCTACAGAGT	GTCTTTGGGGGTTCAAGTCA
Tnf (-0.6 kb)	CGCAGTCAAGATATGGCAGA	CTTGGAGGAAGTGGCTGAAG
Tnf (3' UTR)	GTGGGTGGATTGGAAAGAGA	CTGAATAAAGTCGGCCTTGC
Ccl4 (-4.3 kb)	GACGTGGAAACTTCCCTGAG	GTGCCCACGGTACTTCACTC
Ccl4 (-2.6 kb)	GGTAGACGGGAAACAAACCA	AGAGAAGGGGAGGGAAGAGA
Ccl4 (3' UTR)	TTTGCCTCTATGAGGGTGCT	ACTACGCAGAGCTCCCAGAG

General Conclusions and Future Directions

Chapter 4

Daniel J. Coleman and Arup K. Indra

4.1 General Conclusions and Future Directions

Rates of melanoma incidence as a result of unprotected ultraviolet radiation are on the rise in Oregon and throughout the U.S.; thus better understanding of the molecular mechanisms underlying its formation and progression are needed for the purposes of diagnosis and therapeutic targeting. In this work we have used mouse models to establish multiple roles for Retinoid-X-Receptors in UVR-induced melanocyte homeostasis and melanomagenesis. Loss of RXRα expression in murine epidermal keratinocytes (*Rxrα*$^{ep-/-}$) enhances melanocyte proliferation following an acute UVR dose as a result of increased expression of mitogenic paracrine factors such as EDN1, SCF, and FGF2. Combining keratinocytic RXRα ablation with activated CDK4 (R24C) or oncogenic NRAS (Q61K) mutations in a bigenic mouse model (*Rxrα*$^{ep-/-}$| *Tyr-NRAS*^{Q61K} or *Rxrα*$^{ep-/-}$| *Cdk4*^{R24C}) results in increased number and size of melanomas induced by chronic UVR compared to control mice with the activated CDK4 or oncogenic NRAS mutations alone. Tumors from the bigenic *Rxrα*$^{ep-/-}$ mice show enhanced expression of malignant melanoma and tumor angiogenesis markers; and increased metastases of cells expressing the melanocyte-specific marker TYRP1 to draining lymph nodes are also observed in these animals. Interestingly, the tumor adjacent normal skin of these mice had reduced expression of p53 and PTEN, tumor suppressors commonly downregulated in melanoma [1-3]; suggesting that keratinocytic RXRα loss results in a microenvironment favorable to tumor formation. Loss of p53 expression in these mice could mean functional disruption of p19ARF; a

dangerous combination particularly in *Rxrα*$^{ep-/-}$| *Cdk4*^{R24C} mice as the Rb-INK4a-CDK4 pathway is already dysregulated, analogous to complete functional loss of the Ink4a/ARF locus. Additionally, loss of functional p53 has previously been reported to promote melanoma formation in combination with both mutant CDK4 [4,5] and NRAS [1,2]. Altogether, these results indicate that keratinocytic RXRα expression is involved in mediating cell-cell communication between keratinocytes and melanocytes that when dysregulated results in both promotion and enhanced formation of UVR-induced melanomas. As synergism has been suggested to exist between the Rb-INK4a-CDK4 and MAPK pathways, going forward we aim to investigate the role of keratinocytic RXRα in melanoma when combined with both NRAS and CDK4 mutations in a trigenic *Rxrα*$^{ep-/-}$| *Cdk4*^{R24C} |*Tyr-NRAS*^{Q61K} mouse model. This trigenic mouse line has been generated in our lab and work is currently underway to evaluate melanomagenesis in these animals. In the future we would also like to investigate the cooperative effects of RXRα loss in combination with oncogenic BRAF^{V600E}, as this mutant protein is expressed in a majority of melanomas [6]. Resistance to treatment with drugs that target the mutant BRAF protein [7] can be acquired by melanomas; underscoring the need for additional therapeutic targets for concurrent multidrug treatment strategies.

The role of RXRs in melanocytes themselves had never been thoroughly investigated previously, even though a gradual loss of RXRα expression has been previously observed in the melanoma cells themselves during disease progression [8]. By ablating RXRs α and β specifically in the melanocytes

(*Rxrα/β*$^{mel-/-}$), we observed differential alterations in the post-UVR survival of the melanocytes and the dermal fibroblasts. Loss of melanocytic RXR expression results in defective homeostasis of chemoattractive and chemorepulsive chemokines secreted by melanocytes to attract macrophages and other immune cells following UVR. Alterations in homeostasis of chemokine expression have been previously observed in mice with keratinocyte-specific knockout of RXRs α and β, including *Cxcl10* [9], which is similarly dysregulated in our *Rxrα/β*$^{mel-/-}$ model and is a potential direct binding target of RXRα in melanocytes as determined by Chromatin Immunoprecipitation (ChIP) assay. An overall reduction of immune cell infiltration in *Rxrα/β*$^{mel-/-}$ mice results in less available interferon-γ available in the microenvironment which has a negative effect on post-UVR survival of fibroblasts and melanocytes. However, as the genetic defect in these mice is specifically in the melanocytes, there are dysregulations in the cell-intrinsic apoptosis signaling that allow these cells to overcome a reduction in available IFN-γ and have enhanced survival post-UVR. That was further confirmed by addition of an RXR agonist or RXR antagonist to cultured primary murine melanocytes, in order to simulate loss of either transcriptional repression or activation functions of RXRs, respectively. Interestingly, in both cases we observed reduced post-UVR apoptosis of the cells compared to vehicle controls, suggesting that RXRs can mediate apoptosis in melanocytes independently of IFN-γ via multiple pathways utilizing both activating and repressive functions. It has been previously reported that clonal expansion of keratinocytes expressing a mutant copy of p53 is driven by chronic UVB-induced

apoptosis of surrounding cells resulting in primary papilloma formation [10]. Though correlation between fibroblast apoptosis and melanoma has never been thoroughly examined, it's possible that in our *Rxrα/β*$^{mel-/-}$ model that melanocytes are more likely to incorporate oncogenic mutations stemming from their enhanced ability to survive UVR-induced DNA damage, and increased apoptosis of surrounding cells in the dermis may aid their expansion, favoring melanomagenesis. Future studies are needed to explore the effects of melanocytic RXR α/β ablation on formation of UVR-induced tumors in adult mice; potentially in combination with the activated CDK4 or oncogenic NRAS^{Q61K} mutations used in our bigenic *Rxrα*$^{ep-/-}$ chronic UVR model; and/or BRAF^{V600E} mutations.

A better understanding of the direct gene regulation by RXRs in melanocytes may further enhance our knowledge of its role in these cells. Using motif searching and ChIP-RT-qPCR, we were able to identify two direct proximal promoter targets of RXRα in melanocytes, out of a large list of genes dysregulated in absence of RXRs as found using RT-qPCR arrays. These indirect gene dysregulations may be accounted for by RXR binding to distal promoter/enhancer regions, and/or by *in trans* regulation via enhancer RNAs (eRNAs) [11]; or alternatively these genes may simply be downstream targets of a different gene(s) directly regulated by RXR on its proximal promoter. ChIP for RXRα in melanocytes followed by next generation high-throughput sequencing (ChIP-seq) may be a technique worth employing in the future, in order to elucidate RXR binding genome-wide in melanocytes. We have already had

success with ChIP-seq of RXRα in primary murine keratinocytes (for example see Figure 4.1 A), and a gene ontology (GO) analysis of the data confirmed that purported RXRα binding in this cell type corresponded with genes involved primarily in skin/keratinocyte-specific processes (Figure 4.1 B). ChIP-seq of RXRα in combination with the histone activation (H3K9Ac [12], H3K4Me3 [13]), repression (H3K27Me3 [14]) and enhancer (H3K4Me1 [15]) marks in melanocytes may provide a fast track to better understanding of its involvement in gene-regulatory networks within that specific cell type. Furthermore, data already obtained in keratinocytes will continue to be useful as we seek new directions for investigating the function of keratinocytic RXRα in melanomagenesis and other skin pathologies.

The UVB-induced melanomas we observe in the bigenic *Rxrα*$^{ep-/-}$ mice are largely dermal in nature. Combined with enhanced dermal apoptosis we observe as a result melanocytic RXR ablation, perhaps more focus needs to be put on the distinct melanocyte subpopulations within the skin going forward. The concept of two distinct types of melanocytes in the skin has only come to light recently [16,17]. Armed with this information, it may be useful to investigate the role of RXR ablation in combination with specific blocking or activation of individual mitogenic signaling pathways that have all been previously shown to be upregulated in our *Rxrα*$^{ep-/-}$ mouse studies, such as c-MET-HGF [18] and EDN1/ENDRB [18,19] signaling axes, which have been shown to be more crucial for dermal melanocytes [17]; and SCF-cKIT signaling [18,19], which is a primary requirement for epidermal melanocytes [17]. We are also interested in effects of

αMSH/MC1R signaling as it is crucial for pigmentation [20,21] and MC1R variants are associated with enhanced melanoma risk [21,22]. Work is currently underway to investigate the cooperativity of individual mitogenic signaling pathways with the keratinocytic RXRα signaling in UV-induced keratinoyte and melanocyte homeostasis by using specific blocking peptides or small molecules inhibitors to modulate signaling mediated by each of the paracrine factors (SCF, EDN1, αMSH, and HGF) *in vivo* [Kyryachenko et al, in preparation]. In the future, we may consider investigating the role(s) of the above mentioned signaling pathways in our other mouse models (such as the *Rxrα/β*$^{mel-/-}$ or bigenic *Rxrα*$^{ep-/-}$| *Tyr-NRAS*^{Q61K} and *Rxrα*$^{ep-/-}$| *Cdk4*^{R24C} mice), and/or developing culture conditions for primary melanocytes *in vitro* that are favorable for one subpopulation vs. another.

As RXRs serve as heterodimeric partners for a large number of other Type II nuclear receptors, it may be prudent to investigate the role of other NRs in skin tumorigenesis. We are also interested in heterodimeric partners of RXR, such as Pregnane-X Receptors (PXR), Liver-X-Receptors (LXRs), Vitamin D Receptor (VDR), Retinoic Acid Receptors (RARs) and Peroxisome Proliferator-Activated Receptors (PPARs) in the keratinocytes, whose expression is lost during melanoma progression in humans. PXR is a mediator of drug metabolism and transport [23]. Treatment of melanoma cells with an LXR agonist resulted in induction of apoptosis in a dose-dependent manner [24]. Previously it was found that keratinocyte-specific ablation of PPARγ (*Pparγ*$^{ep-/-}$) resulted in conversion of DMBA-TPA induced epidermal tumors to malignant carcinomas [25]; a similar

phenotype was observed in *Rxrα*$^{ep-/-}$ mice [25], though PPARγ ablation does not appear to enhance formation of melanocytic growths as RXRα loss does [25]. Meanwhile, keratinocyte-specific ablation of vitamin-D receptor (*Vdr*$^{ep-/-}$) does not enhance epidermal DMBA-TPA induced tumorigenesis but does increase formation of melanocytic growths over control mice; though these growths do not undergo malignant transformation as in *Rxrα*$^{ep-/-}$ mice [25]. Polymorphisms in the human *VDR* gene have been previously associated with prognosis of malignant melanoma in patients [26]; a recent genetic analysis of 263 melanoma patients found that a particular nucleotide polymorphisim (SNP) in the VDR correlated with increased numbers of melanocytic nevi, while two other SNPs appeared to confer a protective response [27]. Subsequent studies in mouse models will be necessary to elucidate their role in UV-induced melanomagenesis in combination with activated CDK4 or oncogenic N-RAS. Work is also currently underway in the lab to investigate the melanocyte-specific role of VDR (*Vdr*$^{mel-/-}$) in UVR-induced responses.

Altogether, we have made great strides in elucidating the function of keratinocytic and melanocytic RXRs in melanocyte homeostasis and in melanomagenesis. Much is still left to learn about the molecular mechanisms of melanoma formation; and to that end we are currently pursuing many exciting new leads.

4.2 References

1. Dovey M, White RM, Zon LI (2009) Oncogenic NRAS cooperates with p53 loss to generate melanoma in zebrafish. Zebrafish 6: 397-404.

2. Bardeesy N, Bastian BC, Hezel A, Pinkel D, DePinho RA, et al. (2001) Dual inactivation of RB and p53 pathways in RAS-induced melanomas. Mol Cell Biol 21: 2144-2153.

3. Stahl JM, Cheung M, Sharma A, Trivedi NR, Shanmugam S, et al. (2003) Loss of PTEN promotes tumor development in malignant melanoma. Cancer Res 63: 2881-2890.

4. Muthusamy V, Hobbs C, Nogueira C, Cordon-Cardo C, McKee PH, et al. (2006) Amplification of CDK4 and MDM2 in malignant melanoma. Genes Chromosomes Cancer 45: 447-454.

5. Yang G, Rajadurai A, Tsao H (2005) Recurrent patterns of dual RB and p53 pathway inactivation in melanoma. J Invest Dermatol 125: 1242-1251.

6. Cantwell-Dorris ER, O'Leary JJ, Sheils OM (2011) BRAFV600E: implications for carcinogenesis and molecular therapy. Molecular cancer therapeutics 10: 385-394.

7. Poulikakos PI, Persaud Y, Janakiraman M, Kong X, Ng C, et al. (2011) RAF inhibitor resistance is mediated by dimerization of aberrantly spliced BRAF (V600E). Nature 480: 387-390.

8. Chakravarti N, Lotan R, Diwan AH, Warneke CL, Johnson MM, et al. (2007) Decreased expression of retinoid receptors in melanoma: entailment in tumorigenesis and prognosis. Clin Cancer Res 13: 4817-4824.

9. Li M, Messaddeq N, Teletin M, Pasquali JL, Metzger D, et al. (2005) Retinoid X receptor ablation in adult mouse keratinocytes generates an atopic dermatitis triggered by thymic stromal lymphopoietin. Proc Natl Acad Sci U S A 102: 14795-14800.

10. Zhang W, Hanks AN, Boucher K, Florell SR, Allen SM, et al. (2005) UVB-induced apoptosis drives clonal expansion during skin tumor development. Carcinogenesis 26: 249-257.

11. Melo CA, Drost J, Wijchers PJ, van de Werken H, de Wit E, et al. (2013) eRNAs are required for p53-dependent enhancer activity and gene transcription. Mol Cell 49: 524-535.

12. Karmodiya K, Krebs AR, Oulad-Abdelghani M, Kimura H, Tora L (2012) H3K9 and H3K14 acetylation co-occur at many gene regulatory elements, while H3K14ac marks a subset of inactive inducible promoters in mouse embryonic stem cells. BMC Genomics 13: 424.

13. Lauberth SM, Nakayama T, Wu X, Ferris AL, Tang Z, et al. (2013) H3K4me3 interactions with TAF3 regulate preinitiation complex assembly and selective gene activation. Cell 152: 1021-1036.

14. Au SL-K, Wong CC-L, Lee JM-F, Wong C-M, Ng IO-L (2013) EZH2-mediated H3K27me3 is involved in epigenetic repression of deleted in liver cancer 1 in human cancers. PLoS One 8: e68226.

15. Zentner GE, Tesar PJ, Scacheri PC (2011) Epigenetic signatures distinguish multiple classes of enhancers with distinct cellular functions. Genome research 21: 1273-1283.

16. Aoki H, Hara A, Motohashi T, Osawa M, Kunisada T (2011) Functionally distinct melanocyte populations revealed by reconstitution of hair follicles in mice. Pigment Cell Melanoma Res 24: 125-135.

17. Aoki H, Yamada Y, Hara A, Kunisada T (2009) Two distinct types of mouse melanocyte: differential signaling requirement for the maintenance of non-cutaneous and dermal versus epidermal melanocytes. Development 136: 2511-2521.

18. Hyter S, Bajaj G, Liang X, Barbacid M, Ganguli-Indra G, et al. (2010) Loss of nuclear receptor RXRalpha in epidermal keratinocytes promotes the formation of Cdk4-activated invasive melanomas. Pigment Cell Melanoma Res 23: 635-648.

19. Wang Z, Coleman DJ, Bajaj G, Liang X, Ganguli-Indra G, et al. (2011) RXRalpha ablation in epidermal keratinocytes enhances UVR-induced DNA damage, apoptosis, and proliferation of keratinocytes and melanocytes. J Invest Dermatol 131: 177-187.

20. Lin JY, Fisher DE (2007) Melanocyte biology and skin pigmentation. Nature 445: 843-850.

21. Abdel-Malek ZA, Knittel J, Kadekaro AL, Swope VB, Starner R (2008) The Melanocortin 1 Receptor and the UV Response of Human Melanocytes—A Shift in Paradigm†. Photochemistry and photobiology 84: 501-508.

22. Landi MT, Bauer J, Pfeiffer RM, Elder DE, Hulley B, et al. (2006) MC1R germline variants confer risk for BRAF-mutant melanoma. Science 313: 521-522.

23. Swales KE, Moore R, Truss NJ, Tucker A, Warner TD, et al. (2012) Pregnane X receptor regulates drug metabolism and transport in the vasculature and protects from oxidative stress. Cardiovascular research 93: 674-681.

24. Zhang W, Jiang H, Zhang J, Zhang Y, Liu A, et al. (2014) Liver X receptor activation induces apoptosis of melanoma cell through caspase pathway. Cancer cell international 14: 16.

25. Indra AK, Castaneda E, Antal MC, Jiang M, Messaddeq N, et al. (2007) Malignant transformation of DMBA/TPA-induced papillomas and nevi in the skin of mice selectively lacking retinoid-X-receptor alpha in epidermal keratinocytes. J Invest Dermatol 127: 1250-1260.

26. Hutchinson PE, Osborne JE, Lear JT, Smith AG, Bowers PW, et al. (2000) Vitamin D receptor polymorphisms are associated with altered prognosis in patients with malignant melanoma. Clinical Cancer Research 6: 498-504.

27. Ogbah Z, Visa L, Badenas C, Ríos J, Puig-Butille JA, et al. (2013) Serum 25-hydroxyvitamin D3 levels and vitamin D receptor variants in melanoma patients from the Mediterranean area of Barcelona: 25-hydroxyvitamin D3 levels and VDR variants in melanoma patients from Barcelona. BMC medical genetics 14: 26.

Figure 4.1 Sample data from ChIP-seq experiment performed in murine epidermal keratinocytes

(A) ChIP-seq was performed in primary murine keratinocytes using a specific antibody for RXRα; in addition to specific antibodies against two general markers of transcriptional activation (Histone 3, Lysine 4 tri-methylation (H3K4Me3) and Histone 3, Lysine 9 acetylation (H3K9Ac)). Raw data was aligned to the mouse genome (mm9) using Bowtie and the generated .BED file was then analyzed using four different peak-calling programs (HOMER, QuEST, MACS and MACS2) and output bigWig (.bw) and bigBed (.bb) files were plotted using the UCSC Genome Browser. Comparable results were observed using each program. Depicted is a sample browser window of peaks called using the most stringent of the four programs, MACS2; which called 8004 significantly-enriched peaks for RXRα binding genome-wide in keratinocytes. (B) Using the data assembled by the Gene Ontology Project, peaks identified via ChIP-seq can be correlated to adjacent genes and their associated phenotypes. A GO analysis on our RXRα ChIP-seq reveals many phenotypes associated with the skin, with the top eight hits shown here. These results demonstrate that RXRα plays a ubiquitous role in skin and confirms the specificity of the experiment. It may be a powerful tool to further investigate the pathways by which keratinocytic RXRα influences melanocytes; the technique can also be employed in the future to analyze genome-wide binding of RXRs in other cell types such as melanocytes.

A

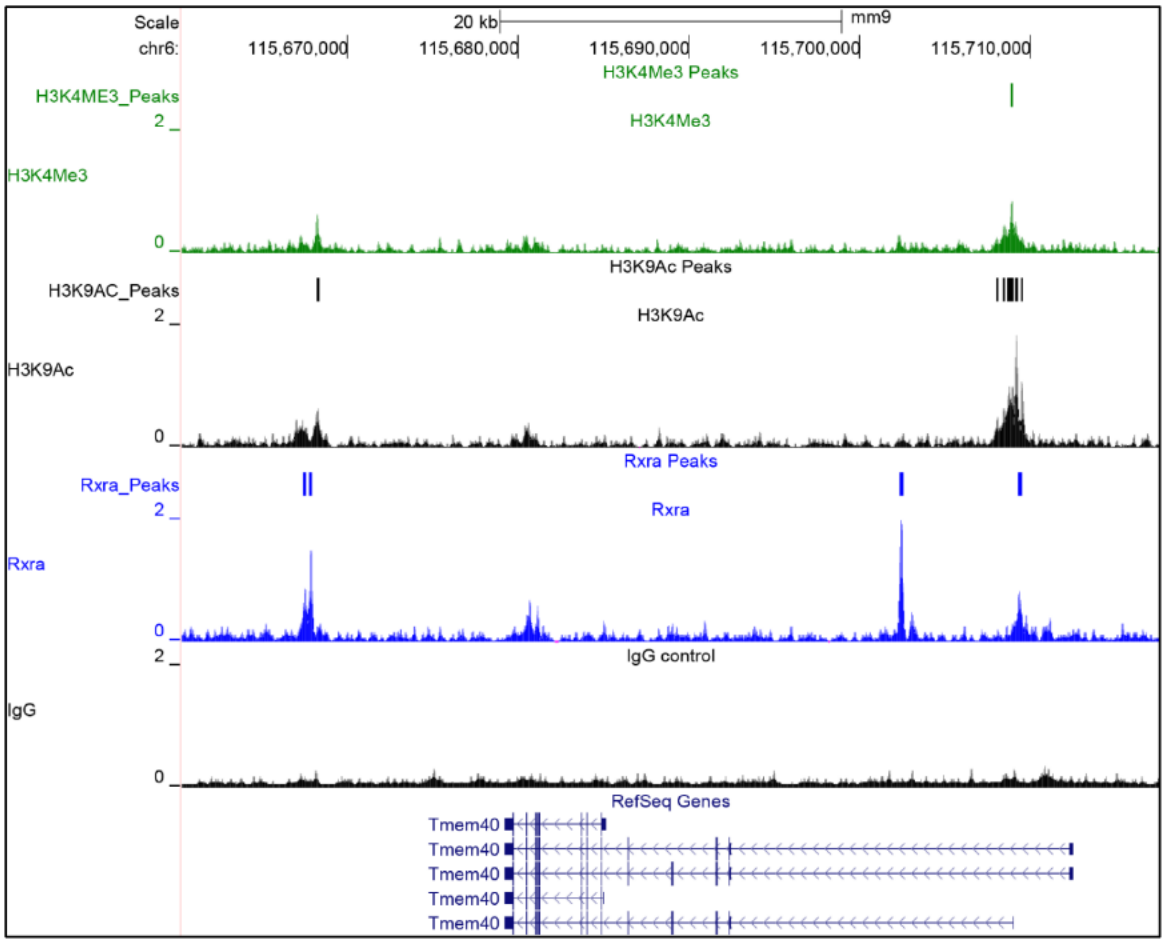

B

Top 8 GO Hits

	Mouse Phenotype
1	abnormal epidermal layer morphology
2	abnormal epidermis stratum corneum morphology
3	abnormal skin physiology
4	hyperkeratosis
5	absent epidermis stratum corneum
6	abnormal hair follicle morphology
7	shiny skin
8	abnormal cell differentiation

Figure 4.1

Bibliography

"Centers for Disease Control and Prevention. Melanoma diagnosis rates are the result of a number of different factors, including: race (melanoma affects Caucasians at a much greater rate than other racial groups), type of UV exposure (intermittent versus cumulative exposure), sun protection behaviors in childhood and adulthood, geographic mobility of the population, risk awareness of the population and geography (e.g., latitude and elevation)."

"National Cancer Institute and Centers for Disease Control and Prevention. (2009) State Cancer Profiles. U.S. state-level and Oregon county-level incidence data query. Incidence data based on data from the State's Cancer Registry, the SEER November 2008 data submission, and the CDC's National Program of Cancer Registries Cancer Surveillance System (NPCR-CSS) November 2008 and January 2009 data submissions. Retrieved March 29, 2010, from http://statecancerprofiles.cancer.gov/."

"National Cancer Institute and Centers for Disease Control and Prevention. (2009). State Cancer Profiles. U.S. state-level and Oregon county-level mortality data query. Mortality data based on the National Vital Statistics System public use data file. Retrieved March 29, 2010, from http://statecancerprofiles.cancer.gov/."

Abdel-Malek, Z. A., J. Knittel, et al. (2008). "The Melanocortin 1 Receptor and the UV Response of Human Melanocytes—A Shift in Paradigm†." Photochemistry and photobiology **84**(2): 501-508.

Ackermann, J., M. Frutschi, et al. (2005). "Metastasizing melanoma formation caused by expression of activated N-RasQ61K on an INK4a-deficient background." Cancer Res **65**(10): 4005-4011.

Agar, N. and A. R. Young (2005). "Melanogenesis: a photoprotective response to DNA damage?" Mutation Research/Fundamental and Molecular Mechanisms of Mutagenesis **571**(1): 121-132.

Alla, V., D. Engelmann, et al. (2010). "E2F1 in melanoma progression and metastasis." J Natl Cancer Inst **102**(2): 127-133.

Aoki, H., A. Hara, et al. (2011). "Functionally distinct melanocyte populations revealed by reconstitution of hair follicles in mice." Pigment Cell Melanoma Res **24**(1): 125-135.

Aoki, H., Y. Yamada, et al. (2009). "Two distinct types of mouse melanocyte: differential signaling requirement for the maintenance of non-cutaneous and dermal versus epidermal melanocytes." Development **136**(15): 2511-2521.

Ariotti, S., J. B. Beltman, et al. (2012). "Tissue-resident memory CD8+ T cells continuously patrol skin epithelia to quickly recognize local antigen." Proc Natl Acad Sci U S A **109**(48): 19739-19744.

Au, S. L.-K., C. C.-L. Wong, et al. (2013). "EZH2-mediated H3K27me3 is involved in epigenetic repression of deleted in liver cancer 1 in human cancers." PLoS One **8**(6): e68226.

Bardeesy, N., B. C. Bastian, et al. (2001). "Dual inactivation of RB and p53 pathways in RAS-induced melanomas." Mol Cell Biol **21**(6): 2144-2153.

Bastien, N., J.-P. Therrien, et al. (2013). "Cytosine containing dipyrimidine sites can be hotspots of cyclobutane pyrimidine dimer formation after UVB exposure." Photochemical & Photobiological Sciences **12**(8): 1544-1554.

Baxter, L. L. and W. J. Pavan (2002). "The oculocutaneous albinism type IV gene Matp is a new marker of pigment cell precursors during mouse embryonic development." Mech Dev **116**(1-2): 209-212.

Baynash, A. G., K. Hosoda, et al. (1994). "Interaction of endothelin-3 with endothelin-B receptor is essential for development of epidermal melanocytes and enteric neurons." Cell **79**(7): 1277-1285.

Bleyer, A., O'Leary, M., Barr, R., & Ries, L.A.G. (Eds.). (2006). "Cancer Epidemiology in Older Adolescents and Young Adults 15 to 29 Years of Age, Including SEER Incidence and Survival: 1975-2000. National Cancer Institute, NIH Pub. No. 06-5767. Bethesda, MD. Retrieved March 13, 2009, from http://seer.cancer.gov/publications/aya/."

Bourguet, W., P. Germain, et al. (2000). "Nuclear receptor ligand-binding domains: three-dimensional structures, molecular interactions and pharmacological implications." Trends Pharmacol Sci **21**(10): 381-388.

Brash, D. E. and W. A. Haseltine (1982). "UV-induced mutation hotspots occur at DNA damage hotspots."

Cantwell-Dorris, E. R., J. J. O'Leary, et al. (2011). "BRAFV600E: implications for carcinogenesis and molecular therapy." Molecular cancer therapeutics **10**(3): 385-394.

Carmeliet, P., L. Moons, et al. (2001). "Synergism between vascular endothelial growth factor and placental growth factor contributes to angiogenesis and plasma extravasation in pathological conditions." Nat Med **7**(5): 575-583.

Chakravarti, N., R. Lotan, et al. (2007). "Decreased expression of retinoid receptors in melanoma: entailment in tumorigenesis and prognosis." Clin Cancer Res **13**(16): 4817-4824.

Chambon, P. (1996). "A decade of molecular biology of retinoic acid receptors." FASEB J **10**(9): 940-954.

Christoffels, V. M., W. M. Hoogaars, et al. (2004). "T-box transcription factor Tbx2 represses differentiation and formation of the cardiac chambers." Dev Dyn **229**(4): 763-770.

Conway, S. J. (1999). "Novel expression of the goosecoid transcription factor in the embryonic mouse heart." Mech Dev **81**(1-2): 187-191.

Costa, D. B., B. Halmos, et al. (2007). "BIM mediates EGFR tyrosine kinase inhibitor-induced apoptosis in lung cancers with oncogenic EGFR mutations." PLoS Med **4**(10): 1669-1679; discussion 1680.

Dave, V. P. and D. Kaul (2010). "Coronary heart disease: Significance of liver X receptor α genomics." World journal of cardiology **2**(6): 140.

de Gruijl, F. R., H. J. van Kranen, et al. (2001). "UV-induced DNA damage, repair, mutations and oncogenic pathways in skin cancer." Journal of Photochemistry and Photobiology B: Biology **63**(1): 19-27.

Delmas, V., S. Martinozzi, et al. (2003). "Cre-mediated recombination in the skin melanocyte lineage." Genesis **36**(2): 73-80.

Denning, M. F. (2012). "Specifying protein kinase C functions in melanoma." Pigment Cell Melanoma Res **25**(4): 466-476.

Dieu, M. C., B. Vanbervliet, et al. (1998). "Selective recruitment of immature and mature dendritic cells by distinct chemokines expressed in different anatomic sites." J Exp Med **188**(2): 373-386.

Dighe, A. S., E. Richards, et al. (1994). "Enhanced in vivo growth and resistance to rejection of tumor cells expressing dominant negative IFN gamma receptors." Immunity **1**(6): 447-456.

Dilworth, F. J., C. Fromental-Ramain, et al. (2000). "ATP-driven chromatin remodeling activity and histone acetyltransferases act sequentially during transactivation by RAR/RXR In vitro." Mol Cell **6**(5): 1049-1058.

Dovey, M., R. M. White, et al. (2009). "Oncogenic NRAS cooperates with p53 loss to generate melanoma in zebrafish." Zebrafish **6**(4): 397-404.

Dunn, G. P., C. M. Koebel, et al. (2006). "Interferons, immunity and cancer immunoediting." Nat Rev Immunol **6**(11): 836-848.

Dutertre, S., M. Cazales, et al. (2004). "Phosphorylation of CDC25B by Aurora-A at the centrosome contributes to the G2-M transition." J Cell Sci **117**(Pt 12): 2523-2531.

Eller, M. S., T. Maeda, et al. (1997). "Enhancement of DNA repair in human skin cells by thymidine dinucleotides: evidence for a p53-mediated mammalian SOS response." Proceedings of the National Academy of Sciences **94**(23): 12627-12632.

Eller, M. S., K. Ostrom, et al. (1996). "DNA damage enhances melanogenesis." Proceedings of the National Academy of Sciences **93**(3): 1087-1092.

Eller, M. S., M. Yaar, et al. (1994). "DNA damage and melanogenesis." Nature **372**(6505): 413.

Epstein, F. H., B. A. Gilchrest, et al. (1999). "The pathogenesis of melanoma induced by ultraviolet radiation." New England Journal of Medicine **340**(17): 1341-1348.

Fang, G., H. Yu, et al. (1998). "The checkpoint protein MAD2 and the mitotic regulator CDC20 form a ternary complex with the anaphase-promoting complex to control anaphase initiation." Genes Dev **12**(12): 1871-1883.

Forman, B. M., P. Tontonoz, et al. (1995). "15-Deoxy-delta 12, 14-prostaglandin J2 is a ligand for the adipocyte determination factor PPAR gamma." Cell **83**(5): 803-812.

Gao, Y., D. O. Ferguson, et al. (2000). "Interplay of p53 and DNA-repair protein XRCC4 in tumorigenesis, genomic stability and development." Nature **404**(6780): 897-900.

Gibejova, A., F. Mrazek, et al. (2003). "Expression of macrophage inflammatory protein-3 beta/CCL19 in pulmonary sarcoidosis." Am J Respir Crit Care Med **167**(12): 1695-1703.

Giguere, V., E. S. Ong, et al. (1987). "Identification of a receptor for the morphogen retinoic acid." Nature **330**(6149): 624-629.

Glass, C. K. and M. G. Rosenfeld (2000). "The coregulator exchange in transcriptional functions of nuclear receptors." Genes Dev **14**(2): 121-141.

Griffith, T. S., T. Brunner, et al. (1995). "Fas ligand-induced apoptosis as a mechanism of immune privilege." Science **270**(5239): 1189-1192.

Guan, H., G. Zu, et al. (2003). "Neuronal repellent Slit2 inhibits dendritic cell migration and the development of immune responses." J Immunol **171**(12): 6519-6526.

Haake, A., G. A. Scott, et al. (2001). "Structure and function of the skin: overview of the epidermis and dermis." The Biology of the skin **2001**: 19-45.

Hall, B. K. (2009). The neural crest and neural crest cells in vertebrate development and evolution, Springer.

Hermanson, O., C. K. Glass, et al. (2002). "Nuclear receptor coregulators: multiple modes of modification." Trends Endocrinol Metab **13**(2): 55-60.

Heyman, R. A., D. J. Mangelsdorf, et al. (1992). "9-cis retinoic acid is a high affinity ligand for the retinoid X receptor." Cell **68**(2): 397-406.

Horner, M. J., Ries, L.A.G., Krapcho, M., Neyman, N., Aminou, R., Howlader, N., Altekruse, S.F., Feuer, E.J., Huang, L., Mariotto, A., Miller, B.A., Lewis, D.R., Eisner, M.P., Stinchcomb, D.G., & Edwards, B.K. (Eds.). (2009). "SEER Cancer Statistics Review, 1975-2006, Section 16: Melanoma of the Skin. Based on November 2008 SEER data submission, posted to the SEER web site, 2009. National Cancer Institute. Bethesda, MD. Retrieved March 29, 2010, from http://seer.cancer.gov/csr/1975_2006/."

Hutchinson, P. E., J. E. Osborne, et al. (2000). "Vitamin D receptor polymorphisms are associated with altered prognosis in patients with malignant melanoma." Clinical Cancer Research **6**(2): 498-504.

Hyter, S., G. Bajaj, et al. (2010). "Loss of nuclear receptor RXRalpha in epidermal keratinocytes promotes the formation of Cdk4-activated invasive melanomas." Pigment Cell Melanoma Res **23**(5): 635-648.

Hyter, S., D. J. Coleman, et al. (2013). "Endothelin-1 is a transcriptional target of p53 in epidermal keratinocytes and regulates ultraviolet-induced melanocyte homeostasis." Pigment Cell Melanoma Res **26**(2): 247-258.

Hyter, S. and A. K. Indra (2013). "Nuclear hormone receptor functions in keratinocyte and melanocyte homeostasis, epidermal carcinogenesis and melanomagenesis." FEBS Lett **587**(6): 529-541.

Indra, A. K., E. Castaneda, et al. (2007). "Malignant transformation of DMBA/TPA-induced papillomas and nevi in the skin of mice selectively lacking retinoid-X-receptor alpha in epidermal keratinocytes." J Invest Dermatol **127**(5): 1250-1260.

Jakob, J. A., R. L. Bassett, et al. (2012). "NRAS mutation status is an independent prognostic factor in metastatic melanoma." Cancer **118**(16): 4014-4023.

Janowski, B. A., P. J. Willy, et al. (1996). "An oxysterol signalling pathway mediated by the nuclear receptor LXR alpha." Nature **383**(6602): 728-731.

Jing, H., E. Vassiliou, et al. (2003). "Prostaglandin E2 inhibits production of the inflammatory chemokines CCL3 and CCL4 in dendritic cells." J Leukoc Biol **74**(5): 868-879.

Jordan, S. A. and I. J. Jackson (2000). "MGF (KIT ligand) is a chemokinetic factor for melanoblast migration into hair follicles." Dev Biol **225**(2): 424-436.

Kaplan, D. H., V. Shankaran, et al. (1998). "Demonstration of an interferon gamma-dependent tumor surveillance system in immunocompetent mice." Proc Natl Acad Sci U S A **95**(13): 7556-7561.

Karmodiya, K., A. R. Krebs, et al. (2012). "H3K9 and H3K14 acetylation co-occur at many gene regulatory elements, while H3K14ac marks a subset of inactive inducible promoters in mouse embryonic stem cells." BMC Genomics **13**: 424.

Karst, A. M., K. Levanon, et al. (2011). "Stathmin 1, a marker of PI3K pathway activation and regulator of microtubule dynamics, is expressed in early pelvic serous carcinomas." Gynecol Oncol **123**(1): 5-12.

Keeley, E. C., B. Mehrad, et al. (2008). "Chemokines as mediators of neovascularization." Arterioscler Thromb Vasc Biol **28**(11): 1928-1936.

Kim, C. H., L. M. Pelus, et al. (1999). "CCR7 ligands, SLC/6Ckine/Exodus2/TCA4 and CKbeta-11/MIP-3beta/ELC, are chemoattractants for CD56(+)CD16(-) NK cells and late stage lymphoid progenitors." Cell Immunol **193**(2): 226-235.

Kim, C. H., L. M. Pelus, et al. (1998). "CK beta-11/macrophage inflammatory protein-3 beta/EBI1-ligand chemokine is an efficacious chemoattractant for T and B cells." J Immunol **160**(5): 2418-2424.

Kim, C. H., L. M. Pelus, et al. (1998). "Macrophage-inflammatory protein-3 beta/EBI1-ligand chemokine/CK beta-11, a CC chemokine, is a chemoattractant with a specificity for macrophage progenitors among myeloid progenitor cells." J Immunol **161**(5): 2580-2585.

Kliewer, S. A., S. S. Sundseth, et al. (1997). "Fatty acids and eicosanoids regulate gene expression through direct interactions with peroxisome proliferator-activated receptors alpha and gamma." Proc Natl Acad Sci U S A **94**(9): 4318-4323.

Kobayashi, N., T. Muramatsu, et al. (1993). "Melanin reduces ultraviolet-induced DNA damage formation and killing rate in cultured human melanoma cells." Journal of investigative dermatology **101**(5).

Kobayashi, T., K. Urabe, et al. (1994). "Tyrosinase related protein 1 (TRP1) functions as a DHICA oxidase in melanin biosynthesis." EMBO J **13**(24): 5818-5825.

Kohrgruber, N., M. Groger, et al. (2004). "Plasmacytoid dendritic cell recruitment by immobilized CXCR3 ligands." J Immunol **173**(11): 6592-6602.

Kos, L., A. Aronzon, et al. (1999). "Hepatocyte growth factor/scatter factor-MET signaling in neural crest-derived melanocyte development." Pigment Cell Res **12**(1): 13-21.

Kunisada, T., S. Z. Lu, et al. (1998). "Murine cutaneous mastocytosis and epidermal melanocytosis induced by keratinocyte expression of transgenic stem cell factor." J Exp Med **187**(10): 1565-1573.

Kwong, L. N., J. C. Costello, et al. (2012). "Oncogenic NRAS signaling differentially regulates survival and proliferation in melanoma." Nat Med **18**(10): 1503-1510.

Landi, M. T., J. Bauer, et al. (2006). "MC1R germline variants confer risk for BRAF-mutant melanoma." Science **313**(5786): 521-522.

Lassus, P., X. Opitz-Araya, et al. (2002). "Requirement for caspase-2 in stress-induced apoptosis before mitochondrial permeabilization." Science **297**(5585): 1352-1354.

Lauberth, S. M., T. Nakayama, et al. (2013). "H3K4me3 interactions with TAF3 regulate preinitiation complex assembly and selective gene activation." Cell **152**(5): 1021-1036.

Le Douarin, N. and C. Kalcheim (1999). The neural crest, Cambridge University Press.

Lee, C. H. and L. N. Wei (1999). "Characterization of receptor-interacting protein 140 in retinoid receptor activities." J Biol Chem **274**(44): 31320-31326.

Leid, M., P. Kastner, et al. (1992). "Multiplicity generates diversity in the retinoic acid signalling pathways." Trends Biochem Sci **17**(10): 427-433.

Leid, M., P. Kastner, et al. (1992). "Purification, cloning, and RXR identity of the HeLa cell factor with which RAR or TR heterodimerizes to bind target sequences efficiently." Cell **68**(2): 377-395.

Li, M., H. Chiba, et al. (2001). "RXR-alpha ablation in skin keratinocytes results in alopecia and epidermal alterations." Development **128**(5): 675-688.

Li, M., A. K. Indra, et al. (2000). "Skin abnormalities generated by temporally controlled RXRalpha mutations in mouse epidermis." Nature **407**(6804): 633-636.

Li, M., N. Messaddeq, et al. (2005). "Retinoid X receptor ablation in adult mouse keratinocytes generates an atopic dermatitis triggered by thymic stromal lymphopoietin." Proc Natl Acad Sci U S A **102**(41): 14795-14800.

Li, Z., D. Metze, et al. (2004). "Expression of SOCS-1, suppressor of cytokine signalling-1, in human melanoma." J Invest Dermatol **123**(4): 737-745.

Liang, X., S. Bhattacharya, et al. (2012). "Delayed cutaneous wound healing and aberrant expression of hair follicle stem cell markers in mice selectively lacking Ctip2 in epidermis." PLoS One **7**(2): e29999.

Lin, H. H., D. E. Faunce, et al. (2005). "The macrophage F4/80 receptor is required for the induction of antigen-specific efferent regulatory T cells in peripheral tolerance." J Exp Med **201**(10): 1615-1625.

Lin, J. Y. and D. E. Fisher (2007). "Melanocyte biology and skin pigmentation." Nature **445**(7130): 843-850.

Mackenzie, M. A., S. A. Jordan, et al. (1997). "Activation of the receptor tyrosine kinase Kit is required for the proliferation of melanoblasts in the mouse embryo." Dev Biol **192**(1): 99-107.

Maeda, T., M. Eller, et al. (1998). "Thymidine dinucleotide enhances DNA repair in human skin cells." J Dermatol Sci **16**: S17.

Mangelsdorf, D. J., E. S. Ong, et al. (1990). "Nuclear receptor that identifies a novel retinoic acid response pathway." Nature **345**(6272): 224-229.

Marlow, R., P. Strickland, et al. (2008). "SLITs suppress tumor growth in vivo by silencing Sdf1/Cxcr4 within breast epithelium." Cancer Res **68**(19): 7819-7827.

Martinez-Pomares, L., N. Platt, et al. (1996). "Macrophage membrane molecules: markers of tissue differentiation and heterogeneity." Immunobiology **195**(4-5): 407-416.

Mehrad, B., M. P. Keane, et al. (2007). "Chemokines as mediators of angiogenesis." Thromb Haemost **97**(5): 755-762.

Melo, C. A., J. Drost, et al. (2013). "eRNAs are required for p53-dependent enhancer activity and gene transcription." Mol Cell **49**(3): 524-535.

Merkel, M., R. H. Eckel, et al. (2002). "Lipoprotein lipase: genetics, lipid uptake, and regulation." J Lipid Res **43**(12): 1997-2006.

Moreno-Bueno, G., F. Portillo, et al. (2008). "Transcriptional regulation of cell polarity in EMT and cancer." Oncogene **27**(55): 6958-6969.

Muthusamy, V., C. Hobbs, et al. (2006). "Amplification of CDK4 and MDM2 in malignant melanoma." Genes Chromosomes Cancer **45**(5): 447-454.

Na, H. K., E. H. Kim, et al. (2012). "Diallyl trisulfide induces apoptosis in human breast cancer cells through ROS-mediated activation of JNK and AP-1." Biochem Pharmacol **84**(10): 1241-1250.

Nevins, J. R. (2001). "The Rb/E2F pathway and cancer." Hum Mol Genet **10**(7): 699-703.

Newkirk, K. M., A. E. Parent, et al. (2007). "Snai2 expression enhances ultraviolet radiation-induced skin carcinogenesis." Am J Pathol **171**(5): 1629-1639.

Ngo, V. N., H. L. Tang, et al. (1998). "Epstein-Barr virus-induced molecule 1 ligand chemokine is expressed by dendritic cells in lymphoid tissues and strongly attracts naive T cells and activated B cells." J Exp Med **188**(1): 181-191.

Nissan, X., L. Larribere, et al. (2011). "Functional melanocytes derived from human pluripotent stem cells engraft into pluristratified epidermis." Proc Natl Acad Sci U S A **108**(36): 14861-14866.

Oba, J., T. Nakahara, et al. (2011). "Expression of c-Kit, p-ERK and cyclin D1 in malignant melanoma: an immunohistochemical study and analysis of prognostic value." J Dermatol Sci **62**(2): 116-123.

Ogbah, Z., L. Visa, et al. (2013). "Serum 25-hydroxyvitamin D3 levels and vitamin D receptor variants in melanoma patients from the Mediterranean area of Barcelona: 25-hydroxyvitamin D3 levels and VDR variants in melanoma patients from Barcelona." BMC medical genetics **14**(1): 26.

Orlov, I., N. Rochel, et al. (2012). "Structure of the full human RXR/VDR nuclear receptor heterodimer complex with its DR3 target DNA." EMBO J **31**(2): 291-300.

Otero, K., A. Vecchi, et al. (2010). "Nonredundant role of CCRL2 in lung dendritic cell trafficking." Blood **116**(16): 2942-2949.

Ouelle, D. E., F. Zindy, et al. (1995). "Alternative reading frames of the< i> INK4a</i> tumor suppressor gene encode two unrelated proteins capable of inducing cell cycle arrest." Cell **83**(6): 993-1000.

Payne, A. S. and L. A. Cornelius (2002). "The role of chemokines in melanoma tumor growth and metastasis." J Invest Dermatol **118**(6): 915-922.

Perissi, V. and M. G. Rosenfeld (2005). "Controlling nuclear receptors: the circular logic of cofactor cycles." Nat Rev Mol Cell Biol **6**(7): 542-554.

Petkovich, M., N. J. Brand, et al. (1987). "A human retinoic acid receptor which belongs to the family of nuclear receptors." Nature **330**(6147): 444-450.

Pfeifer, G. P. and A. Besaratinia (2012). "UV wavelength-dependent DNA damage and human non-melanoma and melanoma skin cancer." Photochemical & Photobiological Sciences **11**(1): 90-97.

Pollock, P. M., F. Yu, et al. (1995). "Evidence for uv induction of CDKN2 mutations in melanoma cell lines." Oncogene **11**(4): 663-668.

Poulikakos, P. I., Y. Persaud, et al. (2011). "RAF inhibitor resistance is mediated by dimerization of aberrantly spliced BRAF (V600E)." Nature **480**(7377): 387-390.

Puigserver, P., Z. Wu, et al. (1998). "A cold-inducible coactivator of nuclear receptors linked to adaptive thermogenesis." Cell **92**(6): 829-839.

Rachez, C., B. D. Lemon, et al. (1999). "Ligand-dependent transcription activation by nuclear receptors requires the DRIP complex." Nature **398**(6730): 824-828.

Ramirez, J. A., J. Guitart, et al. (2005). "Cyclin D1 expression in melanocytic lesions of the skin." Ann Diagn Pathol **9**(4): 185-188.

Rane, S. G., S. C. Cosenza, et al. (2002). "Germ line transmission of the Cdk4R24C mutation facilitates tumorigenesis and escape from cellular senescence." Mol Cell Biol **22**(2): 644-656.

Rane, S. G., P. Dubus, et al. (1999). "Loss of Cdk4 expression causes insulin-deficient diabetes and Cdk4 activation results in beta-islet cell hyperplasia." Nat Genet **22**(1): 44-52.

Rass, K. and J. Reichrath (2008). UV damage and DNA repair in malignant melanoma and nonmelanoma skin cancer. Sunlight, Vitamin D and Skin Cancer, Springer**:** 162-178.

Recio, J. A., F. P. Noonan, et al. (2002). "Ink4a/arf deficiency promotes ultraviolet radiation-induced melanomagenesis." Cancer Res **62**(22): 6724-6730.

Ren, J. G., C. Jie, et al. (2005). "How PEDF prevents angiogenesis: a hypothesized pathway." Med Hypotheses **64**(1): 74-78.

Richmond, A., J. Yang, et al. (2009). "The good and the bad of chemokines/chemokine receptors in melanoma." Pigment Cell Melanoma Res **22**(2): 175-186.

Rigel, D. S., Friedman, R.J., & Kopf, A.W. (1996). "The Incidence of Malignant Melanoma in the United States: Issues as We Approach the 21st Century. Journal of the American Academy of Dermatology, 34(5), 839-847."

Savoldi-Barbosa, M. and E. T. Sakamoto-Hojo (2001). "Influence of interferon-gamma on radiation-induced apoptosis in normal and ataxia-telangiectasia fibroblast cell lines." Teratog Carcinog Mutagen **21**(6): 417-429.

Sbodio, J. I., H. F. Lodish, et al. (2002). "Tankyrase-2 oligomerizes with tankyrase-1 and binds to both TRF1 (telomere-repeat-binding factor 1) and IRAP (insulin-responsive aminopeptidase)." Biochem J **361**(Pt 3): 451-459.

Seghezzi, G., S. Patel, et al. (1998). "Fibroblast growth factor-2 (FGF-2) induces vascular endothelial growth factor (VEGF) expression in the endothelial cells of forming capillaries: an autocrine mechanism contributing to angiogenesis." J Cell Biol **141**(7): 1659-1673.

Serrano, M., G. J. Hannon, et al. (1993). "A new regulatory motif in cell-cycle control causing specific inhibition of cyclin D/CDK4." Nature **366**(6456): 704-707.

Sharpless, N. and L. Chin (2003). "The INK4a/ARF locus and melanoma." Oncogene **22**(20): 3092-3098.

Sheppard, K. E. and G. A. McArthur (2013). "The cell-cycle regulator CDK4: an emerging therapeutic target in melanoma." Clin Cancer Res **19**(19): 5320-5328.

Shibutani, S., M. Takeshita, et al. (1991). "Insertion of specific bases during DNA synthesis past the oxidation-damaged base 8-oxodG."

Simpson, R. U. and H. F. DeLuca (1980). "Characterization of a receptor-like protein for 1,25-dihydroxyvitamin D3 in rat skin." Proc Natl Acad Sci U S A **77**(10): 5822-5826.

Sotillo, R., J. F. García, et al. (2001). "Invasive melanoma in Cdk4-targeted mice." Proceedings of the National Academy of Sciences **98**(23): 13312-13317.

Stahl, J. M., M. Cheung, et al. (2003). "Loss of PTEN promotes tumor development in malignant melanoma." Cancer Res **63**(11): 2881-2890.

Steel, K. P., D. R. Davidson, et al. (1992). "TRP-2/DT, a new early melanoblast marker, shows that steel growth factor (c-kit ligand) is a survival factor." Development **115**(4): 1111-1119.

Street, S. E., E. Cretney, et al. (2001). "Perforin and interferon-gamma activities independently control tumor initiation, growth, and metastasis." Blood **97**(1): 192-197.

Suzuki, F., T. Nanki, et al. (2005). "Inhibition of CX3CL1 (fractalkine) improves experimental autoimmune myositis in SJL/J mice." J Immunol **175**(10): 6987-6996.

Swales, K. E., R. Moore, et al. (2012). "Pregnane X receptor regulates drug metabolism and transport in the vasculature and protects from oxidative stress." Cardiovascular research **93**(4): 674-681.

Tamai, M., A. Kawakami, et al. (2006). "Significant inhibition of TRAIL-mediated fibroblast-like synovial cell apoptosis by IFN-gamma through JAK/STAT pathway by translational regulation." J Lab Clin Med **147**(4): 182-190.

Tole, S., I. M. Mukovozov, et al. (2009). "The axonal repellent, Slit2, inhibits directional migration of circulating neutrophils." J Leukoc Biol **86**(6): 1403-1415.

Tornaletti, S. and G. P. Pfeifer (1994). "Slow repair of pyrimidine dimers at p53 mutation hotspots in skin cancer." Science **263**(5152): 1436-1438.

Underhill, C., M. S. Qutob, et al. (2000). "A novel nuclear receptor corepressor complex, N-CoR, contains components of the mammalian SWI/SNF complex and the corepressor KAP-1." J Biol Chem **275**(51): 40463-40470.

Verhaegen, M., A. Checinska, et al. (2012). "E2F1-dependent oncogenic addiction of melanoma cells to MDM2." Oncogene **31**(7): 828-841.

Wang, D., C. R. Stockard, et al. (2008). "Immunohistochemistry in the evaluation of neovascularization in tumor xenografts." Biotech Histochem **83**(3): 179-189.

Wang, Z., D. J. Coleman, et al. (2011). "RXRalpha ablation in epidermal keratinocytes enhances UVR-induced DNA damage, apoptosis, and proliferation of keratinocytes and melanocytes." J Invest Dermatol **131**(1): 177-187.

Wang, Z., J. S. Kirkwood, et al. (2013). "Transcription factor Ctip2 controls epidermal lipid metabolism and regulates expression of genes involved in sphingolipid biosynthesis during skin development." J Invest Dermatol **133**(3): 668-676.

Wang Z, Zhang LJ, Guha G, Li S, Kyrylkova K, et al. (2012) Selective ablation of Ctip2/Bcl11b in epidermal keratinocytes triggers atopic dermatitis-like skin inflammatory responses in adult mice. PLoS One 7: e51262.

Wolfel, T., M. Hauer, et al. (1995). "A p16INK4a-insensitive CDK4 mutant targeted by cytolytic T lymphocytes in a human melanoma." Science **269**(5228): 1281-1284.

Wu, J. Y., L. Feng, et al. (2001). "The neuronal repellent Slit inhibits leukocyte chemotaxis induced by chemotactic factors." Nature **410**(6831): 948-952.

Xue, Y., R. Gibbons, et al. (2003). "The ATRX syndrome protein forms a chromatin-remodeling complex with Daxx and localizes in promyelocytic leukemia nuclear bodies." Proc Natl Acad Sci U S A **100**(19): 10635-10640.

Yamazaki, F., H. Okamoto, et al. (2005). "Development of a new mouse model (xeroderma pigmentosum a-deficient, stem cell factor-transgenic) of ultraviolet B-induced melanoma." J Invest Dermatol **125**(3): 521-525.

Yancopoulos, G. D., S. Davis, et al. (2000). "Vascular-specific growth factors and blood vessel formation." Nature **407**(6801): 242-248.

Yang, G., A. Rajadurai, et al. (2005). "Recurrent patterns of dual RB and p53 pathway inactivation in melanoma." J Invest Dermatol **125**(6): 1242-1251.

Yang, J. and A. Richmond (2004). "The angiostatic activity of interferon-inducible protein-10/CXCL10 in human melanoma depends on binding to CXCR3 but not to glycosaminoglycan." Mol Ther **9**(6): 846-855.

Yoshida, H., T. Kunisada, et al. (2001). "Review: melanocyte migration and survival controlled by SCF/c-kit expression." J Investig Dermatol Symp Proc **6**(1): 1-5.

Zaidi, M. R., S. Davis, et al. (2011). "Interferon-gamma links ultraviolet radiation to melanomagenesis in mice." Nature **469**(7331): 548-553.

Zentner, G. E., P. J. Tesar, et al. (2011). "Epigenetic signatures distinguish multiple classes of enhancers with distinct cellular functions." Genome research **21**(8): 1273-1283.

Zhang, W., A. N. Hanks, et al. (2005). "UVB-induced apoptosis drives clonal expansion during skin tumor development." Carcinogenesis **26**(1): 249-257.

Zhang, W., H. Jiang, et al. (2014). "Liver X receptor activation induces apoptosis of melanoma cell through caspase pathway." Cancer cell international **14**(1): 16.

Zuo, L., J. Weger, et al. (1996). "Germline mutations in the p16INK4a binding domain of CDK4 in familial melanoma." Nat Genet **12**(1): 97-99.